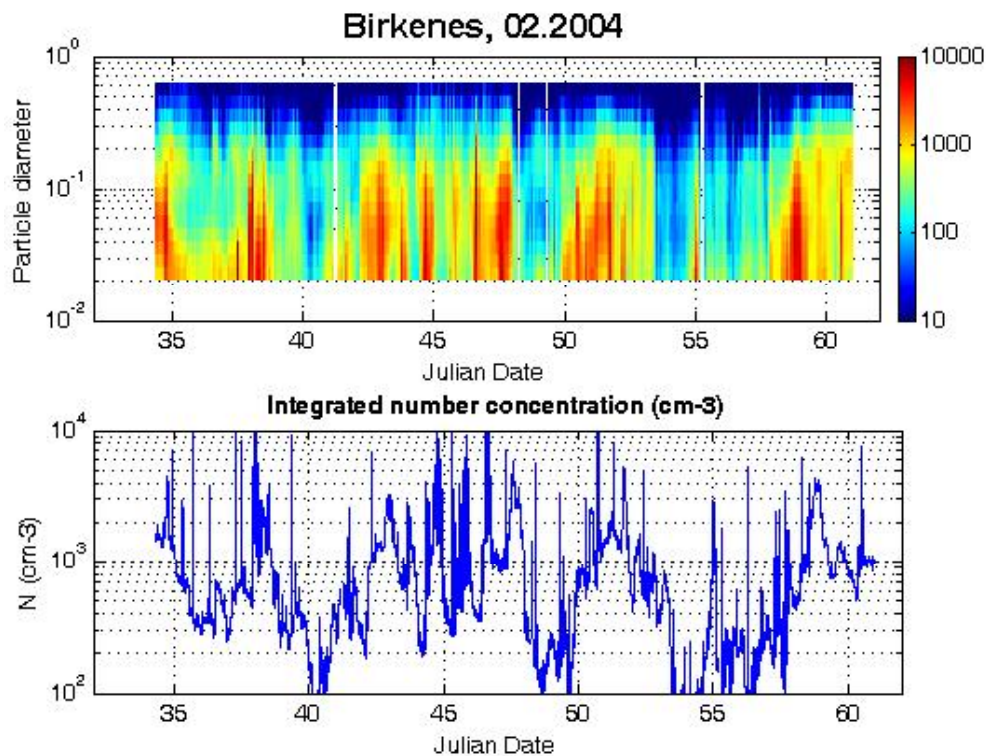


Measurements of Particulate Matter: Status Report 2005



NILU : EMEP/CCC-Report 5/2005
REFERENCE : O-98134
DATE : AUGUST 2005

**EMEP Co-operative Programme for Monitoring and Evaluation
of the Long-range Transmission of Air Pollutants
in Europe**

**Measurements of Particulate Matter:
Status Report 2005**



Norwegian Institute for Air Research
P.O. Box 100, N-2027 Kjeller, Norway

Edited by Karl Espen Yttri

List of Contributors

Wenche Aas¹, Lucie Dzumbova², Maria Cristina Facchini³, Thodoros Glytsos²,
Jan Erik Hanssen¹, Thomas Holzer-Popp⁴, Øystein Hov⁵, S. Gerard Jennings⁶,
Ilias Kopanakis², Markku Kulmala⁷, Mihalis Lazaridis², Gerrit de Leeuw⁸,
Chris Lunder¹, Jakub Ondracek², Jan Schaug¹, Robin Schoemaker⁸,
Kjetil Tørseth¹, Christoph Wehrli⁹ and Karl Espen Yttri¹

- 1 Chemical Co-ordinating Centre of EMEP
Norwegian Institute for Air Research
P.O. Box 100, NO-2027 Kjeller, Norway
- 2 Technical University of Crete
Department of Environmental Engineering
Polytechniopolis, GR-73100 Chania, Greece
- 3 CNR, Institute of Atmospheric Sciences and Climate
Via P. Gobetti 101, IT-40129 Bologna, Italy
- 4 DLR German Aerospace Center
German Remote Sensing Data Center (DFD)
P.O. Box 1116, DE-82234 Wessling, Germany
- 5 Meteorological Institute
P.O. Box 43 Blindern, NO-0313 Oslo, Norway
- 6 National University of Ireland
Department of Experimental Physics
Atmospheric Research Group / Environmental Change Institute
Galway, Ireland
- 7 University of Helsinki
Department of Physics
FIN-00014 Helsinki, Finland
- 8 Netherlands Organisation for Applied Scientific Research
TNO-Physics and Electronics Laboratory
P.O. Box 96864, NL-2509 JG The Hague, The Netherlands
- 9 Physikalisch-Meteorologisches Observatorium Davos
Dorfstrasse 33, CH-7260 Davos Dorf, Switzerland

Executive summary

The present report contains seven separate contributions on recent EMEP- and EMEP-related activities, concerning particulate matter. A summary of these contributions is given below.

In 2003 measurements of PM₁₀ were taken up by three more countries, namely Denmark, Sweden and Slovenia. Thus, ten countries currently report concentrations of PM₁₀, whereas seven of these measure PM_{2.5} as well. Two more countries reported PM_{2.5} for 2003, namely Italy and Sweden. Furthermore, two sites in Austria and Switzerland reported concentrations of PM₁ in addition to the concentrations of PM₁₀ and PM_{2.5}. Although the number of countries and sites that reports concentrations of particulate matter increase year by year, the total number of 36 sites only covers a small part of Europe. Thus, effort should be made to increase the number of sites, and even more important, to increase the number of countries reporting concentrations of particulate matter.

None of the EMEP sites exceeded the annual limit value (40 µg/m³) for the protection of human health, set by the EU in the first Daughter Directive as a goal for 2005. However, the limit value for daily averages of PM₁₀ (50 µg/m³) was exceeded at the Italian site IT04 on 87 days and on 49 days at the Austrian site AT02. The EU has so far set no limit value for PM_{2.5} concentrations. However, five of the EMEP sites reported annual mean concentrations of PM_{2.5} above the PM_{2.5} standard of 15 µg/m³ of the US EPA.

There are still only a few sites within EMEP that have reported concentrations of particulate matter more than for a few years. However, based on measurements from the Austrian, the German and the Swiss sites, there seem to be an upward trend for PM₁₀ after 2000 in parts of central Europe. Data from the Swiss sites indicates that this increase in PM₁₀ follow after a downward trend during the period 1997-2000. The data shows that the increase in PM₁₀ mainly can be attributed to the fine (PM_{2.5}) fraction. The Norwegian site Birkenes show no clear trend like the sites in Central Europe.

A chapter is included that addresses the concentration of particulate matter in the Eastern Mediterranean area. Continuous measurements of particulate matter from this region are scarce. Furthermore, this part of Europe is situated on the outskirts of the domain area of the EMEP model, and receives a significant part of its aerosol loading from outside Europe. Thus, these measurements provides important information concerning the particulate matter level, the seasonal variation, and the contributing sources. It is argued that climatologically changes taking place in other parts of the world is likely to increase the particulate matter loading in the eastern Mediterranean area, both through increased input from natural sources and from anthropogenic sources. During the measurement period (April 2003-June 2005) the mean concentration of PM₁₀ was $35.1 \pm 17.9 \mu\text{g m}^{-3}$, whereas the mean concentration of PM_{2.5} was equal to $27.1 \pm 10.8 \mu\text{g m}^{-3}$. The particulate matter concentration was significantly increased during Saharan dust events. The concentration of particulate matter was found to be higher during

summer than during winter. This was attributed to the influence of Saharan dust events during summer and increased levels of precipitation during winter.

The increased focus on the carbonaceous fraction of ambient aerosols, and the lack of data concerning this parameter in Europe in general, initiated the EMEP EC/OC campaign, which took place from the 1st July 2002–1st July 2003. Levels of organic carbon, elemental carbon and total carbon obtained during this campaign were reported last year (EMEP/CCC, 2004). In the present report, additional chemical analyses of the carbonaceous fraction of the filter samples from this campaign are presented. The main objective has been to provide estimates of the different carbonaceous subfractions and to assess the contribution of residential wood burning as a source of particulate matter.

Levels of water-soluble organic matter (WSOC) and water-insoluble organic matter (WINSOC) were determined, amongst other reasons, to provide a more accurate estimate of the organic matter content in ambient aerosols in rural background areas. WINSOC was the dominant fraction at 11 of the 13 sites investigated, ranging from 43%-83% of the organic carbon (OC) fraction. The relative contribution of WSOC to OC ranged from 17%-57%. Converting WSOC to water-soluble organic matter (WSOM) by using a conversion factor of 2.1, and WINSOC to water-insoluble organic matter (WINSOM) by using a conversion factor of 1.3, WSOM was found to dominate the organic matter (OM) fraction at the majority of the sites, ranging from 24%-68%. Further, it is argued that adding levels of WSOM and WINSOM is the better way to provide concentrations of OM. The advantage of this approach is that it accounts for the relative contribution of WSOM and WINSOM to OM, which was found to vary considerably between the 13 European background sites investigated. If concentrations of WSOM and WINSOM are not available, the next best approach to provide levels of OM was obtained by multiplying OC by a factor of 1.6, compared to using conversion factors of 1.4 and 2.0. (This conclusion is valid given that a factor of 2.1 is used to convert WSOC to WSOM and a factor of 1.3 is used to convert WINSOC to WINSOM). The results presented underlines the importance of a priori knowledge of which subfractions of OC prevails.

Levels of the organic constituent levoglucosan, which is a source specific tracer of wood burning, was quantified to address the spatial and seasonal variation of residential wood burning at 13 European rural background sites, and to estimate the relative contribution of wood smoke particles to the ambient level of PM₁₀. The presence of levoglucosan was demonstrated at all sites investigated. It is argued that the spatial variation reported can be attributed to population density and proximity to urban areas. Thus, the situation of the measurement site is important for the concentrations observed. Concentrations of levoglucosan was 1.3-5.9 times higher during winter compared to summer at the sites investigated, reflecting the increased impact from residential wood burning as the ambient temperature drops during winter. It is argued that wildfires contribute to the level of levoglucosan observed during summer, however, it is not known to what extent. On an annual basis particulate matter from residential wood burning accounted for 1.7% to 10.2% of PM₁₀. Providing corresponding estimates for the winter season, the concentration was found to increase for all sites investigated.

The study indicates that particulate emission from residential wood burning is not a major contributor to PM₁₀ at rural background sites in Europe.

EMEP/CCC (2003) has previously underlined the benefit of including optical aerosol measurements within EMEP, in particular for modelling purposes. Furthermore, an increased emphasis on providing particle number size distribution measurements has been emphasized. Thus, two contributions concerning these topics have been included.

Measurements of AOD (Aerosol Optical Density) at 501 nm at Ny-Ålesund clearly illustrate the problem of Arctic Haze in the boundary layer during the Arctic spring. This is attributed to poor dispersion during winter. During summer, precipitation scavenges the aerosols and the water-soluble gases. Furthermore, an example of satellite AOD measurement is presented. An AOD map over Europe for August 2000, retrieved from ATSR-2 data, provides information on the spatial variation of aerosols, hot spots and other regions with high aerosol loading. The results are validated by comparison with collocated AERONET sun photometer AOD measurements, within 30 minutes of the satellite overpass. The sun-photometer AOD are determined with an accuracy of 0.02, whereas the ATSR-2 AOD accuracy over land is 0.05. An example of how satellite measurements provide retrieved percentage contribution of basic aerosol components to AOD₅₅₀ is shown. The measurements distinguish between insoluble aerosols with high/low absorption, water-soluble aerosols, diesel/biomass burning soot, coarse/accumulation mode sea salt aerosols, and mineral aerosols with high/low hematite content. In addition, it is shown that this kind of measurement has the ability to distinguish between a high and a low relative humidity component for hygroscopic aerosols.

Particle number size distribution measurements obtained at the Norwegian site Birkenes (NO01) are presented. The instruments measures aerosol size distributions in the range between 19.0 nm and 643.2 nm. Particle number size distributions for February and July 2004 are shown to illustrate that the number concentrations are considerably higher during winter compared to summer. It is believed that this seasonal variation can be attributed to higher biogenic activity during spring and summer compared to the winter. However, seasonal changes in air masses, a lower number of particle formation events due to less incoming solar radiation, and a higher rate of precipitation and overall cloudiness may be contributing factors. An example of what most likely is a local particle formation event, taking place during late April, is presented. Small Aitken mode particles appear at noon, which most likely originate from the growth of nucleation mode particles. Over a period of one day these Aitken particles grow into the accumulation mode following coagulation and condensation. As the formation of new particles stop during night and resume the next day, supports that these particles are of biogenic origin. When segregating data into days with and without nucleation events a diurnal variation was revealed that was much more pronounced on days with nucleation events than without. For days with nucleation events there was an initial increase of small particles between 08:00-12:00 that escalated during the day reaching maximum concentrations between 16:00-20:00. Thereafter the size shifted towards larger particles. This daily pattern is interpreted as growth of the small, initially formed particles.

The last contribution to the report is about CREATE, which is a Thematic Project delivered under the 5th Framework Programme “Energy, Environment and Sustainable Development” in support of Global Monitoring for Environment and Security (GMES). GMES represents the main European contribution to the Group on Earth Observation (GEO). The project was established to address issues relating to measuring, modelling and monitoring of atmospheric aerosols within the priority theme: Global Atmosphere Monitoring. The primary objective of CREATE has been to construct, use and deliver an European aerosol database. This database can be found at www.nilu.no/projects/ccc/create/database.htm.

Data linked to the following aerosol parameters have been submitted to the database: Total aerosol number concentration, Aerosol (PM₁₀, PM_{2.5}) mass concentration, aerosol particle size distribution, aerosol inorganic composition (nitrate, ammonium and sulphate), mass concentration of organic carbon, black carbon and total carbon and aerosol radiative data (aerosol absorption, scattering coefficient and aerosol optical depth at specified wavelengths). All these data can be downloaded from the Internet from the before mentioned Internet address, which has been specially created both for the submission of aerosol data and for access to data. The database is run by EMEP and is housed at NILU. The database caters for all the aerosol parameters sited above except the for aerosol optical depth, which is submitted to the World Data Centre for Aerosols (WDCA) (<http://ies.irc.cec.eu.int/wdca/>). Technical information on instrumentation, techniques, meta data, references, data sources and comments for selected aerosols parameters can be found in Appendix B of the CREATE Final Report, which is accessible from the CREATE web site (<http://macehead.nuigalway.ie/create>).

It has previously been stated that information on size distribution measurements, even for a small number of EMEP sites, would be of great benefit for understanding aerosol dynamic processes (EMEP/CCC, 2003). Through the CREATE project more advanced and otherwise unavailable data from research groups in Europe can be added to the EMEP data base and make it more complete.

Contents

	Page
Executive summary	5
1. Measurements of particulate matter in EMEP sites during 2003	11
1.1 PM mass	11
1.2 PM speciation	14
1.3 Trends for PM.....	15
2. Particulate Matter Measurements at the Akrotiri research station on the island of Crete, Greece	17
2.1 Introduction	17
2.2 Methodology.....	19
2.3 Number concentration measurements	23
2.4 Analysis of the Particulate Matter Concentration Sources.....	23
2.5 Conclusions	29
3. Levels and relative contributions of water-insoluble organic carbon and water-soluble organic carbon at rural background sites in Europe	31
3.1 Introduction	31
3.2 Aerosol sampling.....	32
3.3 Quantification of water-insoluble organic carbon and water- soluble organic carbon.....	33
3.4 Concentrations of WINSOC and WSOC and their relative contribution to OC.....	33
3.5 Ambient concentrations of water-soluble organic matter (WSOM) and water-insoluble organic matter (WINSOM) and their relative contribution to OM.....	36
3.6 Conclusion.....	38
4. Impact of residential wood burning at rural background sites in Europe	39
4.1 Introduction	39
4.2 Aerosol sampling.....	40
4.3 Quantification of levoglucosan.....	41
4.4 Annual mean concentration of levoglucosan	41
4.5 Summer vs. winter.....	43
4.6 Relative contribution of individual monosaccharides anhydrides (MA) to the total MA concentration.....	46
4.7 Relative contribution of wood burning to PM ₁₀	47
4.8 Conclusion.....	48
5. Aerosol size distribution measurements at the EMEP site Birkenes (Norway).....	49
6. European aerosol optical depth measurements from ground and space.....	55
6.1 Three years' measurements in Ny-Ålesund with the WMO-GAW precision-filter-radiometer.....	56

6.2	ATSR-2 retrieved spatial distribution of aerosols over Europe	57
6.3	Synergetic ENVISAT aerosol optical depth and type.....	59
7.	Construction, use and delivery of an European aerosol database.....	63
7.1	Introduction	63
7.2	European Aerosol Database	63
7.3	Descriptions of aerosol data sets, housed at NILU	64
7.4	Technical information on instrumentation, techniques used, meta-data, references, data sources and comments for selected aerosol parameters	65
7.5	Summary	67
7.5.1	Size resolved aerosol composition measurements	68
8.	References	71
Annex 1	Overview of sampling methods for particulate matter 2003.....	77
Annex 2	Time series of particulate matter mass concentrations at EMEP stations in 2002 and 2003.....	81
Annex 3	Trends in yearly mean particulate mass concentrations at selected EMEP stations	107

Measurements of Particulate Matter: Status Report 2005

1. Measurements of particulate matter in EMEP sites during 2003

by J.E. Hanssen and W. Aas

1.1 PM mass

Measurements of PM₁₀ were reported from Denmark, Sweden and Slovenia in 2003 in addition to those countries reporting the preceding years. In total 10 Parties now report PM₁₀ from 36 sites and seven of the Parties also measure PM_{2.5} at 22 sites. Austria and Switzerland are in addition also measuring PM₁ at one site each. From April 2003, continuous measurements of PM₁₀ have also been performed at Vreedepeel in The Netherlands. In addition three Parties have reported Suspended Particulate Matter (SPM) from six sites measured either gravimetrically after a non-specific air intake (CH01 and SK02 and SK07, or by the Black Smoke method (SE05, SE08 and SE14). The annual averages of particulate matter from different size bins are given in Table 1.1. Maps of the annual averages of PM₁₀ and PM_{2.5} can be seen in Figure 1.1 and Figure 1.2.

The location of sites, as well as more statistics has been given by Hjellbrekke (2005). Details on sampling methods for particulate matter are given in Annex 1. It is seen that different samplers (high- and medium volume samplers) and different filter types have been used. Also monitors (TEOM and beta gauge) giving hourly values are included.

Time series of the PM data for 2002 and 2003 are given in Annex 2. A complete set of data, including raw data, annual statistics and monthly means, can be downloaded from the web at <http://www.nilu.no/projects/ccc/> under "Measurement data".

It should be noted that in addition to the relatively small PM₁₀ EMEP network, a much larger network, with rural stations, urban background sites as well as measurements in hotspots, is run in Europe in the European Union and that data from this network is collected in the AirBase data base. For 2002 AirBase contains data from approximately 160 PM₁₀ monitoring stations classified as regional background stations (for metadata and statistics, see http://air-climate.eionet.eu.int/databases/airbase/index_html). Many of these stations are EMEP stations. It should, however, be kept in mind that there are differences related to the classification of stations in the two databases. Siting criteria differ a bit between EMEP and EoI-related station. Thus, "Regional background" EoI stations may in some cases not be as strictly background as the EMEP stations.

In Chapter 7 information about the CREATE database for aerosols is given. Other aerosol data from Europe may also be found in the WMO-GAW database for aerosols (GAW-WDCA) at <http://rea.ei.jrc.it/netshare/wilson/WDCA/>.

Table 1.1: Annual average of particulate matter measurements 2003.

Code	PM ₁₀	PM _{2.5}	PM ₁
AT0002R	31.1	24.7	14.1
AT0004R	13.6	-	-
AT0005R	12.3	-	-
CH0002R	25.3	19.8	-
CH0003R	23.2	-	-
CH0004R	14.7	11.0	8.5
CH0005R	15.2	-	-
DE0002R	21.6	16.5	-
DE0003R	13.1	10.1	-
DE0004R	18.5	13.8	-
DE0005R	14.1	-	-
DE0007R	17.6	-	-
DE0008R	13.2	-	-
DE0009R	19.8	-	-
DE0041R	22.8	-	-
DK0005R	24.8	-	-
ES0007R	21.4	9.4	-
ES0008R	19.8	11.0	-
ES0009R	11.5	7.2	-
ES0010R	23.8	15.8	-
ES0011R	16.6	8.0	-
ES0012R	16.1	7.7	-
ES0013R	12.6	8.0	-
ES0014R	19.6	13.3	-
ES0015R	14.2	7.2	-
ES0016R	14.6	9.3	-
IT0001R	28.2	-	-
IT0004R	39.8	28.5	-
NO0001R	6.7	4.4	-
NO0099R	18.7	7.3	-
SE0011R	15.4	10.5	-
SE0012R	6.7	4.8	-
SE0035R	3.6	1.7	-
SI0008R	21.3	-	-
SK0004R	15.7	-	-
SK0005R	23.3	-	-
SK0006R	21.6	-	-

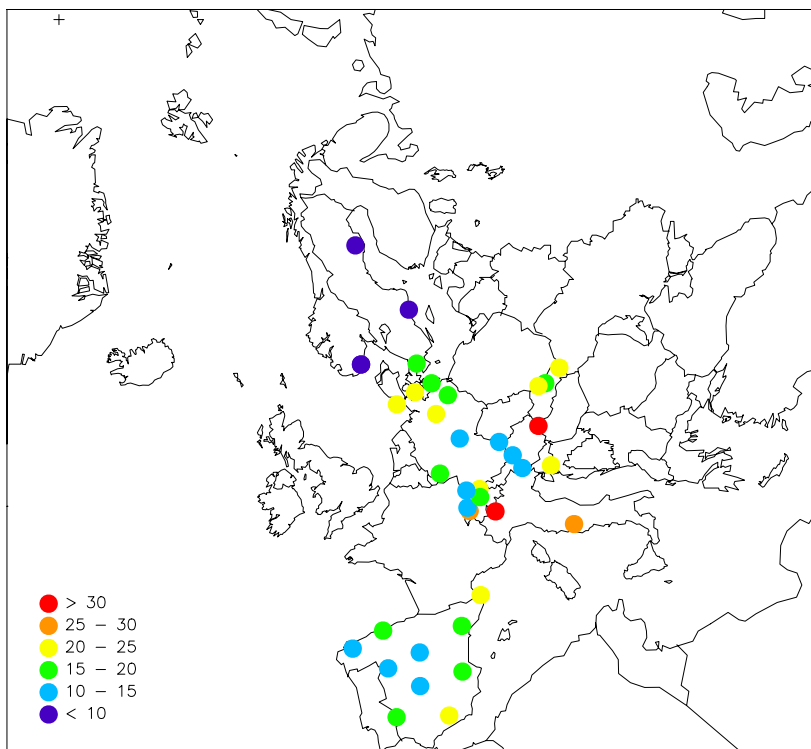


Figure 1.1: Annual 2003 averages PM_{10} mass measurements. Unit $\mu\text{g}/\text{m}^3$.

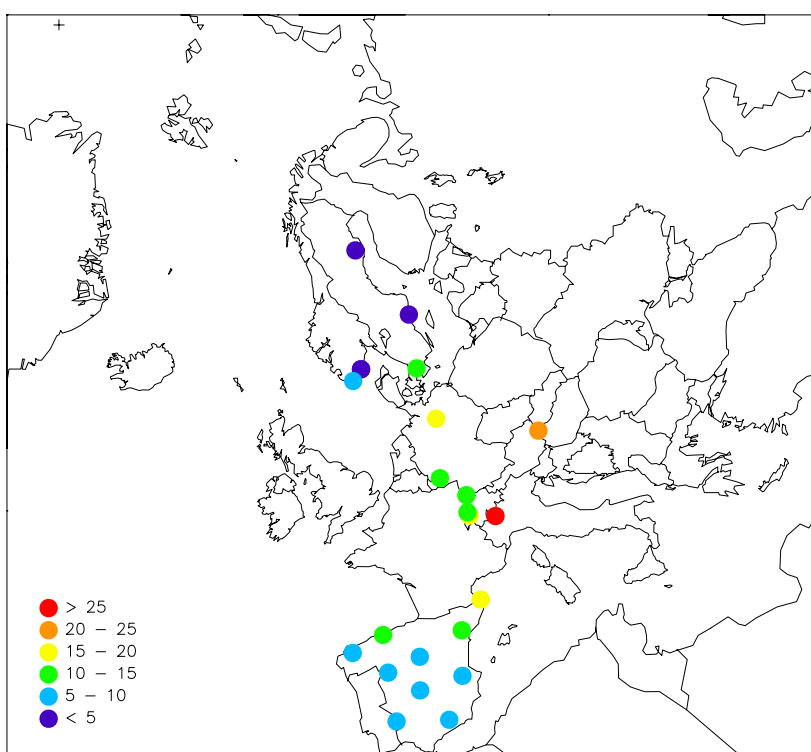


Figure 1.2: Annual 2003 averages $PM_{2.5}$ mass measurements. Unit $\mu\text{g}/\text{m}^3$.

None of the EMEP sites exceeded the annual limit value ($40 \mu\text{g}/\text{m}^3$) for the protection of human health, set by EU in the first Daughter Directive as a goal for 2005 (Table 1.2). However, Ispra (IT04) with $39.8 \mu\text{g}/\text{m}^3$ is very close. The limit value for daily average ($50 \mu\text{g}/\text{m}^3$) was exceeded at IT04 on 87 days in 2003. At Illmitz in Austria (AT02) this limit value was exceeded on 49 days.

Table 1.2: EU limit values for PM_{10} and date to be met, for health-protection.

Compound	Limit/ target value	Value	Remarks	Date to be met
Particulate matter (PM_{10}) Stage 1	Annual average	$40 \mu\text{g}/\text{m}^3$		01.01.2005
	Daily average	$50 \mu\text{g}/\text{m}^3$	May be exceeded up to 35 days a year	01.01.2005
Particulate matter (PM_{10}) Stage 2	Annual average	$20 \mu\text{g}/\text{m}^3$	Indicative	01.01.2010
	Daily average	$50 \mu\text{g}/\text{m}^3$	Indicative; may be exceeded up to 7 days a year	01.01.2010

No limit value has so far been set for $\text{PM}_{2.5}$ concentrations in the EU. The revised $\text{PM}_{2.5}$ standard from the United States EPA is $15 \mu\text{g}/\text{m}^3$ for the annual arithmetic mean. Five of the EMEP sites reported higher values than this.

1.2 PM speciation

Attempting to assess the mass closure of PM_{10} , four selected EMEP sites with partly speciation measurements were chosen. The EC and OM concentrations used were provided from the EMEP EC/OC measurement campaign described in the last year's report (EMEP/CCC, 2004) and used together with reported concentrations of main ions in aerosols for 2003, Figure 1.3. As these measurements only partly represent the same time period, it increases the uncertainty of the results. However, the concentrations do not change much from year to year.

Not all sites measure all ions, thus the labels in Figure 1.3 are not identical for the different sites. In particular, it should be noted that sea-salt is not measured at the Dutch site, but that it is expected to account for a significant part of the unaccounted mass.

In general, the unspecified fraction is relatively large. Most likely, a significant part of the unspecified fraction can be attributed to mineral dust and water associated with the particulate matter. In addition, uncertainties related to the chemical analysis and the mass concentration determination, along with the conversion factor used to convert organic carbon (OC) into organic matter (OM), should be accounted for. As can be seen from Figure 1.3, the highest contribution to the particulate mass can be attributed to the OM fraction, ranging from 20%-45%.

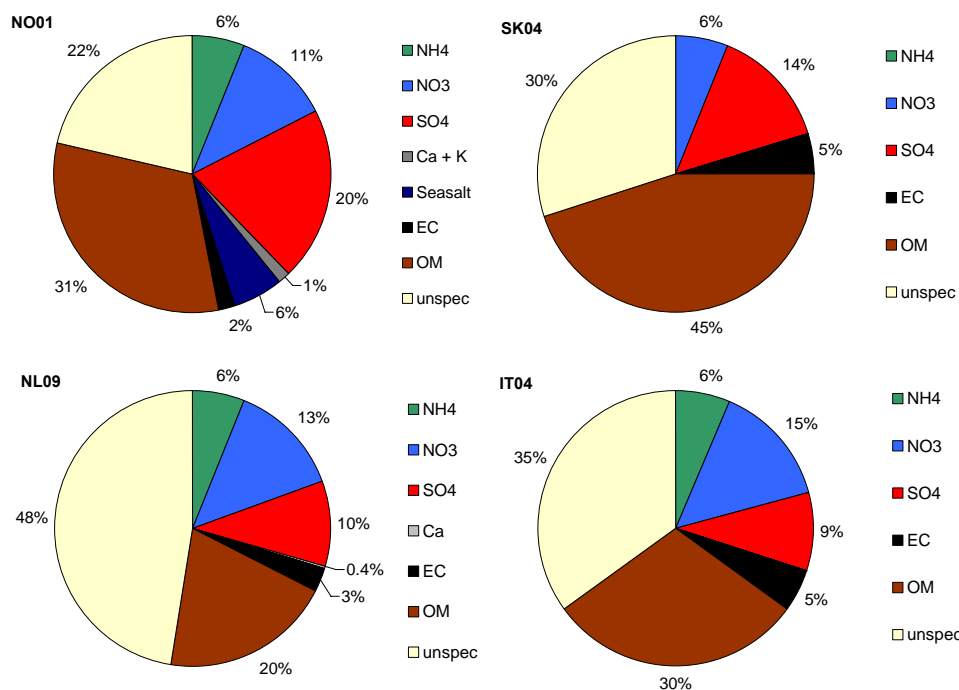


Figure 1.3: Speciation of PM_{10} mass. PM_{10} mass, EC and OM concentrations are taken from the measurement campaign for the period 2002.07.01–2003.07.01. OM is OC multiplied by a factor of 1.6 (IT04) or 2.0 (SK04, NO01, NL09). The concentrations of the inorganic ions are from 2003, and are provided from filterpack (NO, SK, NL) and PM_{10} (IT) measurements.

1.3 Trends for PM

Although there are only a few EMEP sites that have reported PM-data for more than a few years, it may still be valuable to look for trends for those having reported concentrations for at least four years. In Annex 3 plots are given for 15 sites for PM_{10} and seven sites for $PM_{2.5}$ for sites in Austria, Switzerland, Germany and Norway.

For the Austrian sites, Illmitz, St. Koloman and Vorhegg (AT02, AT04 and AT05) there seems to be a gradually upward trend after 2000 for PM_{10} . At Illmitz also $PM_{2.5}$ is gradually increasing. The data shows that the increase is mainly due to the fine ($PM_{2.5}$) part of PM_{10} . The reason for the yearly average of $PM_{2.5}$ being higher than for PM_{10} in 1999 at Illmitz can be attributed to the few months that have $PM_{2.5}$ data.

For the Swiss sites, it seems that the upward trend in the last years follows a downward trend from 1997 to 2000. Also for these sites, it seems that changes in the fine fraction dominates the PM_{10} trend.

Also most of the German sites show increased concentrations after 2000, and again this is mainly caused by the increased fine fraction.

The Norwegian site (Birkenes, NO01) do not show any clear trend like the other sites in the central parts of Europe.

2. Particulate Matter Measurements at the Akrotiri research station on the island of Crete, Greece

M. Lazaridis, I. Kopanakis, T. Glytsos, L. Dzumbova, J. Ondracek, Ø. Hov, M. Kulmala and K. Tørseth

2.1 Introduction

The focus of the current study is on the PM₁₀ and PM_{2.5} ambient levels at the Akrotiri research station on the island of Crete, Greece. This work presents one of the first studies of continuous aerosol monitoring in the Eastern Mediterranean area.

At the north of the Mediterranean Sea a number of highly populated European countries exist with industrial, semi-industrial, and rural economies, whilst to the south is Africa. A detailed wind trajectory analysis shows that more than 60% of air masses, which arrive in the Eastern Mediterranean, come from the N-NW and 13-16% from the Sahara (Guerzoni et al., 1990). Air masses from the N-NW contain particles related to industrial and urban inputs; those from Sahara carry predominantly mineral dust. Transport of Saharan dust occurs mostly during the spring and summer and causes non-continuous crustal aerosol pulses to the Mediterranean area (Bergametti et al., 1989). On the other hand, precipitation scavenging during the rainy season from October and May reduces aerosol concentrations (Dulac et al., 1987). The summer time is characterised by low-inversion layers, and strong sunlight, causing photochemical smog. Moreover, forest fires, which occur during the summer months in the Mediterranean region, increase black carbon and organic mass in general, and fine particle emissions. Thus, the Mediterranean Sea constitutes an area where atmospheric particles originating from continental natural and anthropogenic sources, marine sources and gas-to-particle conversion exist simultaneously. Furthermore, specific meteorological conditions result in high temporal variability of aerosol concentrations. It should be noted that the meteorological conditions in the Mediterranean area also are quite influential for the Central and Southern European weather (Millán et al., 1997).

Most of the studies on the chemical composition of Mediterranean particulate aerosol have been conducted in the western and north-western region (Bergametti et al., 1989; Dulac et al., 1987) or on the eastern coast including Turkey and Israel (Luria et al., 1996; Maenhaut et al., 1999). However relatively few studies have been undertaken in the southern part of the Eastern Mediterranean and Greece (Danalatos and Glavas, 1999).

The loading of air pollution and particulate matter in the Eastern Mediterranean troposphere is strongly linked to the prevailing atmospheric circulation regime over the region. It has been found that the projected changes for 2071-2100 in the SRES B2 scenario (Special Report on Emission Scenarios under IPCC; B2 lies close to the lower end of the scenario range described in SRES) in mean summer precipitation and large-scale circulations over Europe are consistent with the observed changes over the last 25 years as seen in the data from the National Centre for Environmental Prediction (NCEP) reanalysis (Pal et al., 2004). The

change in circulation patterns imply an increased likelihood for drier summers over most of Western and Southern Europe and wetter summers over Finland and Western Russia. It has been concluded that a decrease in mean precipitation results in an increase in the occurrence of drought. The observed drying trend in Western/Central Europe and wetter trend in Western Russia is likely to continue in the future (Pal et al., 2004). The results indicate significant changes in the intensity and persistence of summer flood and drought over the European region (Pal et al., 2004). The Central Mediterranean and Central/Western Europe were identified to be particularly vulnerable to increases in both summer flood and drought. These results show that the probability distribution function of summer precipitation shifts towards the drier side and with a widening of its tails in this century. More frequent dry and hot summers in the Mediterranean could imply a much higher PM loading both because the likelihood of dust storms increases, the oxidative capacity of the atmosphere may increase since the ozone concentrations become more elevated as the photochemical production increases (higher biogenic emissions, perhaps shorter chemical lifetimes of the precursors), and because the residence time in the boundary layer is likely to increase as there is slow subsidence in high pressure cells, and because the main boundary loss term for ozone (dry deposition) becomes less efficient in drought due to the closing of plant stomata under drought stress.

Also based on the NCEP reanalysis data, but with a different regional climate model and emission scenario, scientists (Meehl and Tebalki, 2004) arrive at similar conclusions as that of Pal et al. (2004). Heat waves are in general associated with specific atmospheric circulation patterns represented by semi-stationary 500 hPa positive height anomalies that dynamically produce subsidence, clear skies, warm-air advection and prolonged hot conditions at the surface (Meehl and Tebalki, 2004). Drought often ensues at the surface, intensifying the heat wave. In a "business-as-usual" emission scenario, the mean base state change for future climate shows 500-hPa height anomalies of about 50 geopotential metres over France for the end of the 21st century, and the 500-hPa increase over the Mediterranean (and over Southern United States as well) for future climate are directly associated with more intense heat waves in those regions. The 500-hPa height anomalies over the Mediterranean are shown to be most strongly related to positive warm season precipitation anomalies over the Indian monsoon region and positive convective anomalies that come with it that drive mid-latitude teleconnection patterns in response to anomalous tropical convective heating in future climate (Meehl and Tebalki, 2004). The Indian Ocean has warmed more than any other ocean basin (Kerr, 2003). These calculations are in support of the link between the Indian subcontinent monsoon and the probability of drought in the Eastern Mediterranean and drought in the Sahel with implications for higher loading of both natural mineral dust and man made particles over the Mediterranean basin.

The link between climate change and the air pollution loading over the Mediterranean has been elaborated also in the literature. It was found that by forcing a climate model with the maximum and minimum monthly mean observed Mediterranean Sea surface temperatures large precipitation reductions of 10% to 50% in the Mediterranean region, the Middle East and the Eastern Sahel were seen (Lelieveld et al., 2002). The difference between the maximum and minimum

sea surface temperature in the Mediterranean was taken as an approximation to the upper limit of the aerosol surface cooling effect during the past decades; the aerosol radiative forcing over the summertime Mediterranean is among the highest in the world (as much as 18 W/m^2). Drought in Eastern Sahel coincides with maximum sulphate forcing over the Mediterranean (Lelieveld et al., 2002). As shown, intensified Indian subcontinent monsoon over a warmer Indian Ocean reduces precipitation over Eastern Sahel and Eastern Mediterranean, reducing the scavenging of sulphate and increasing the mineral dust fraction of PM (Meehl and Tebalki, 2004).

From the above it is evident that Southern Europe is characterised with large changes over the past few decades linked to a large increase in population, and land-use alterations. The above changes have had an impact on the atmospheric composition and consequently on the quality of life, including possible impact on human health (European Commission, 2001). Human-induced forcing in the Mediterranean area is an increasing problem with complex consequences to quality of life and effects on radiative climate forcing as discussed above. In addition, regional climate change in Southern Europe may have an effect on atmospheric composition and air quality standard violations in these areas.

Notably, there is scarce information concerning continuous aerosol measurements studies to reveal the atmospheric composition and variability of particulate matter (PM) and its contribution to air quality and human health in the Mediterranean area. On this basis continuous aerosol measurements were started during 2003 at the Akrotiri research monitoring station on the island of Crete (Greece). In the current study the focus is on the ambient levels of PM_{10} and $\text{PM}_{2.5}$ and the influence of African dust outbreaks on the particulate matter concentration.

Particulate matter measurements (PM_{10} , $\text{PM}_{2.5}$) were performed at the Akrotiri research station (April 2003-June 2005) on the island of Crete in combination with statistical and back trajectory analysis. The aerosol concentration at the Akrotiri station shows a large variability during the year. Regional transport contributes significantly to the aerosol concentration levels, whereas low aerosol concentrations were observed during storm episodes. Elevated concentrations were observed during Saharan dust events. The PM_{10} concentration was equal to $35.10 \pm 17.85 \mu\text{g/m}^3$ whereas the $\text{PM}_{2.5}$ concentration was equal to $27.11 \pm 10.81 \mu\text{g/m}^3$. The concentration of particulate matter undergoes a seasonal change characterised by higher concentration during summer (PM_{10} : $38.84 \pm 10.40 \mu\text{g/m}^3$; $\text{PM}_{2.5}$: $27.84 \pm 8.47 \mu\text{g/m}^3$) than during winter (PM_{10} : $28.71 \pm 11.35 \mu\text{g/m}^3$).

2.2 Methodology

PM_{10} and $\text{PM}_{2.5}$ were measured at the rural site Akrotiri, which is situated on the island of Crete (Greece). The station ($35^{\circ}31\text{N}$, $24^{\circ}03\text{E}$) is a coastal site eastward of Chania at an elevation of 180 m. PM_{10} was sampled during the period 15.04.03-10.03.04, whereas $\text{PM}_{2.5}$ was sampled during the period 10.03.04-30.06.05.

The region of interest includes parts of Southern Greece, which is a typical marine environment characterized by a large number of islands. The main urban and

industrial areas in this region are located along the coast of the Greek mainland. The region is characterized by a complicated topography combined with strong winds and long sunny and humid periods.

Concentrations of PM₁₀, PM_{2.5}, O₃ and meteorological variables are continuously measured at the Akrotiri station. Levels of PM₁₀ and PM_{2.5} are measured using an automatic beta radiation attenuation monitor (FH 62 I-R). The monitoring period for the wind direction and the speed data started on the 15 April 2003, whereas the temperature and humidity measurements started on the 4 January 2003.

The particulate matter measurements show that the seasonal evolution of PM₁₀ was characterized by a summer maximum. This is consistent with the majority of rural environments in the Mediterranean region (Rodriguez et. al, 2002).

High PM₁₀ concentrations, as shown in Figure 2.1, were also associated with elevated O₃ levels at the station during regional transport from Central Europe. In general, strong NW winds were dominant during the year, which gave rise to elevated concentration of particulate matter on a regional scale. In particular, between 15.11.03-05.12.03 the regional transport component dominates.

To detect the real structure of the dust episodes in time, the whole time series of PM₁₀ concentrations is presented. As can be seen in Figure 2.1, many dust episodes are temporally very short. Still the data reveal that high aerosol concentrations were observed during the whole measurement period with an average concentration for October 2003 and February 2004 equal to 45.8 µg/m³ and 40 µg/m³, respectively. The reason for the elevated concentrations during these two months was the outbreak of a number of Saharan dust episodes.

From 10.03.04 to 30.06.05 PM_{2.5} measurements were performed using the same automatic beta attenuation monitor with a PM_{2.5} pre-impactor. The daily average concentrations are shown in Figure 2.2.

The average PM_{2.5} concentration during the measurement period was 27.11 µg/m³. There were three periods in which the PM_{2.5} concentration reached high values (up to several hundred µg/m³), all which correspond to Saharan dust episodes. On the 27.03.04 the average concentration was 73.8 µg/m³, on the 01.05.04 the concentration was 64.5 µg/m³, and on the 05.05.04 the concentration reached 98.4 µg/m³. The last Saharan dust episode was very intense with a considerable reduction in the visibility. At 09:00 h on 05.05.04 the PM_{2.5} concentration reached 364 µg/m³.

The time series of data available for the PM_{2.5} concentrations are presented in Figure 2.3. In general, the Saharan dust episodes do not last very long, although with some exceptions (e.g. 05.05.04). During dust episodes it is evident that the PM_{2.5} levels are affected by the Saharan intrusion. This is in agreement with similar observations reported in the literature (Rodriguez et al., 2004). The lowest observed PM_{2.5} value reported for the measurement period was 12.25 µg/m³ (25.03.04). The air masses, which reached the Akrotiri station on this date, originated from the West Mediterranean Sea. Figure 2.4 shows the monthly mean concentration of PM_{2.5} for the period March 2004-June 2005.

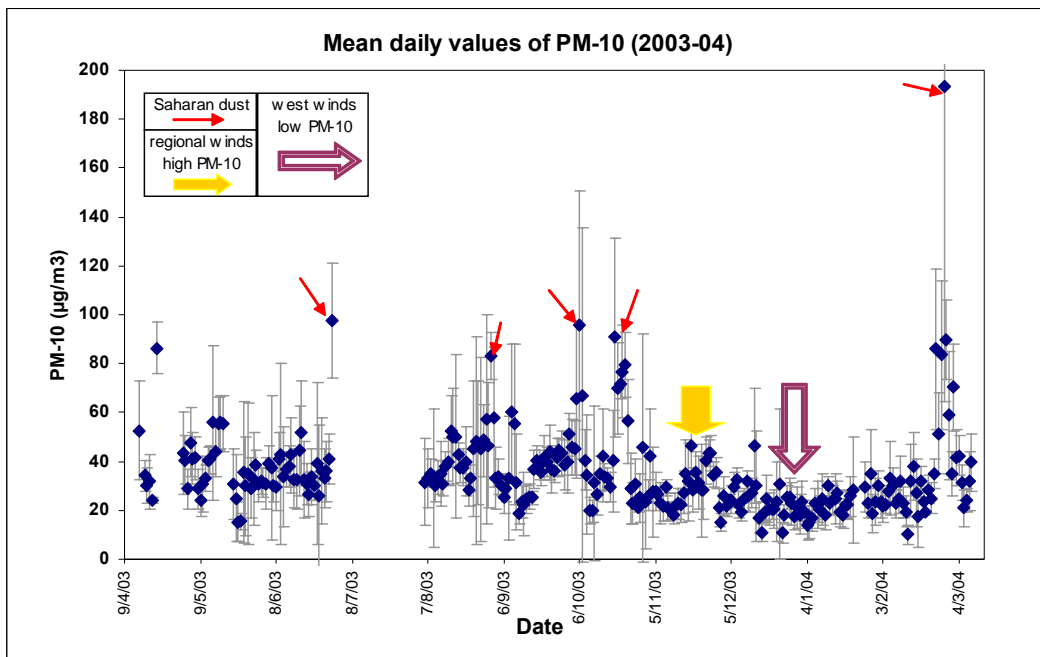


Figure 2.1: Daily mean PM₁₀ concentrations at the Akrotiri research station between 09.04.03-04.03.04.

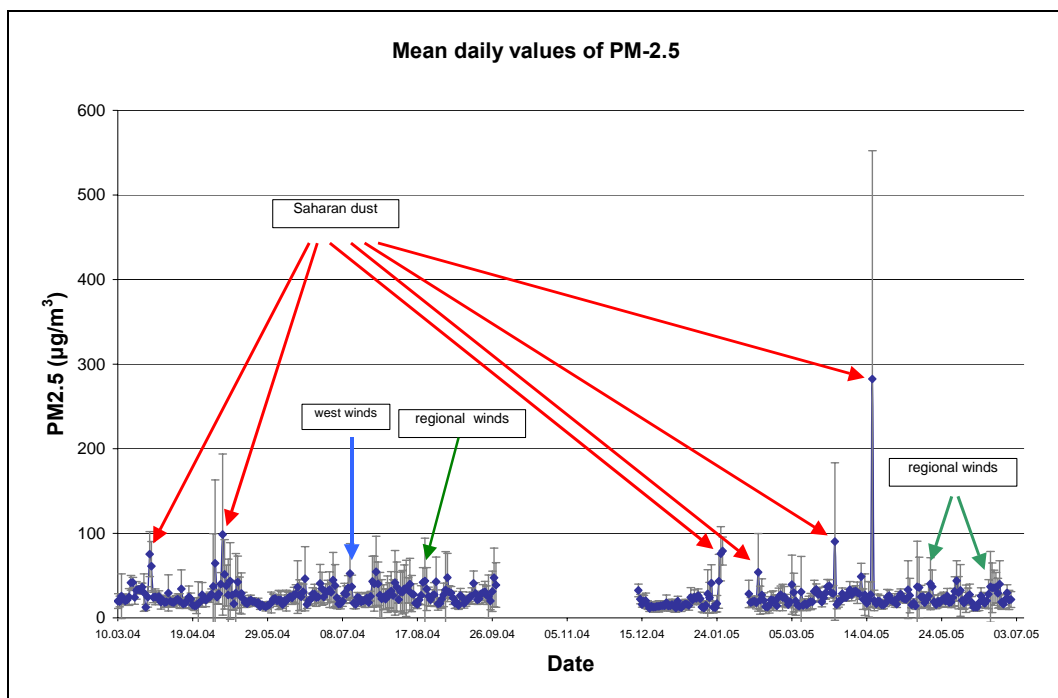


Figure 2.2: Daily mean PM_{2.5} concentrations between 10.03.04-30.06.05.

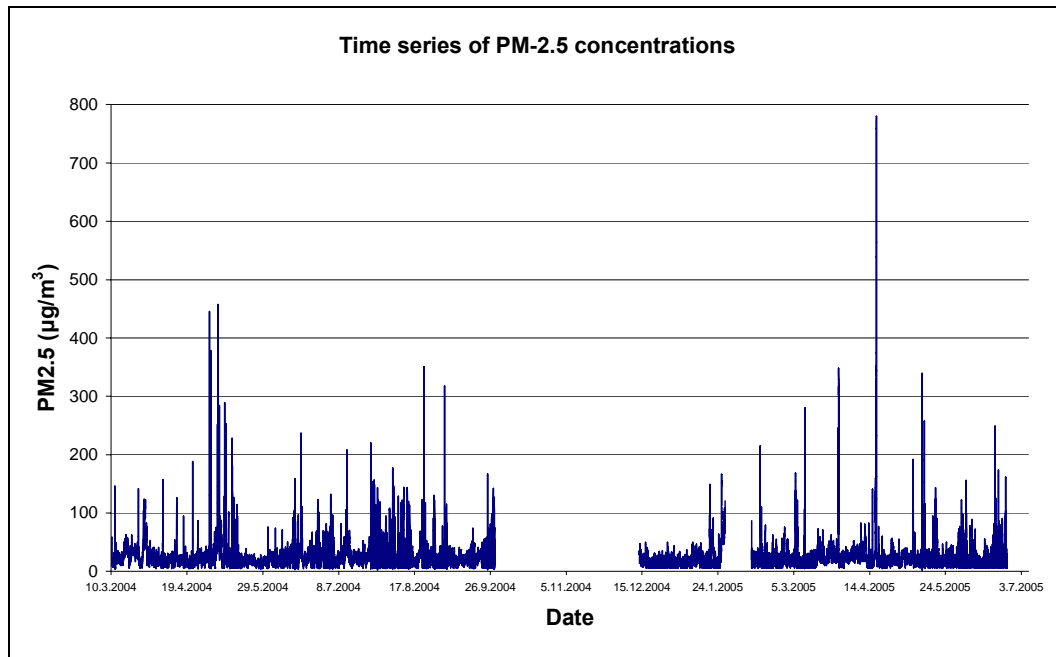


Figure 2.3: Time series of PM_{2.5} concentrations (all data available for Akrotiri, 10.03.04-30.06.05).

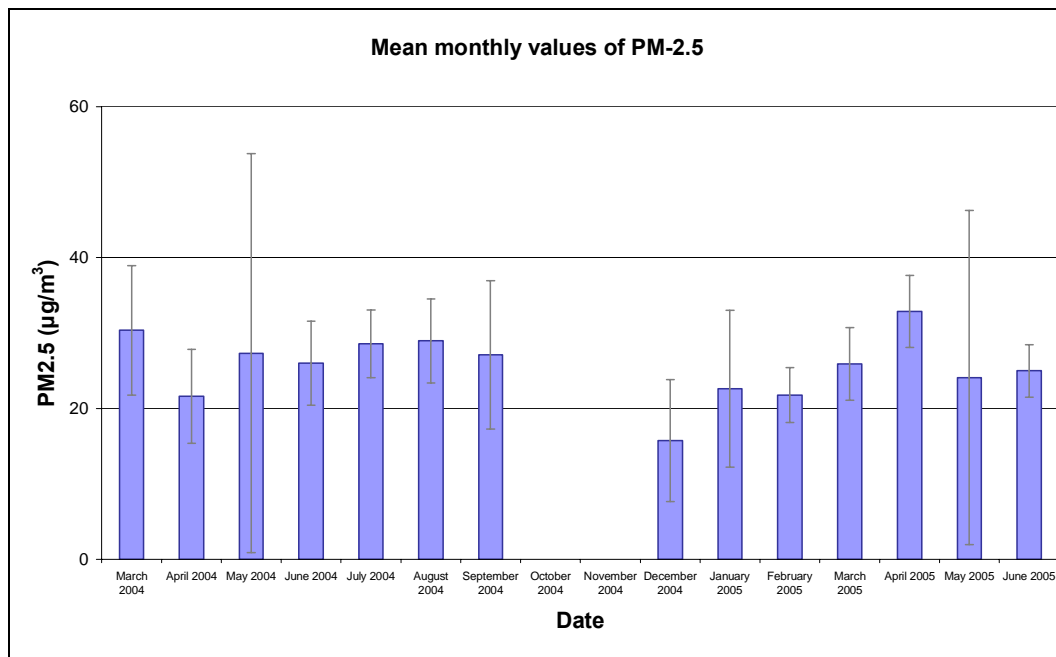


Figure 2.4: Monthly mean PM_{2.5} concentrations during March 2004-June 2005 at the Akrotiri research station (Crete, Greece).

2.3 Number concentration measurements

Condensation particle counter (CPC) (Grimm CPC 5403) measurements of aerosol number concentration were performed during the period from 22.06.05 until 30.06.05. The particle counter was used to gain first insight into the particle number concentration together with the particle mass concentration. In continuation of the aerosol particle measurements at the Akrotiri station the CPC will be equipped with a DMA (Differential Mobility Analyser) tube to form a SMPS (scanning mobility particle sizer) for particle size distribution measurements.

Figure 2.5 shows the measurements of aerosol particle mass ($PM_{2.5}$) (Figure 2.5a) and number concentrations for the same time period (Figure 2.5b). There is no general correlation between the mass concentration and total particle number concentration.

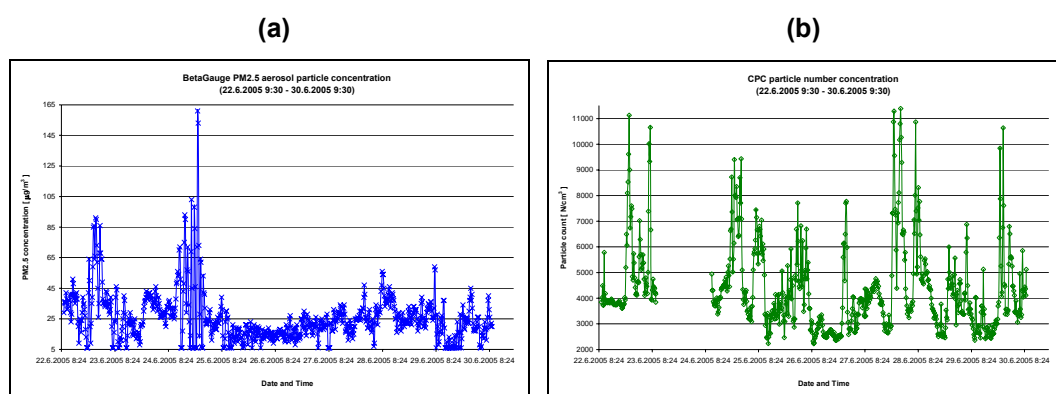


Figure 2.5: Particulate matter measurements between 22.06.05-30.06.05.
(a) mass concentration of $PM_{2.5}$, (b) number size distribution data.

Higher night values (from 20:00 until 1:00) and morning values (around 7:00 and 8:00) is probably due to increased local traffic. Some of the high peaks on the CPC time slope early in the morning can also be induced by the nucleation of very small particles due to photochemical reactions. Some of these high peaks cannot be seen on Beta gauge time slope.

Back trajectory calculations show that the peaks on the CPC time slope are not influenced by aerosol transport from areas with high aerosol mass concentration. Rather do the air masses tend to originate from north during these occasions.

2.4 Analysis of the Particulate Matter Concentration Sources

The origin of the $PM_{2.5}$ concentrations on the Akrotiri station was studied using a statistical analysis of the data and back trajectory modelling. Trajectories were obtained using the HYSPLIT4 Model, developed by the Air Resources Laboratory of the National Oceanic and Atmospheric Administration (NOAA) (NOAA, 2002; Draxler, 1994). The 3-dimensional trajectories were computed for the coordinates 35.53N, 24.06E, which are the coordinates of the Akrotiri region, for 12:00 am for each day of measurements. The trajectories were 120h (5 days) long. The wind data were retrieved from NOAA and had a time resolution of 6 hours and spatial resolution of 191 Km.

Back trajectory analysis for the Akrotiri research station is shown in Figure 2.6. Figure 2.6a shows that the air masses on the 05.05.04 passed over Northern Africa whereas in Figure 2.6b it can be seen that the air masses on the 25.03.04 came from the west. The 05.05.04 is a day with very high $PM_{2.5}$ concentration values due to a Saharan dust episode (24h mean for $PM_{2.5}$, $98.4 \mu\text{g}/\text{m}^3$, maximum concentration $364 \mu\text{g}/\text{m}^3$). At the 25.03.04, the lowest $PM_{2.5}$ concentration for the whole measurement period was observed (average 24h $PM_{2.5}$ concentration $12.25 \mu\text{g}/\text{m}^3$). This can be explained by the fact that the air masses originated from the Atlantic Ocean and that they mainly passed over the Mediterranean Sea before they arrived at/passed over the Akrotiri station. Figure 2.6c shows the regional transport of air masses from Central Europe, which passes the Attica region leading to elevated concentration of $PM_{2.5}$ ($44.65 \mu\text{g}/\text{m}^3$).

For the first four months of 2005 four peaks of $PM_{2.5}$ can be seen. For the first peak (26.02.05) the air masses passed over Northern Africa close to the ground for more than 72 h prior to coming over the Akrotiri station (average 24h $PM_{2.5}$ concentration $81.3 \mu\text{g}/\text{m}^3$, maximum value $166 \mu\text{g}/\text{m}^3$) (Figure 2.7a). In Figure 2.7b it can be seen that the air masses passed over Scandinavia and Western Europe before they passed over Northern Africa and finally arrived Akrotiri (average 24h $PM_{2.5}$ concentration $79.0 \mu\text{g}/\text{m}^3$, maximum value $121 \mu\text{g}/\text{m}^3$).

Such comments we can do for the next two peaks on the 15.02.05 (average 24h $PM_{2.5}$ concentration $53.77 \mu\text{g}/\text{m}^3$, maximum value $215 \mu\text{g}/\text{m}^3$) and on the 28.03.05 (average 24h $PM_{2.5}$ concentration $93.0 \mu\text{g}/\text{m}^3$, maximum value $348 \mu\text{g}/\text{m}^3$) where air masses were coming from North Africa (Figure 2.8).

Finally, the 17.04.05 was a day with very high $PM_{2.5}$ concentration values due to a Saharan dust episode (average 24h $PM_{2.5}$ concentration $282.4 \mu\text{g}/\text{m}^3$, maximum value $780 \mu\text{g}/\text{m}^3$). The air masses passed over Northern Africa close to the ground for more than 36 h prior to coming over the monitoring station.

A statistical analysis has been performed using the back-trajectory data for each day of the measurement period, constructing maps for the origin of the air masses. Four sectors have namely used the north-west (NW), north-east (NE), south-west (SW) and south-east (SE) directions.

Each trajectory was divided into five segments. Each segment was assigned to one of the sectors mentioned before. Finally, the length of each bar shown in the map, is proportional to the frequency of each wind sector from which the air masses origin. The colour of the bars shows particulate matter levels of the air originating from each sector.

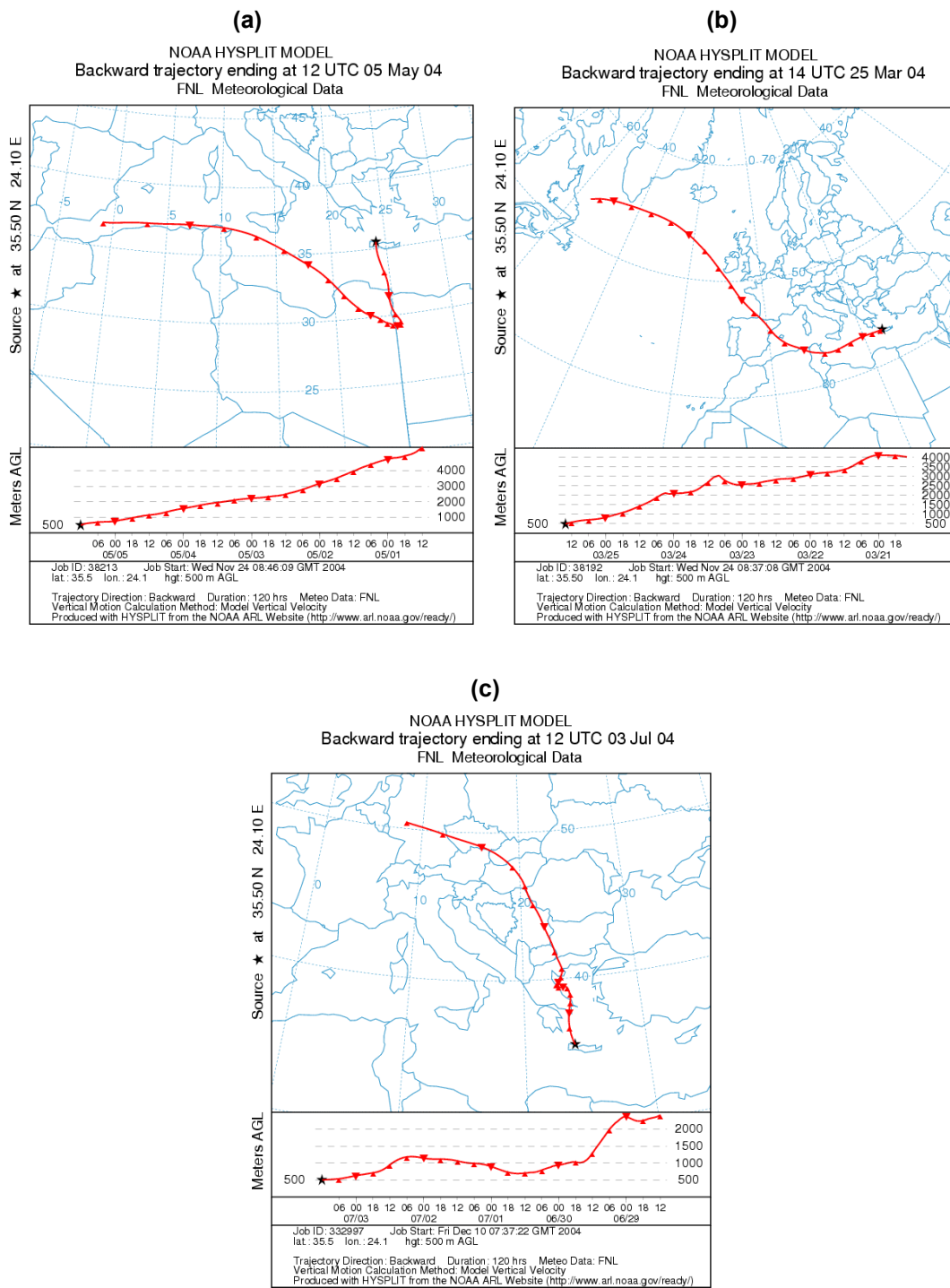


Figure 2.6: Back trajectories calculated by the HYSPLIT4 Model (NOAA, 2002) for (a) 5 May 2004, (b) 25 March 2004, (c) 3 July 2004.

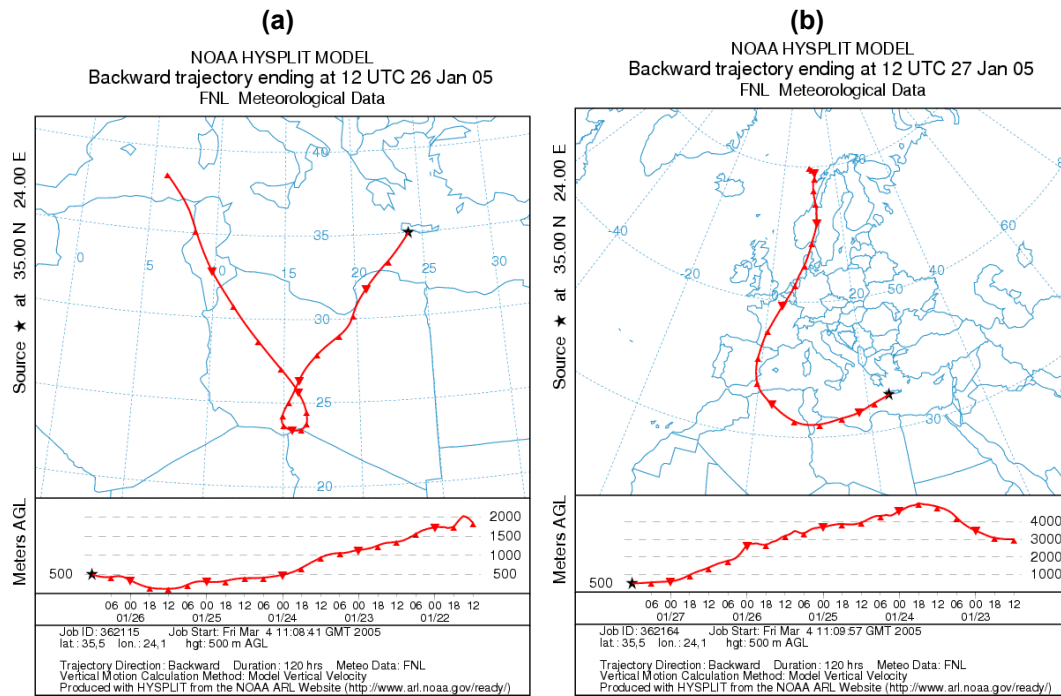


Figure 2.7: Back trajectories calculated by the HYSPLIT4 Model (NOAA, 2002) for (a) 26.01.05, (b) 27.01.05.

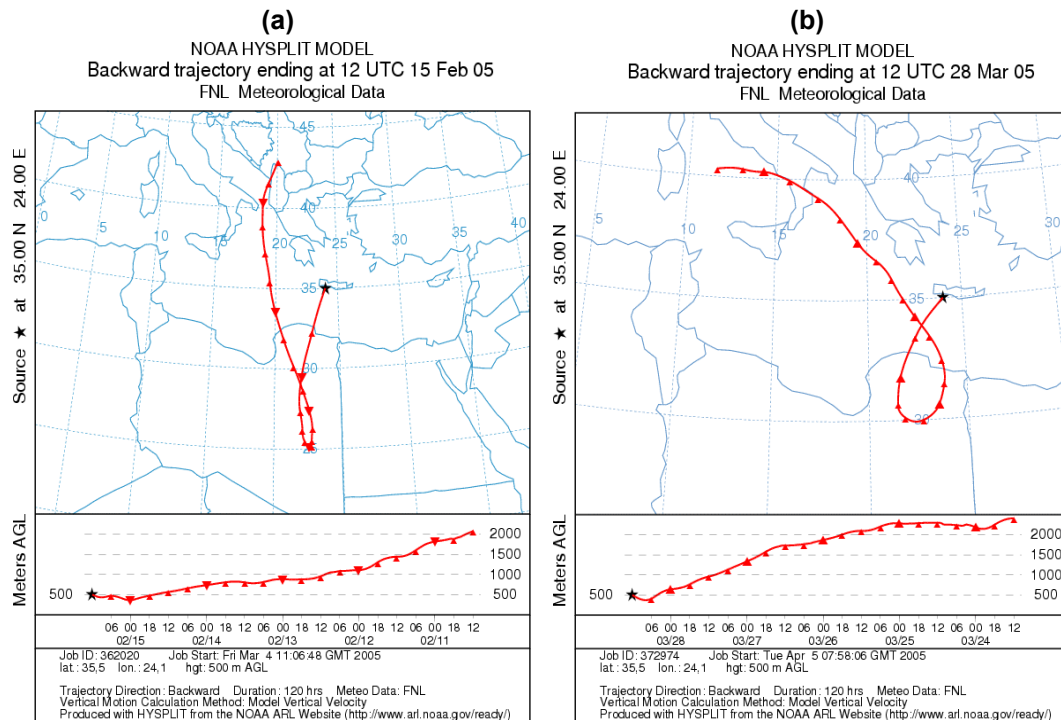


Figure 2.8: Back trajectories calculated by the HYSPLIT4 Model (NOAA, 2002) for (a) 15.02.05, (b) 28.03.05.

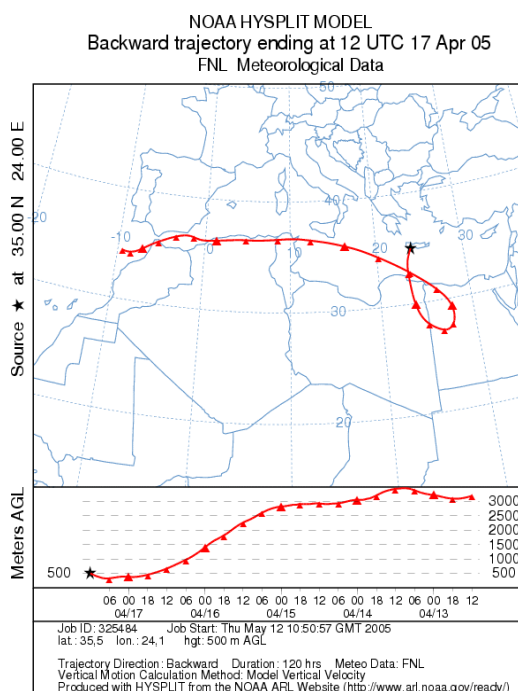


Figure 2.9: Back trajectories calculated by the HYSPLIT4 Model (NOAA, 2002) for 17.04.05.

Figure 2.10 and Figure 2.11 show the frequency distribution of the $PM_{2.5}$ concentration at the Akrotiri research station during spring 2004 and summer 2004, respectively. The $PM_{2.5}$ concentrations originating from the southerly directions were in general higher (for example for spring 2004, SE: $32.3 \mu\text{g}/\text{m}^3$, SW: $40.1 \mu\text{g}/\text{m}^3$) than from the northerly directions (NW: $24.0 \mu\text{g}/\text{m}^3$, NE: $21.6 \mu\text{g}/\text{m}^3$), whereas the corresponding figures for the northerly directions was $24.0 \mu\text{g m}^{-3}$ for NW and $27.6 \mu\text{g m}^{-3}$ for NE.

From the analysis made, major differences in episodicity were detected, comparing southerly and northerly directions. The frequency and length of dust episodes in the area of Akrotiri were increased when the air masses originated from southern directions and especially from the Saharan desert. Based on the $PM_{2.5}$ measurements made, it is shown that the high aerosol concentrations occur during specific short time intervals (1-3 days) in situations with southerly winds having passed over North Africa. When the air masses originated from the NW and NE, the PM levels were lower. However, elevated concentrations at the Akrotiri station occur during transport from the north when the air masses pass over the European continent.

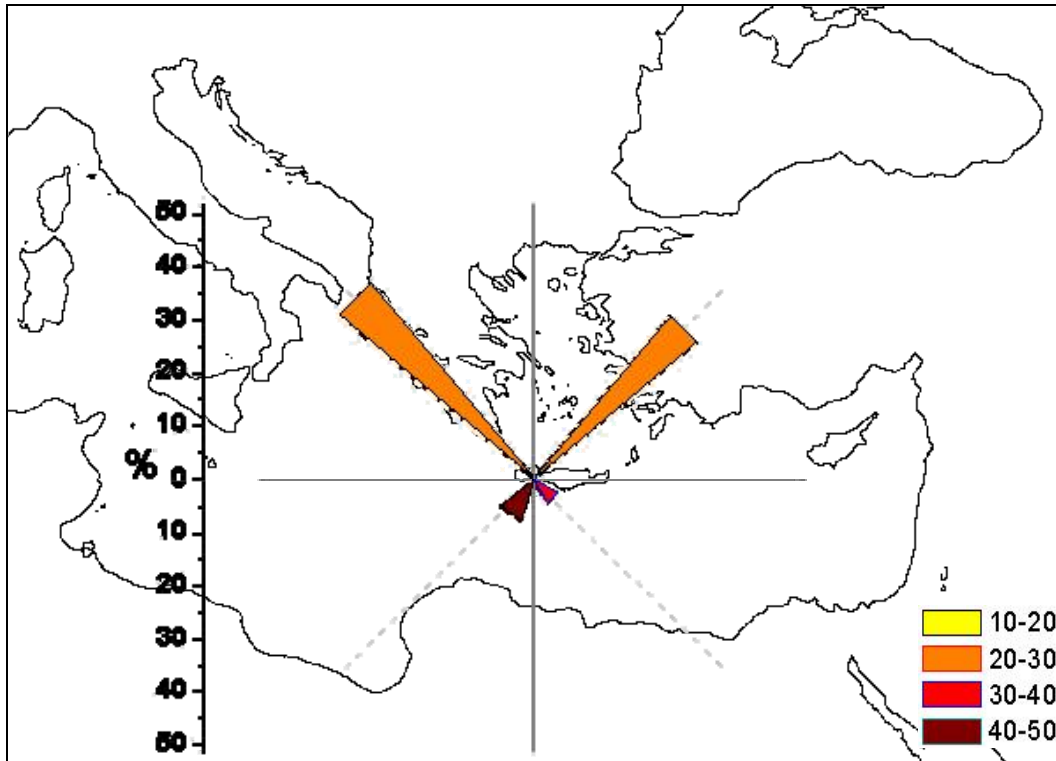


Figure 2.10: Origin of the air masses and corresponding average $PM_{2.5}$ concentration ($\mu\text{g}/\text{m}^3$) for the spring 2004 period.

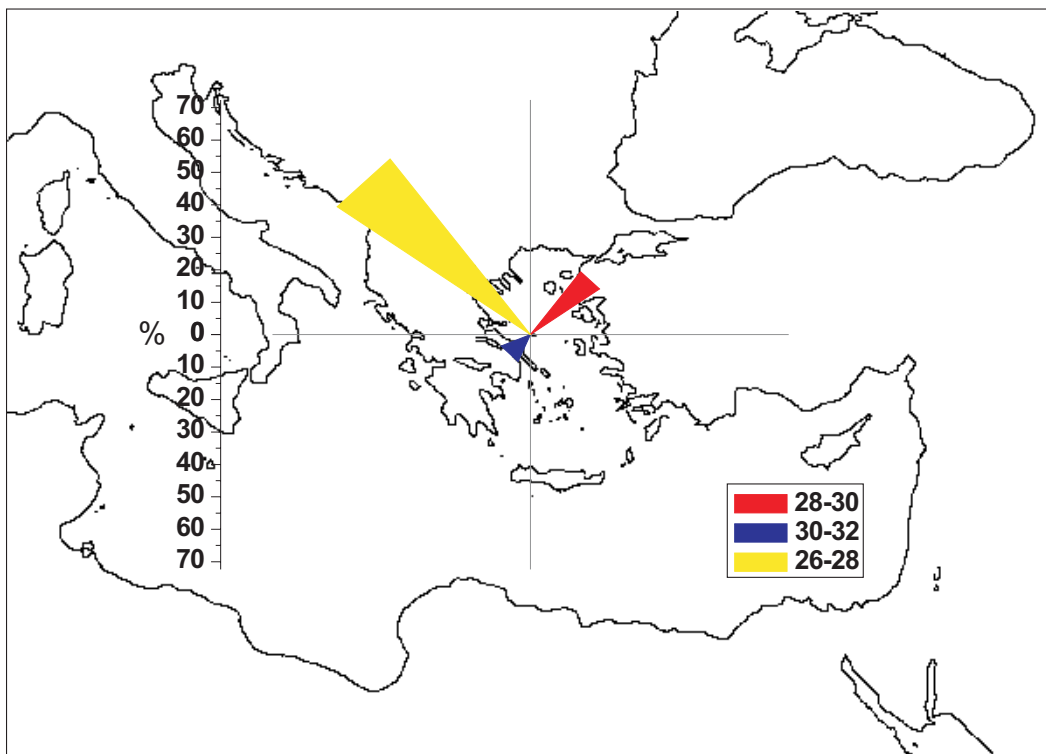


Figure 2.11: Origin of the air masses and corresponding average $PM_{2.5}$ concentration ($\mu\text{g}/\text{m}^3$) for the summer 2004 period.

2.5 Conclusions

The ambient PM₁₀ and PM_{2.5} concentrations at the Akrotiri research station on Crete (Greece) show a large variability with elevated concentrations during Saharan dust episodes, whereas low PM₁₀ and PM_{2.5} concentrations occurred during winter storms and when air masses originated from the western parts of the Mediterranean Sea and the Atlantic Ocean.

Transport from the Greek mainland and the European continent contributes significantly to the particulate matter levels in the area since the prevailing wind direction is northerly throughout the year. The particulate matter concentrations at Akrotiri during transport from northerly direction are elevated, but considerably lower than the concentrations during outbreaks of African dust.

The EU annual average PM₁₀ standard of 40 µg/m³ is not exceeded in the area. The EU 2010 annual average PM₁₀ standard of 20 µg/m³ is, however, exceeded. Besides, the US-EPA annual average PM_{2.5} standard of 15 µg/m³ is exceeded in the area.

3. Levels and relative contributions of water-insoluble organic carbon and water-soluble organic carbon at rural background sites in Europe

by K.E. Yttri and M.C. Facchini

3.1 Introduction

The organic carbon fraction of ambient aerosols contains a high number of individual organic compounds. Thus, a full characterization of this carbonaceous subfraction on the molecular level for the purpose of mass-closure is an insurmountable task. This great diversity has necessitated the implementation of operational definitions for bulk fractions of the carbonaceous material, such as elemental carbon (EC) and organic carbon (OC). At present, EC and OC are commonly reported in literature, although the wide range of different analytical techniques applied, and the lack of standardized sampling procedures, introduce a significant level of uncertainty to the results obtained.

The OC fraction is commonly separated according to its solubility in water. This extraction step is easily performed as an extension of the analysis of EC and OC, and provides additional information about the carbonaceous fraction without having to invest too much extra work. The resulting subfractions provided by the water-extraction, being water-insoluble organic carbon (WINSOC) and water-soluble organic carbon (WSOC), are of interest for a number of reasons: Firstly, WSOC seems to influence the ambient aerosols ability to act as cloud condensation nuclei (CCN) (Novakov and Corrigan, 1996), and it contributes to the aqueous phase chemistry in clouds and fogs. Secondly, more detailed knowledge concerning which are the constituents of the WINSOC and the WSOC fractions, including their chemical and physical properties, will contribute to clarify if any negative health effects can be associated with these carbonaceous subfractions. Furthermore, it will add to the present knowledge of the chemical composition of the tropospheric aerosol and its sources. Finally, dividing OC into WSOC and WINSOC will provide more accurate estimates of the concentrations of carbonaceous matter in the atmosphere. This is particularly important, as the carbonaceous mass of ambient aerosols probably will become even more important in the future, as the abatement strategies for NO_x and SO_x will reduce the concentrations of precursors of the inorganic components constituting the inorganic aerosol mass.

As the thermal optical analysis only accounts for the carbon content of the organic constituents of the aerosol, a conversion factor converting levels of OC ($\mu\text{g C m}^{-3}$) to levels of organic matter (OM) ($\mu\text{g m}^{-3}$) is needed in order to account for the oxygen, hydrogen, nitrogen and sulphur associated with the molecules. This conversion step is recognized as one of the most important uncertainty factors in mass closure calculations. In a recent study, Turpin and Lim (2001) reevaluated the commonly used conversion factors applied both for urban and rural areas, ranging from 1.2-1.4 (Gray et al., 1986). Their study indicates that a ratio of 1.6 ± 0.2 is a better estimate for urban aerosols. The reason for this increase can be attributed to the increased focus on the highly oxidized secondary organic aerosols, as well as the polyhydroxy compounds associated with primary

biological aerosol particles. Furthermore, conversion factors of 1.9-2.3 were suggested for aged aerosols, whereas conversion factors of 2.2-2.6 were suggested for aerosols originating from biomass burning. In the study by Turpin and Lim (2001), ratios of molecular weight per carbon weight for less water-soluble organic compounds (water solubility < 1 g solute per 100 g water) ranging from 1.1-2.1, and for more water-soluble organic compounds (water solubility > 1 g solute per 100 g water) ranging from 1.5-3.8, were listed. The great difference between the ratios of these two operationally defined groups emphasizes the importance of WSOC and WINSOC data for ambient aerosols. By segregating between WSOC and WINSOC in mass closure studies, and by using conversion factors specific for each of these carbonaceous subfractions, more accurate concentrations of the OM can be obtained. In addition, estimates of water-soluble organic material (WSOM) and water-insoluble organic matter (WINSOM) are provided. However, it has to be recognized that the uncertainties associated with the conversion factors for WINSOC and WSOC still could bias the results.

In the present study, concentrations of WSOC and WINSOC are reported for 13 European rural background sites. Furthermore, levels of water-soluble organic matter (WSOM) and water-insoluble organic matter are calculated. Finally, a comparison of different ways to calculate OM is reported.

3.2 Aerosol sampling

The ambient aerosol content of WINSOC and WSOC was quantified using filter samples collected during the EMEP EC/OC campaign, conducted during the period 1 July 2002–1 July 2003. Table 3.1 provides an overview of the sampling sites included in the campaign, their site category and the sampling equipment used. Aerosol sampling was performed using CEN (European Committee for Standardization) approved or equivalent PM₁₀ samplers, collecting one 24h sample every week (starting Tuesday mornings). Samples were collected on pre-baked quartz fibre filters. The filters content of PM₁₀, elemental carbon, organic carbon and total carbon have been reported previously (Yttri and Kahnert, 2004). The level of levoglucosan has been quantified for a selected number of the filter samples (Chapter 4, this report). A total of 71 samples from 13 of the 14 sites included in the campaign were analysed with respect to WINSOC and WSOC.

Table 3.1: *Sampling sites in the EMEP EC/OC campaign, their site category and sampling equipment used.*

Country	Sampling site	Site category	Aerosol sampler	Filter size	Flow rate
Austria	Illmitz (AT02)	Rural Background	Partisol	47 mm	16.7 l min ⁻¹
Belgium	Ghent (BE02)	Urban Background	Gent Filter Unit	47 mm	17 l min ⁻¹
The Czech Republic	Košetice (CZ03)	Rural Background	FH 95 SEQ	47 mm	38 l min ⁻¹
Finland	Virolahti (FI17)	Rural Background	KFG	47 mm	38 l min ⁻¹
Great Britain	Penicuik (GB46)	Rural	Partisol	47 mm	16.7 l min ⁻¹
Germany	Langenbrügge (DE02)	Rural Background	Hi-Vol (Digitel)	150 mm	500 l min ⁻¹
The Netherlands	Kollumerwaard (NL09)	Rural Background	KFG	47 mm	38 l min ⁻¹
Ireland	Mace Head (IE31)	Rural Background	KFG	47 mm	38 l min ⁻¹
Italy	Ispra (IJRC) (IT04)	Near-city	KFG	47 mm	38 l min ⁻¹
Italy	San Pietro Capofiume (S.P.C) (IT08)	Urban Background	Gent Filter Unit	47 mm	17 l min ⁻¹
Norway	Birkenes (NO01)	Rural Background	KFG	47 mm	38 l min ⁻¹
Portugal	Braganza (PT01)	Rural Background	Hi-Vol (Sierra)	8 x 10 inch	1133 l min ⁻¹
Sweden	Aspvreten (SE12)	Rural Background	Gent Filter Unit	47 mm	17 l min ⁻¹
Slovakia	Stara Lesna (SK04)	Rural Background	Partisol	47 mm	16.7 l min ⁻¹

3.3 Quantification of water-insoluble organic carbon and water-soluble organic carbon

Before analysis, parts of each filter were soaked in Milli-Q water (7 ml for low volume filters and 20 ml for high volume filters) and subjected to sonication (30 min) for extraction of the water-soluble organic material. The dissolved organic material was then quantified using a Shimadzu TOC liquid analyzer (model TC5000A). The determination of WINSOC and WSOC was performed at the Institute of Atmospheric Sciences and Climate of the Italian National Research Council (ISAC-CNR).

3.4 Concentrations of WINSOC and WSOC and their relative contribution to OC

The concentrations of WSOC and WINSOC at the sites investigated are shown in Table 3.2. It should be noted that the samples are not collected on the same dates, which complicates the comparison of the concentrations obtained at the different sites. Further, there are an unequal number of samples collected during summer and winter (Table 3.2). Still, the results reported represent a snapshot of which concentrations of WINSOC and WSOC can be encountered at the sites investigated.

The lowest mean concentration of both WINSOC (0.6 $\mu\text{g C m}^{-3}$) and WSOC (0.1 $\mu\text{g C m}^{-3}$) was reported for the Irish site. The highest concentration for WINSOC was reported for the Italian site San Pietro Capofiume (4.9 $\mu\text{g C m}^{-3}$), whereas the highest concentration of WSOC was reported for the Italian site Ispra (3.6 $\mu\text{g C m}^{-3}$).

Table 3.2: Concentrations of WSOC and WINSOC in PM_{10} , and relative contribution of WSOC and WINSOC to OC in PM_{10} .

Site	Number of samples	Samples Winter : Summer	WSOC ($\mu\text{g C m}^{-3}$)	WINSOC ($\mu\text{g C m}^{-3}$)	WSOC/OC (%)	WINSOC/OC (%)
AT02	n = 5	3 : 2	2.9	3.5	41	59
BE02	n = 4	2 : 2	2.2	3.2	41	59
CZ03	n = 6	6 : 0	1.2	2.5	33	67
DE02	n = 11	6 : 5	1.4	1.7	46	54
GB46	n = 5	5 : 0	0.3	0.7	31	69
IE31	n = 4	2 : 2	0.1	0.6	17	83
IT04	n = 5	3 : 2	3.0	4.9	38	62
IT08	n = 5	3 : 2	3.6	3.7	49	51
NL09	n = 3	2 : 1	1.5	1.5	49	51
NO01	n = 4	4 : 0	0.8	0.7	52	48
PT01	n = 11	6 : 5	1.5	1.1	57	43
SE12	n = 4	2 : 2	0.8	1.2	40	60
SK04	n = 4	2 : 2	1.9	4.3	30	70

WINSOC was the dominant subfraction at all sites investigated, except at the Norwegian and the Portuguese sites, ranging from 43 – 83% of OC (Table 3.2 and Figure 3.1). The highest relative contribution of WINSOC was observed at the Irish site (Mace Head), accounting for 83% of the OC. This finding is in accordance with what has been reported by Krivácsy et al. (2001), finding that WINSOC was the major carbonaceous subfraction at Mace Head, accounting for 59% of OC. In their study, the high relative contribution of WINSOC was related to the less oxidative atmosphere over oceans. Furthermore, the higher frequency of cloud formation over oceans reduces the residence time of the water-soluble compounds in the marine environment compared to the continental environment. It has been suggested that primary biological aerosol particles contributes to the WINSOC material observed at Mace Head (Kleefeld et al., 2002), and that these particles are derived from microorganisms accumulating in the surface layer of the ocean, which are injected into the atmosphere during the formation of jet-drops.

A high relative contribution of WINSOC can also be expected at sites situated close to urban areas due to the impact of emissions from vehicle exhaust. Low WSOC/OC ratios have been reported for several sites influenced by traffic; a ratio of 12.5% (Ruellan and Cachier, 2001) and ratios between 14% and 26% (Mader et al., 2004) have been reported for curbside sites. The most likely explanation for this is low levels of polar oxygenated compounds in vehicular exhaust and the short distance from the source to the sampling site, which leaves little time for oxidation of aerosols and precursor compounds. WINSOC is quite clearly the dominant carbonaceous subfraction at the UK site (69%), the Italian site Ispra (62%), the Belgian site (59%) and the Austrian site (59%) (Table 3.2 and Figure 3.1), which all are located quite close to major urban areas. However, equally high percentages of WINSOC are reported for the Swedish site (60%), the Czech site (67%) and the Slovakian site (70%) as well, which are sites situated further away from urban areas.

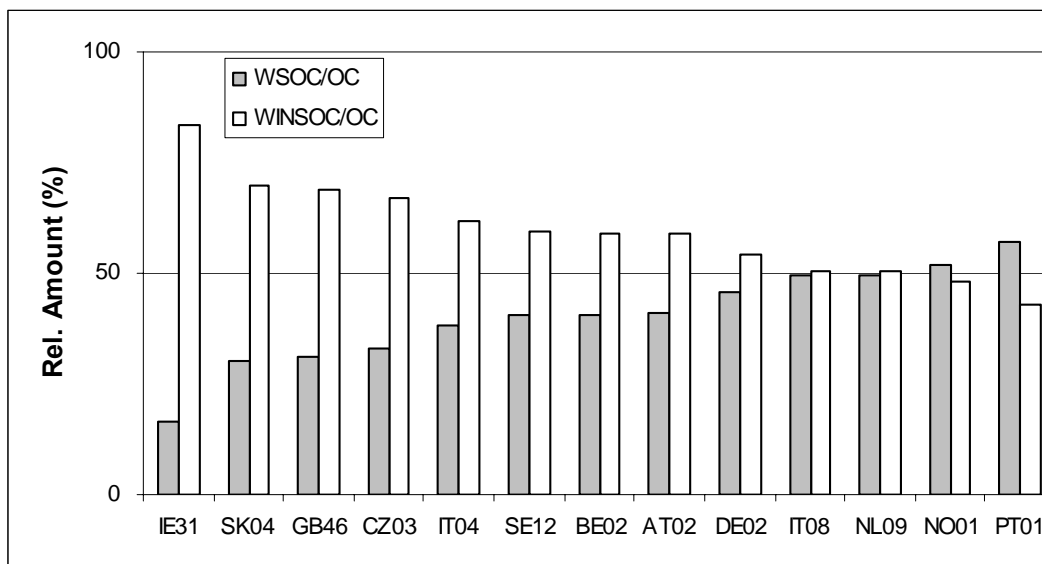


Figure 3.1: Mean WSOC/OC and WINSOC/OC percentages.

The relative contribution of WSOC to OC ranged from 17-57% for the sites investigated (Table 3.2 and Figure 3.1). WSOC was the dominant carbonaceous subfraction at only two of the sites, namely at the Norwegian site (52%) and at the Portuguese site (57%). The major source of particles at the Norwegian site is long-range transported particles. Thus, oxidation of particulate carbonaceous material during long-range atmospheric transport might be a possible explanation for at least a part of the WSOC concentration observed at this site.

Another important source of WSOC is wood burning. Mayol-Bracero et al. (2002) reported that 65% of OC could be attributed to WSOC when studying the chemical composition of aerosols in the Amazon region during the burning season, whereas 77% of OC could be attributed to WSOC in an area heavily influence by residential wood burning in Norway (Yttri et al., 2005a). Indeed, the presence of levoglucosan, which is a tracer of particulate emissions from wood burning, has been demonstrated at all sites participating in the EMEP EC/OC campaign (Chapter 4, this report). Based on ambient aerosol concentrations of levoglucosan, particulate matter originating from wood burning was estimated to account for 1.7-9.0% of the ambient PM_{10} concentration on an annual basis for the sites included in that study. Thus, the relative contribution of WSOC from wood burning to the ambient aerosol content of WSOC is suspected to be substantial. Crude estimates of how much of the ambient aerosol content of WSOC originates from wood burning can be provided combining levels of PM_{Wood} presented in Table 4.1 in Chapter 4 and emission ratios of WSOC from wood burning. Unfortunately, emission ratios of WSOC for wood burning are not readily available, although they can be deduced from studies reported in the literature, such as that of Mayol-Bracero et al. (2002) and Yttri et al. (2005a). Another important source of WSOC is secondary organic aerosols (SOA). Furthermore, highly water-soluble sugars and sugar-alcohols have been associated with primary biological aerosol particles (PBAP) (Graham et al., 2003).

3.5 Ambient concentrations of water-soluble organic matter (WSOM) and water-insoluble organic matter (WINSOM) and their relative contribution to OM

A factor of 2.1 was used to convert WSOC to WSOM, whereas a factor of 1.3 was used to convert WINSOC to WINSOM. The conversion factor used to convert WSOC to WSOM is based on the study by Kiss et al. (2002). To our knowledge their study is the only one who has provided experimentally derived conversion factors for WSOC for a European rural background site (K-puszt). The calculated concentrations of WINSOM and WSOM are presented in Table 3.3. Due to the higher factor used to calculate WSOM compared to WINSOM, the relative contribution of these two subfractions to OM differs from that of WSOC and WINSOC to OC presented in Table 3.2. As can be seen from Table 3.3, WSOM dominates the OM fraction at the majority of the sites, ranging from 24-68%.

Table 3.3: Concentrations of WSOM and WINSOM in PM_{10} , and relative contribution of WSOM and WINSOM to OM in PM_{10} .

Site	WSOM ($\mu\text{g m}^{-3}$)	WINSOM ($\mu\text{g m}^{-3}$)	OM ($\mu\text{g m}^{-3}$)	WSOM/OM (%)	WINSOM/OM (%)
AT02	6.1	4.6	10.7	57	43
BE02	4.6	4.1	8.7	53	47
CZ03	2.6	3.2	5.8	45	55
DE02	3.0	2.2	5.2	58	42
GB46	0.7	1.0	1.7	42	58
IE31	0.2	0.8	1.0	24	76
IT04	6.3	6.4	12.7	49	51
IT08	7.6	4.8	12.4	61	39
NL09	3.2	2.0	5.2	61	39
NO01	1.6	0.9	2.6	63	37
PT01	3.1	1.4	4.6	68	32
SE12	1.7	1.6	3.3	52	48
SK04	3.9	5.6	9.5	41	59

- OM is calculated by according to the following equation: $OM = 2.1 * WSOC + 1.3 * WINSOC$

As previously mentioned, converting OC to OM is recognized as one of the most important factors of uncertainty in mass closure studies. In the present study we have used conversion factors for WSOC and WINSOC instead of for OC to exemplify how this uncertainty can be reduced. The benefit of this approach becomes apparent when considering how the relative contribution of WINSOC and WSOC to OC varies from site to site (Table 3.2) and how great the difference between the conversion factors for these two subfractions are (see introduction). The concentrations of OM provided by this approach, using a factor of 2.1 to convert WSOC into WSOM and a factor of 1.3 to convert WINSOC into WINSOM, is listed in Table 3.3.

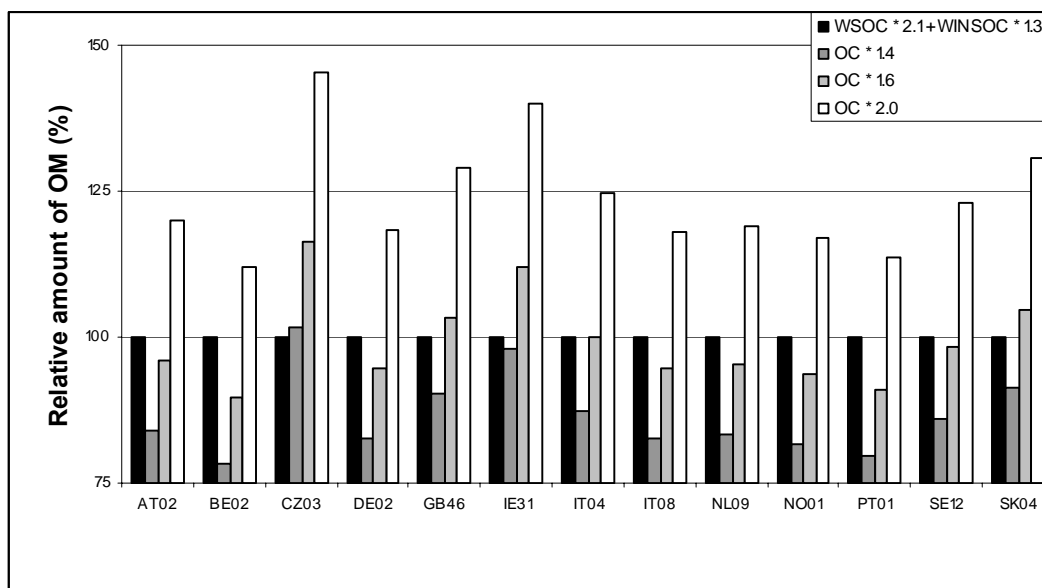


Figure 3.2: Results from calculation of OM by different approaches. The levels of OM obtained by using conversion factors for WSOC (2.1) and WINSOC (1.3) is defined as 100%.

The results presented in Figure 3.2 illustrate the difference obtained by using various approaches to calculate OM. It is assumed that applying conversion factors for subfractions of OC to calculate OM ($OM = WSOC \times 2.1$ and $WINSOC \times 1.3$) currently is the best approach, thus, the results obtained using this method is defined as 100%. Furthermore, OM has been calculated using conversion factors commonly cited and used in the literature, namely 1.4, 1.6 and 2.0. Using a factor of 1.4 generally underestimates the level of OM, accounting for $87\% \pm 7$ (Mean \pm SD) of the reference method for all the sites investigated. The only exception is the Czech site. Moreover, the high relative contribution of WINSOC to OC at the Czech site and at the Irish site actually favors a factor of 1.4 compared to the factors of 1.6 and 2.0. Using a factor of 1.6 both overestimates and underestimates the level of OM depending on the site addressed. Still, the results obtained using this factor comes closest ($99\% \pm 8$) to that of using conversion factors for WSOC and WINSOC. Applying a factor of 2.0 consequently overestimates the level of OM, providing estimates of $124\% \pm 10$ compared to the reference approach. This exercise obviously illustrates the importance of a priori knowledge of which subfractions of OC prevail.

Despite the fact that this approach takes into account the relative contribution of WSOC and WINSOC to OC at the different sites, there are still uncertainties related to the conversion factors applied. Although the conversion factor for WSOC is experimentally obtained from a rural background site in Europe, it can be questioned to what extent it is applicable for a wider range of European sites, which can be influenced by other sources. Furthermore, Kiss et al. (2002) states that 2.1 is a lower estimate for the WSOC fraction. Obviously, more work is needed to provide conversion factors for a wider range of sites than what currently is the case.

3.6 Conclusion

The mean ambient aerosol concentration of WINSOC ranged from $0.58 \mu\text{g C m}^{-3}$ at the Irish site to $4.9 \mu\text{g C m}^{-3}$ at the Italian site Ispra. For WSOC the corresponding range was from $0.12 \mu\text{g C m}^{-3}$ at the Irish site to $3.6 \mu\text{g C m}^{-3}$ at the Italian site San Pietro Capofiume. WINSOC was the dominant subfraction at all sites investigated except at two sites, ranging from 43 – 83%.

Converting WSOC to WSOM by using a conversion factor of 2.1, and WINSOC to WINSOM by using a conversion factor of 1.3, WSOM was found to dominate the OM fraction at the majority of the sites, ranging from 24 – 68%.

It is argued that adding levels of WSOM and WINSOM is the best way to provide concentrations of OM in ambient aerosols. The advantage of this approach is that it accounts for the relative contribution of WSOM and WINSOM to OM, which was found to vary considerably between the 13 European background sites investigated. If concentrations of WSOM and WINSOM are not available, the next best approach to provide levels of OM was obtained by multiplying OC by a factor of 1.6, compared to using conversion factors of 1.4 and 2.0. (This conclusion is valid given that a factor of 2.1 is used to convert WSOC to WSOM and a factor of 1.3 is used to convert WINSOC to WINSOM.)

4. Impact of residential wood burning at rural background sites in Europe

by K.E. Yttri

4.1 Introduction

Wood smoke can be a significant source of fine atmospheric particles. In communities where wood burning is used for residential heating, wood smoke can even dominate the fine particle burden (Fine et al., 2002a). The small size of particles originating from wood burning enables them to remain in the atmosphere for up to one week on average and to be transported over long distances. Their small size, equivalent aerodynamic diameter typically being less than 1 μm (Kleeman et al., 1999), also makes them potentially more harmful, as they can penetrate into the alveolar region of the respiratory system. Wood smoke particles have a high content of carbonaceous material, and organic carbon is the dominating fraction, typically accounting for more than 70% of the aerosol mass ($\text{PM}_{2.5}$) (Fine et al., 2002a; Seinfeld and Pandis, 1998). Several studies have focused on wood burning because wood smoke has a high content of polycyclic aromatic hydrocarbons, which are known to be both mutagenic and carcinogenic (Hawthorne et al., 1992).

Furthermore, energy sources other than fossil fuel is gaining importance on a global scale. This is both due to increased energy prices and the fact that alternative sources of energy have to replace energy based on fossil fuel, as this production will decline significantly within the next decades. In addition, CO_2 emissions from wood burning are not included amongst the greenhouse gases such as CO_2 from fossil fuel. Thus, it can be speculated that the use of firewood as an energy source may increase. In this aspect the long turnover time from old to new and cleaner combustion technology should be notified.

For the reasons mentioned, a reliable tracer of particulate emissions from residential wood burning is warranted. Currently, levoglucosan is the most recognized molecular marker for tracing emissions of particulate matter from residential wood burning. This organic molecule is generated when burning cellulose and hemicellulose at temperatures $> 300^\circ\text{C}$ (Simoneit et al., 1999). These two biopolymers account for 60-80% of the dry weight of wood.

Levoglucosan holds certain features that make it very well suited as a tracer of residential wood burning:

- It is emitted in high concentrations during wood burning, which makes it readily to detect in ambient aerosol samples.
- It has a low vapour pressure due to a high molecular weight, which ensures that the compound partitions to the particulate phase.
- It is associated with fine aerosols only, which makes it possible to trace emissions from wood burning on inter-continental scale.
- It does not undergo chemical reactions in the atmosphere that selectively deplete its concentration between source and receptor site.

Due to these advantageous features, levoglucosan is used in chemical-mass-balance models or principle component analysis techniques, such as positive matrix factorisation, to calculate the contribution of wood smoke particles to the total atmospheric concentration of ambient aerosols. However, ambient concentrations of levoglucosan can provide important information *per se*, positively confirming the presence of emissions from biomass burning, as well as providing estimates of the relative contribution of residential wood burning.

While commonly used to address the impact of residential wood burning in the USA, the use of levoglucosan it is not widespread in Europe. In the present study levoglucosan is used to address the spatial and seasonal variation of residential wood burning at a number of European rural background sites, and to estimate the relative contribution of wood smoke particles to the ambient level of PM₁₀.

4.2 Aerosol sampling

The ambient aerosol content of levoglucosan was quantified using filter samples collected during the EMEP EC/OC campaign, conducted during the period 1 July 2002-1 July 2003. Table 4.1 provides an overview of the sampling sites included in the campaign, their site category and the sampling equipment used. Aerosol sampling was performed using CEN (European Committee for Standardization) approved or equivalent PM₁₀ samplers, collecting one 24h sample every week (starting Tuesday mornings). Samples were collected on pre-baked quartz fibre filters. The filters content of PM₁₀, elemental carbon, organic carbon and total carbon have been reported previously (Yttri and Kahnert, 2004).

Table 4.1: *Sampling sites in the EMEP EC/OC campaign, their site category and sampling equipment used.*

Country	Sampling site	Site category	Aerosol sampler	Filter size	Flow rate
Austria	Illmitz (AT02)	Rural Background	Partisol	47 mm	16.7 l min ⁻¹
Belgium	Ghent (BE02)	Urban Background	Gent Filter Unit	47 mm	17 l min ⁻¹
The Czech Republic	Košetice (CZ03)	Rural Background	FH 95 SEQ	47 mm	38 l min ⁻¹
Finland	Virolahti (FI17)	Rural Background	KFG	47 mm	38 l min ⁻¹
Great Britain	Penicuik (GB46)	Rural	Partisol	47 mm	16.7 l min ⁻¹
Germany	Langenbrügge (DE02)	Rural Background	Hi-Vol (Digitel)	150 mm	500 l min ⁻¹
The Netherlands	Kollumerwaard (NL09)	Rural Background	KFG	47 mm	38 l min ⁻¹
Ireland	Mace Head (IE31)	Rural Background	KFG	47 mm	38 l min ⁻¹
Italy	Ispra (IJRC) (IT04)	Near-city	KFG	47 mm	38 l min ⁻¹
Italy	San Pietro Capofiume (S.P.C) (IT08)	Urban Background	Gent Filter Unit	47 mm	17 l min ⁻¹
Norway	Birkenes (NO01)	Rural Background	KFG	47 mm	38 l min ⁻¹
Portugal	Braganza (PT01)	Rural Background	Hi-Vol (Sierra)	8 x 10 inch	1133 l min ⁻¹
Sweden	Aspvreten (SE12)	Rural Background	Gent Filter Unit	47 mm	17 l min ⁻¹
Slovakia	Stara Lesna (SK04)	Rural Background	Partisol	47 mm	16.7 l min ⁻¹

Ten samples from each of the 14 sites included in the campaign were analysed. Four of the samples were picked from the summer period, including the two periods July 02-September 02 (16-17 July and 10-11 September) and April 03-July 03 (22-23 April and 27-28 May), whereas the other six samples were picked from the winter period lasting from October 02-March 03 (15-16 October, 26-27 November, 17-18 December, 21-22 January, 4-5 February and 4-5 March). The 140 samples selected for analysis were collected on the same ten dates in order to ease the comparison and to get a snapshot of the impact from residential wood burning on these days in Europe.

4.3 Quantification of levoglucosan

Levoglucosan and its isomeric compounds, mannosan and galactosan, were quantified using high-performance liquid chromatography in combination with a high-resolution mass spectrometry based on a time-of-flight principle (Dye and Yttri, 2005). The detection limit for the three isomers is between 20-40 pg injected in the instrument.

4.4 Annual mean concentration of levoglucosan

The annual mean concentrations of levoglucosan are given in Figure 4.1 and Table 4.2. In general the lowest annual levels of levoglucosan are reported for the Northwestern parts of Europe (the Dutch site, the United Kingdom site, the Norwegian site and the Swedish site), whereas the highest concentrations are reported for the Southern, Central and Eastern parts of Europe. However, care should be taken drawing general conclusions, as the situation of the various sites may be highly decisive for the concentrations observed. Notably, residential wood burning has been recognized as a significant contributor to the particulate pollution level in urban areas in Scandinavia (Ramdahl et al., 1984; Yttri et al., 2005b), whereas this is not reflected when addressing the impact from this source at rural background sites in the current study.

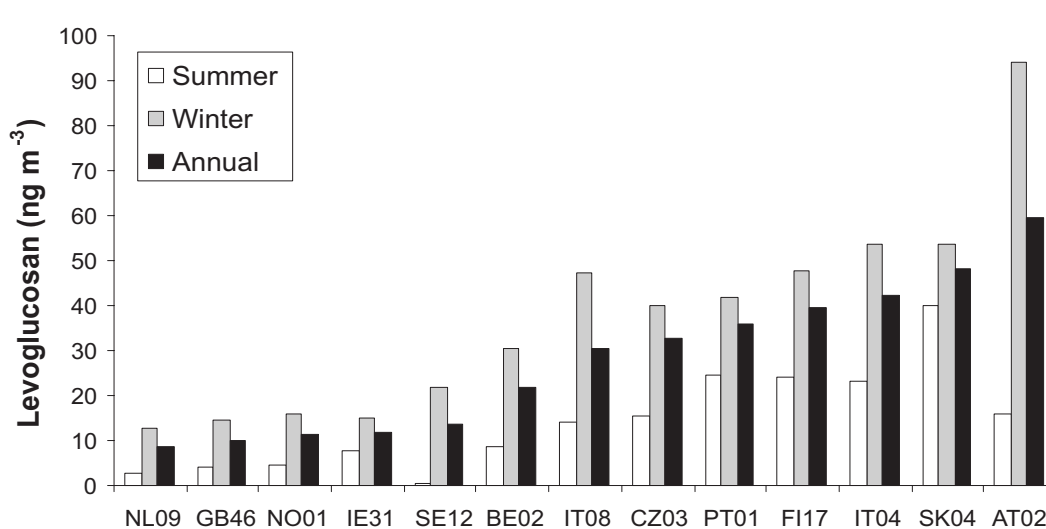


Figure 4.1: Annual and seasonal mean concentration of levoglucosan at the various sites investigated in the present study. For explanation of abbreviations, see Table 4.1.

The highest annual mean concentration of levoglucosan was observed for the Austrian site (59.4 ng m^{-3}), whereas the lowest was reported for the Dutch site (8.73 ng m^{-3}). This spatial variation might be expected, as the Austrian site is located in the densely populated Central Europe, whereas the Dutch site is situated next to the North Sea. Furthermore, the Austrian site is situated close to Bratislava, less than 20 km, and may be influenced by residential wood burning from this area. Indeed, proximity to major urban areas seems to be an important factor decisive for the concentrations observed at the various sites. It should be noted that although residential wood burning is not as common in densely populated areas as in rural areas, possibly reflecting the availability of firewood, the population density makes the urban areas the most exposed both in terms of mean and maximum concentrations. Notably, maximum concentrations of levoglucosan close to (Yttri et al., 2005b) and even higher than $1 \mu\text{g m}^{-3}$ (Zdrahal et al., 2002) have been reported for urban influenced European sites. Thus, the site category, being mainly rural background sites in the present study, may be an important factor for the lower concentrations observed.

Of the sites included in the present study, levoglucosan has previously been reported only for the Ghent site (urban background site) (Zdrahal et al., 2002). In that study both concentrations seen during winter (477 ng m^{-3}) and summer (19.4 ng m^{-3}) are higher than those reported in the present study (30.6 ng m^{-3} during winter and 8.69 during summer) (Table 4.2). This difference is particularly significant for the samples collected during the winter period. It is assumed that this can be attributed to differences in the ambient temperature. It has been shown that the ambient concentration of levoglucosan increases significantly as the ambient temperature drops (Yttri et al., 2005b). Furthermore, meteorological conditions may prevent or promote effective dispersion of emissions from residential wood burning, being highly decisive for the concentrations observed.

Table 4.2: Annual and seasonal mean (min and max) concentrations of levoglucosan (ng m^{-3}) in PM_{10} , annual and winter concentrations of PM_{Wood} ($\mu\text{g m}^{-3}$) for PM_{10} , and relative contribution of PM_{Wood} to PM_{10} for the entire year and the winter season. For explanation of abbreviations, see Table 4.1.

Site	Levoglucosan Annual (ng m^{-3})	Levoglucosan Winter (ng m^{-3})	Levoglucosan Summer (ng m^{-3})	PM_{Wood} Annual ($\mu\text{g m}^{-3}$)	PM_{Wood} Winter ($\mu\text{g m}^{-3}$)	$\text{PM}_{\text{Wood}}/\text{PM}_{10}$ Annual (%)	$\text{PM}_{\text{Wood}}/\text{PM}_{10}$ Winter (%)
AT02	59.4 (n.d.-156)	94.2	15.9	2.47	3.92	6.6 (n.d.-15.1)	8.3
BE02	21.9 (4.5-56.1)	30.6	8.7	0.909	1.27	2.6 (0.4-6.7)	4.3
CZ03	32.9 (5.5-50.6)	39.9	15.5	1.37	1.66	3.8 (0.9-7.1)	4.6
FI17	39.7 (7.1-62.2)	47.6	24.0	1.65	1.98	10.2 (4.3-12.8)	10.3
GB46	10.0 (n.d.-18.2)	14.7	4.1	0.417	0.613	3.9 (n.d.-10.5)	5.4
IE31	12.0 (3.4-29.9)	14.8	7.7	0.498	0.616	3.3 (0.8- 10.9)	3.9
IT04	42.3 (10.2-70.5)	53.8	23.2	1.76	2.24	6.2 (3.0-54.5)	6.8
IT08	30.7 (8.0-80.0)	47.2	14.1	1.28	1.96	3.5 (1.0-7.9)	4.7
NL09	8.7 (n.d.-26.9)	12.7	2.8	0.363	0.527	1.7 (n.d.-3.8)	2.5
NO01	11.3 (n.d.-38.1)	15.8	4.6	0.472	0.658	4.9 (n.d.-61.2)	7.5
PT01	36.0 (2.3-66.9)	41.9	24.4	1.50	1.74	9.0 (0.9-28.7)	10.2
SE12	13.4 (n.d.-61.3)	22.0	0.5	0.559	0.917	4.1 (n.d.-18.2)	6.8
SK04	48.3 (10.8-94.2)	53.8	40.1	2.01	1.96	6.9 (1.3-21.8)	8.3

- Note: The mean ratio of $\text{PM}_{\text{Wood}}/\text{PM}_{10}$ for the entire year and for the winter period is calculated according to the following equation: $(a_{\text{mean}}/b_{\text{mean}})*100$; the min and max value are calculated according to $a/b * 100$ (for $n = i$).
- When calculating PM_{Wood} from ambient levels of levoglucosan it is assumed that levoglucosan accounts for 2.4% of PM_{10} originating from wood burning.

4.5 Summer vs. winter

The concentration of levoglucosan was higher during winter than during summer at all sites investigated (Table 4.2). The highest difference was experienced for the Austrian site where it was 5.9 times higher during winter compared to the summer, whereas the smallest difference was reported for the Slovakian site, where the levoglucosan concentration was only 1.3 times higher during winter than during summer. Although the seasonal variation for the Swedish site is greater, this is not accounted for as levoglucosan was detected in only one of the samples picked from the summer period. This finding clearly illustrates that residential wood burning is far more common during winter than during summer, as expected. The seasonal dependence of residential wood burning is clearly illustrated in Figure 4.2A-M, showing the annual variation of levoglucosan for all sites included in the study. Typically an increase in the levoglucosan concentration is seen going from summer to fall, whereas the maximum concentrations are obtained during winter. Going from winter to spring, the concentrations

decline again. It should be noted that no more than 10 days have been selected for analysis and that this low number hardly is representative for an entire year. Thus, deviation from the annual pattern described can be seen, such as the local minimum for the Slovakian site during February and March (Figure 4.2L) and the continued elevated concentrations at the Finnish site during spring (Figure 4.2J). For the Slovakian site the drop in the levoglucosan concentration for February and March, compared to the preceding and the proceeding months, leads to a small difference between the summer (40.1 ng m^{-3}) and the winter concentration (53.8 ng m^{-3}) of levoglucosan. However, the relative contribution of levoglucosan to PM_{10} for these two days is in accordance with the other samples collected during winter at this site, as the PM_{10} concentrations are low as well. Further, the great geographical variation of the sites most probably influences the annual variation of levoglucosan. Obviously the winter lasts longer at the sites in Scandinavia compared to those in Central and Southern Europe, as well as at those sites located at a certain altitude such as the Slovakian, the Czech and the Portuguese sites.

In the study by Zdrahal et al. (2002) the concentration of levoglucosan was over 20 times higher during winter compared to the summer for the Ghent site. A correspondingly high difference between summer and winter has been reported for a suburban site in Norway (Yttri et al., 2005b). A likely explanation for the smaller differences seen when comparing concentrations of levoglucosan obtained during summer and winter in the present study is that the influence from residential wood burning on the days picked during the winter period is rather modest. As previously discussed, the site category most likely have a significant impact on the mean and the maximum concentrations observed, as these figures seems to be linked to the population density. Thus, this factor can explain the smaller differences between winter and summer reported for the rural background sites in the present study compared to the figures reported for urban influenced areas (Zdrahal et al., 2002; Yttri et al., 2005b).

The study confirms that levoglucosan is present in a significant number of samples at the sites investigated also during summer, although in much lower concentrations than during winter. This finding indicates that residential wood burning also takes place during summer. However, wildfires can contribute to the level of levoglucosan as well. Indeed, high concentrations of fine aerosols were reported above the boundary layer in Europe during summer 2003 and suggestions were made that this could be attributed to emissions from wildfires in Siberia (Mattis et al., 2003). Furthermore, Niemi et al. (2004) showed that large-scale agricultural field burning in Eastern Europe resulted in high concentrations of fine particles in Scandinavia. Without further investigation, any attempt to distinguish between the contribution of levoglucosan from wildfires and residential wood burning during summer becomes speculative. Nevertheless, attempts should be made to estimate the contribution of particulate matter from wildfires in the Northern hemisphere to the fine particulate level in Europe. Currently, this source is not included in chemical transport models calculating the particulate concentrations for Europe.

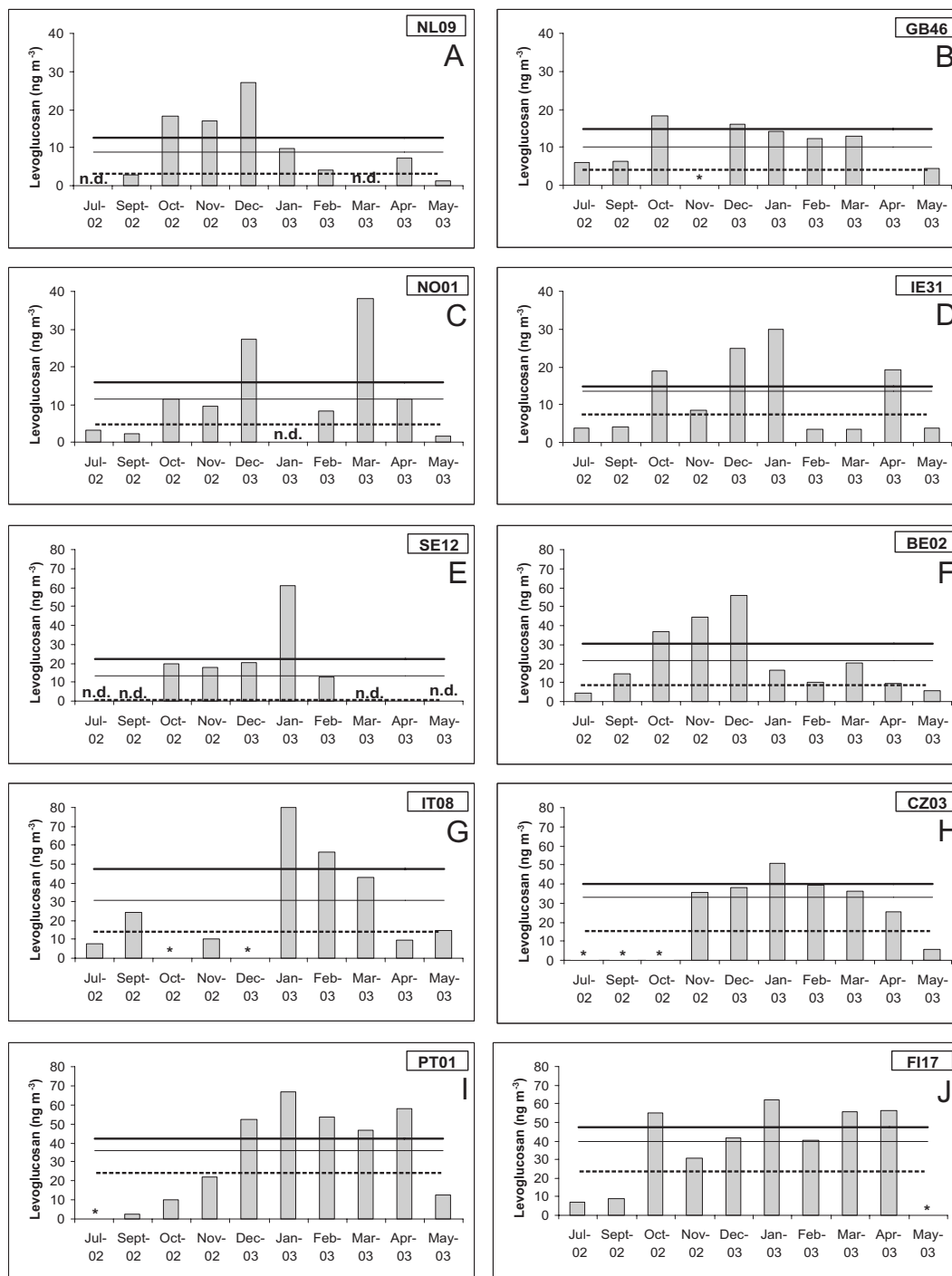


Figure 4.2: Annual variation of levoglucosan at the various sites investigated in the present study. For explanation of abbreviations, see Table 4.1. Annual mean concentration of levoglucosan (—), mean concentration of levoglucosan during winter (—) and mean concentration of levoglucosan during summer (-----). Note that the figures do not display monthly values, but rather one day of sampling for the months listed.

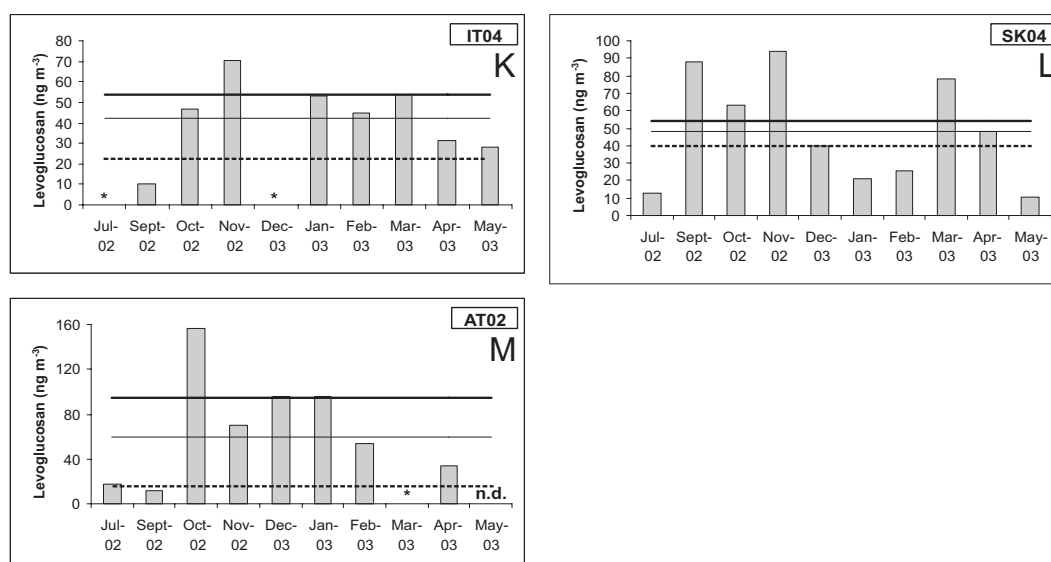


Figure 4.2, cont.

4.6 Relative contribution of individual monosaccharides anhydrides (MA) to the total MA concentration

The relative contribution of the individual monosaccharide anhydrides to the total concentration of monosaccharide anhydrides did not vary much from site to site (Table 4.3). Moreover, the results presented in Table 4.3 correspond well with what has been reported for three European sites previously (Zdrahál et al. 2002; Yttri et al., 2005b). The results are also in accordance with results reported from the Amazon region during the wet season (Zdrahál et al., 2002). Results from a study measuring monosaccharide anhydrides at three different sites in the USA (Nolte et al., 2001) indicate that levoglucosan may account for a somewhat greater fraction of the total MA concentration at those sites than what is seen in the current study.

Table 4.3: Relative contribution of the individual monosaccharide anhydrides (MA) to the total concentration of MA (Mean \pm SD) (%).

Site	Galactosan/MA	Mannosan/MA	Levoglucosan/MA	No of samples
AT02	5.2 (1.4)	15 (2.3)	80 (2.4)	(n=6)
BE02	5.6 (1.0)	17 (3.6)	78 (4.5)	(n=5)
CZ03	8.3 (1.5)	23 (4.2)	69 (5.4)	(n=6)
FI17	8.2 (2.6)	20 (4.7)	71 (6.9)	(n=8)
IE31	8.6 (0.9)	19 (1.9)	72 (1.9)	(n=5)
IT04	-	-	-	
IT08	7.0 (1.3)	15 (5.1)	78 (6.3)	(n=5)
NL09	7.0 (1.3)	18 (1.0)	75 (0.44)	(n=4)
NO01	6.4 (0.9)	21 (3.5)	73 (3.5)	(n=5)
PT01	6.6 (2.4)	14 (3.0)	79 (4.7)	(n=6)
SK04	7.5 (1.5)	19 (3.5)	73 (3.8)	(n=8)
SE212	5.8 (0.9)	22 (2.2)	72 (2.4)	(n=5)
GB46	6.0 (1.6)	24 (2.4)	70 (3.1)	(n=3)
Mean	6.9 (1.1)	18.9 (3.3)	74 (3.7)	(n=12)

No significant differences could be seen comparing the relative contribution of the individual monosaccharide anhydrides to the total concentration of monosaccharide anhydrides, when comparing summer and winter. It should be noted that this was performed for a couple of sites only due to the low number of samples during summer where all three isomers were present.

4.7 Relative contribution of wood burning to PM₁₀

Based on stable levoglucosan to PM emission ratios, the concentration of PM from wood burning can be estimated based on the samples content of levoglucosan. In the present study it is assumed that levoglucosan accounts for 2.4% of the particulate emissions from wood burning. This percentage is taken from the study by Yttri et al. (2005b) and is based on sampling in a source specific region. This percentage is in the lower end of what has been reported for a number of American tree types, ranging from 1% to 26% (Fine et al., 2001, 2002b, 2004). It should be noted that emission tests performed with the most commonly used European wood types at a wide range of burn rates, must be performed to take full advantage of levoglucosan as a tracer for residential wood burning. Still, in the study performed by Fine et al. (2002a) regionally averaged compound-specific emission rates shows that the relative amount of levoglucosan emitted per gram organic carbon in wood smoke varies by less than a factor of two across all regions of the United States.

By using the before-mentioned ratio of levoglucosan to PM of 2.4%, the contribution of particulate matter originating from wood burning (PM_{Wood}) has been estimated for the sites included in the study (Table 4.2). The results show that PM_{Wood} varies between 0.363 µg m⁻³ at the Dutch (NL09) site and 2.47 µg m⁻³ at the Austrian site (AT02). On an annual basis the mean relative concentrations of PM_{Wood} to PM₁₀ do not vary too much between the sites investigated, ranging from 1.7% at the Dutch site to 10.2% at the Finnish site. This result indicates that residential wood burning is not a major source contributing to PM₁₀ at rural background sites in Europe. Accounting for the fact that particles emitted from wood burning almost exclusively reside in the fine fraction (< PM_{2.5}) the relative importance of this source will be greater for PM_{2.5}. Typically, PM_{2.5} accounts for approximately 70% of PM₁₀ at rural background sites in Europe, except for some countries in the Mediterranean region where the percentage is somewhat lower, mainly due to the high impact from resuspension. Thus, the relative contribution of particulate matter from residential wood burning is approximately 30% higher for PM_{2.5} than for PM₁₀. Estimates of the relative contribution of PM_{Wood} to PM₁₀ for the winter period are provided in Table 4.2. The results show that the relative contribution of PM_{Wood} to PM₁₀ is higher during winter compared to the estimate provided for the entire year for all sites included, ranging from 2.5% at the Dutch site to the 10.3% at the Finnish site.

For some sites the maximum relative contribution of PM_{Wood} to PM₁₀ was quite high, such as for the Norwegian site (61.2%) and the Italian site Ispra (54.5%). For the Norwegian site the high maximum level can be attributed to the low PM₁₀ concentration (0.78 µg m⁻³) for the day in question. For the Ispra site, a combination of a low PM₁₀ concentration (5.4 µg m⁻³) and the highest reported concentration of levoglucosan for this site, could explain the high maximum level reported.

4.8 Conclusion

The presence of levoglucosan in ambient aerosols was demonstrated at all sites investigated. The mean annual concentration of levoglucosan varied from 8.73 ng m⁻³ at the Dutch site to 59.4 ng m⁻³ at the Austrian site. It is argued that the spatial variation reported can be attributed to population density and proximity to urban areas. Thus, the situation of the measurement site is important for the concentrations observed. Furthermore, temperature, meteorological conditions and ambient temperature will be equally important for the concentrations observed.

Concentrations of levoglucosan was higher during winter compared to summer at all sites investigated, reflecting the increased impact from residential wood burning as the ambient temperature drops during winter. The concentrations observed during winter were 1.3-5.9 times higher than reported during summer. It is argued that wildfires contribute to the level of levoglucosan observed during summer, however, it is not known to what extent.

On an annual basis particulate matter from residential wood burning accounted for 1.7% (the Dutch site) to 10.2% (the Finnish site) of PM₁₀. Providing corresponding estimates for the winter season the concentration was found to increase for all sites investigated.

Although residential wood burning has been recognized as a significant source of ambient air fine particulate pollution in several urban communities, the present study indicates that particulate emission from residential wood burning is not a major contributor to PM₁₀ at rural background sites in Europe.

5. Aerosol size distribution measurements at the EMEP site Birkenes (Norway)

by C. Lunder

Particle mass is mostly determined by particles in the accumulation mode (0.1-1.0 μm) and by coarse particles (2.5-10 μm), whereas Aitken (0.030-100 μm) and nucleation (smaller than 30 nm) mode particles make a negligible contribution to PM_{10} , $\text{PM}_{2.5}$, and even PM_1 mass. On the other hand, coarse particles contribute little to particle number densities. The main contribution to the particle number concentration comes from ultra fine particles (UFP) ($d_p < 100$ nm), i.e. nucleation mode and the Aitken particles, and to a lesser extent from particles in the accumulation mode. A better characterisation of UFP is needed to facilitate our understanding of adverse health effects of aerosols. In addition a better understanding of the dynamic growth of Aitken particles to accumulation mode, particles by heterogeneous chemical processes is needed. Furthermore, accurate prediction of aerosol number concentrations is important for estimating the indirect climate forcing of aerosols.

The size distribution of aerosols is an important parameter that impacts the transport and deposition properties of particles in the atmosphere, their optical properties, and their ability to act as cloud condensation nuclei. The optical properties determine the direct climate effect of aerosols, whereas their role as cloud condensation nuclei is the origin of the indirect climate forcing effect of aerosols. Detailed information on particle size distributions can provide valuable information for the validation of air pollution models (EMEP, 2003), for source attribution, and for understanding the formation, transport, and deposition of particles in the atmosphere (Tunved et al., 2003a). Size distribution data is also an indispensable input parameter for modelling the radiative effects of aerosols (Myhre and Stordal, 2001; Kahnert and Kylling, 2004).

Nucleation particles are formed from precursor gases and quickly grow within a few hours by condensation of gases or by coagulation with other particles. Aitken particles can originate from primary emission (e.g. diesel soot) or from growing nucleation particles. Accumulation particles have the longest lifetime (up to 2 weeks). Most accumulation particles originate from Aitken particles, which grow within a few days to accumulation size (by heterogeneous liquid phase reactions, condensation, and coagulation). Most coarse mode particles (larger than 1000 nm) originate from primary emitted particles (mainly sea salt and mineral dust). However, precursor gases (e.g. H_2SO_4 and HNO_3) can chemically interact with coarse mode particles (containing e.g. NaCl , CaCO_3), thus adding mass (e.g. sulphate, nitrate) to the aerosols. Coarse mode particles have high deposition rates and thus short lifetimes in the atmosphere. Accumulation particles are most important for long-range transport due to their long lifetime, whereas nucleation and Aitken particles usually originate from local sources. Thus by investigating aerosol size distributions we can distinguish between locally formed particles and those originating from more distant source regions.

One of the most extensive networks for measuring particle number distributions in Europe is a Nordic network comprising several Swedish and Finnish stations, and, since autumn 2002, the EMEP station at Birkenes. This report presents some of the results obtained with the Differential Mobility Particle Sizer (DMPS) instrument installed at Birkenes, which measures aerosol size distributions in the diameter range between 19.0 nm and 643.2 nm.

Figure 5.1 and Figure 5.2 show time series of number size distributions (upper panel) and total number concentrations (lower panel) measured in February 2004 and July 2004, respectively. Particle numbers are considerably lower in winter than in summer, which is in agreement with published data from other Nordic background stations (Tunved et al., 2003b). A potential explanation for the seasonal variation in particle number concentration might be a higher biogenic activity in springtime, which produces larger amounts of organic vapours that contribute to the growth of aerosol particles by condensing onto existing particles. However, it can also be explained by seasonal changes in air masses, lower rate of incoming solar radiation and thus less new particle formation during the winter period and/or a higher rate of precipitation and overall cloudiness during the winter (Tunved et al., 2003b).

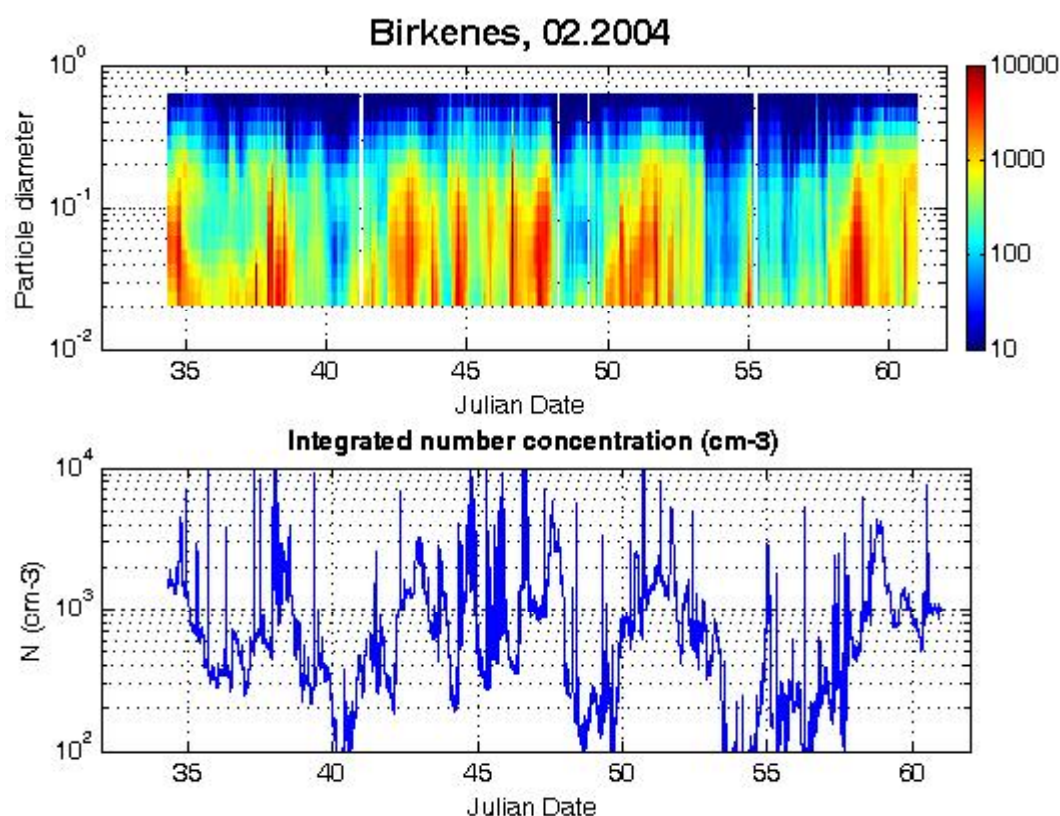


Figure 5.1: Spectral plot of aerosol number as a function of size distribution (μm) and Julian Date (upper panel) and time series of total number concentration (lower panel) at Birkenes in February 2004.

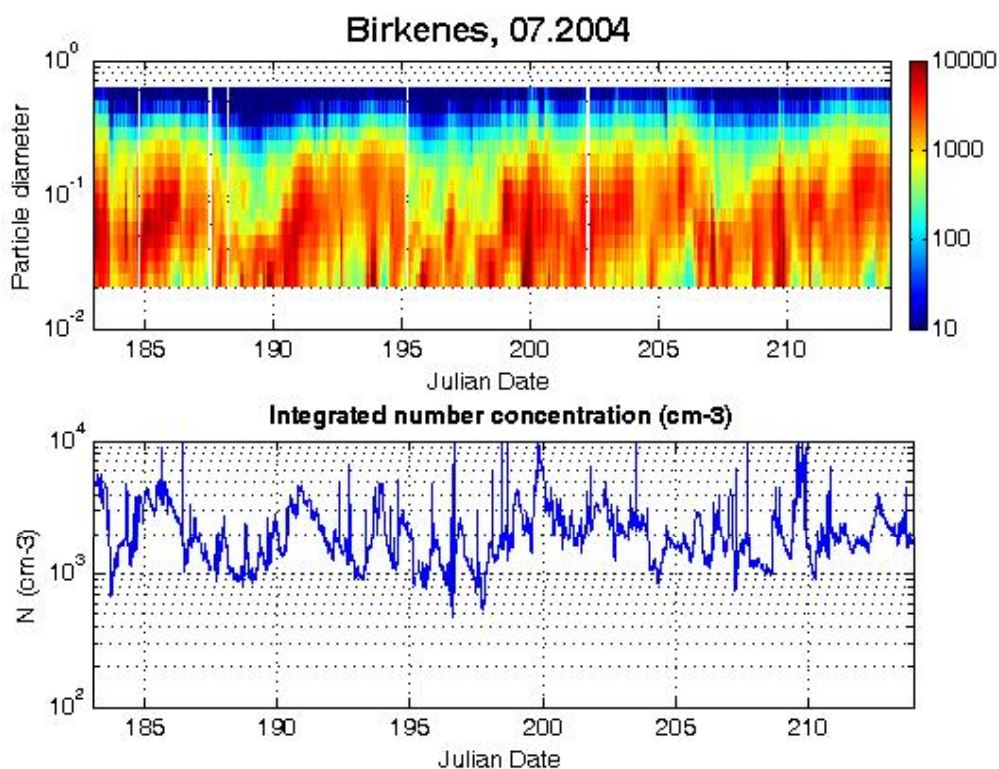


Figure 5.2: Spectral plot of aerosol number as a function of size distribution (μm) and Julian Date (upper panel) and time series of total number concentration (lower panel) at Birkenes in September 2004.

Figure 5.3 presents a 2-day period in early spring. High particle number concentrations (lower panel) are correlated with the appearance of nucleation mode particles and new small Aitken particles, most likely due to local nucleation events. Also the dynamic growth of the Aitken particles to accumulation size on the time scale of 1-3 days is observed.

Diurnal variations were observed and most of the nucleation events were characterized by a sharp increase of nuclei mode number concentration around noon. The frequency of nucleation events in 2004 at Birkenes has been shown to be largest around spring and summertime. This seasonal variation has been observed at similar sites (Tunved et al., 2003b).

Figure 5.3 shows an episode of dynamic particle growth process. At noon (Julian day 116.5) small Aitken particles appear, which most likely originate from the growth of nucleation mode particles. These particles come from local, possibly biogenic sources. Over a period of a day it is observed that the Aitken particles grow to accumulation mode. These nucleation events stop at night and resume in the morning of the next day. This diurnal variation in the production of new particles supports the hypothesis that these particles are of biogenic origin. During night time the growth process of the Aitken particles to accumulation mode continues. Comparison of the upper and lower panel also shows that peaks in number concentrations are usually accompanied by the appearance of new small

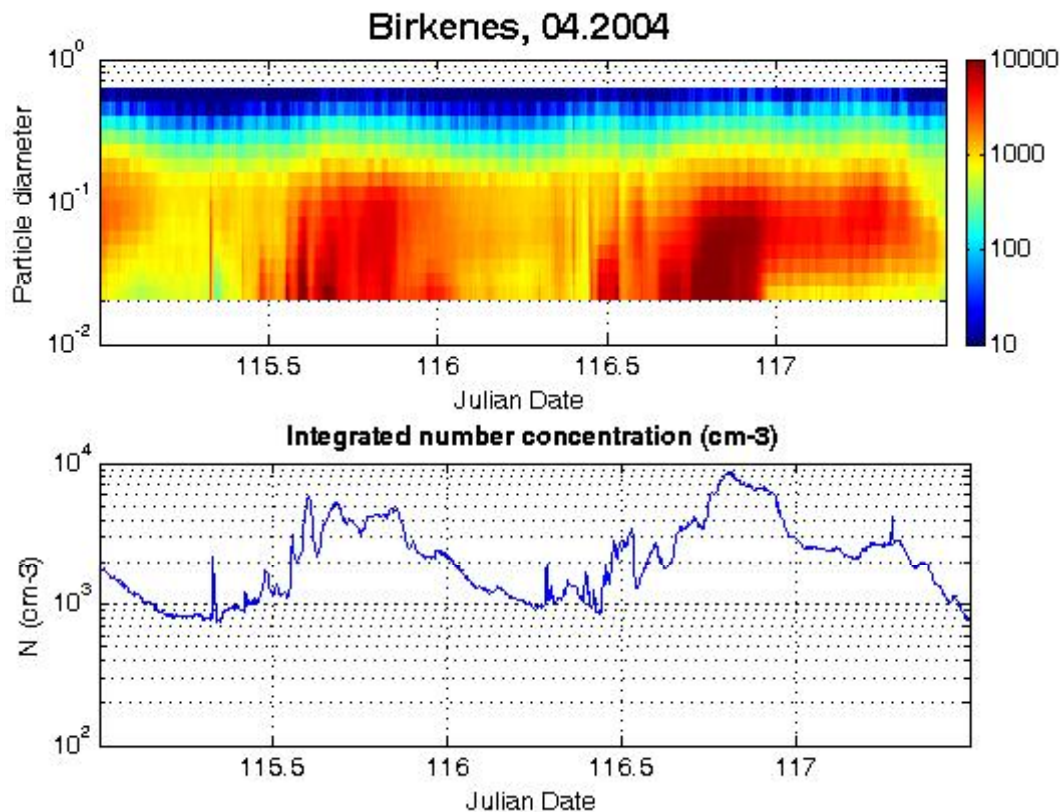


Figure 5.3: A 2-day period in early spring 2004 with local particle formations and diurnal variations.

Aitken particles. This demonstrates that small particles make the dominant contribution to number concentrations. The reason for this is coagulation of particles, and condensation, which are the important dynamic processes (Kerminen et al., 2001). Coagulation and condensation increase the average particle size while decreasing particle number concentration.

In Figure 5.4 the composite time dependent average size distribution for Birkenes during March-May 2004 are depicted. The data have been divided into 4 hrs intervals and calculated as the average value of the integral of scans during the period of the year. The data was further divided into one sub-set with days with typical nucleation events and another with days where nucleation events were not observed. The diurnal variation is much more pronounced in the sub-set with nucleation events compared the sub-set without. In the case of nucleation events there was an initial increase of small particles in the time interval between 08:00-12:00 and 12:00-16:00 and even more pronounced during 16:00-20:00. Hereafter the size is shifted towards larger particles during 20:00-24:00. This behaviour could be interpreted as growth of the small, initially formed, particles.

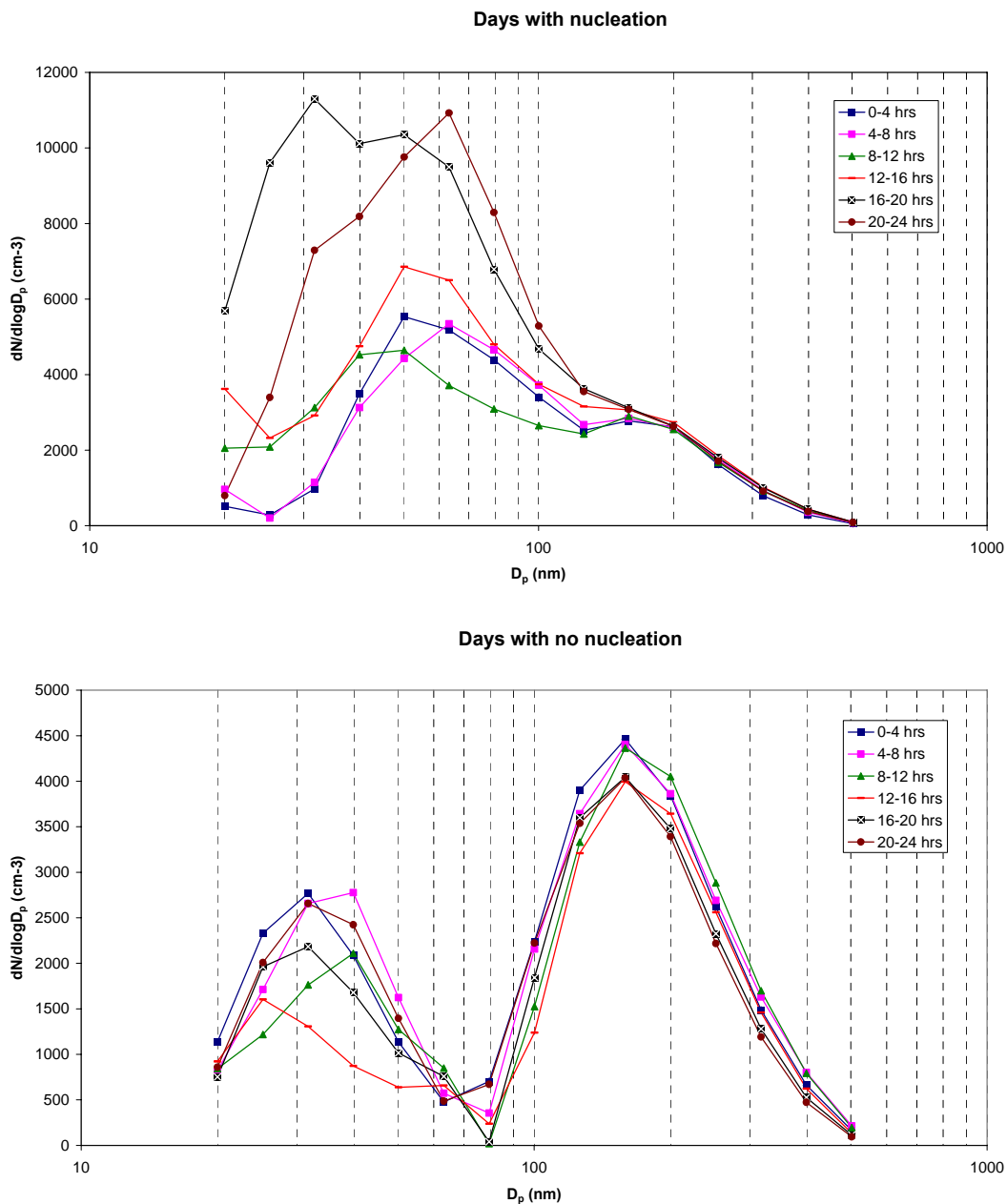


Figure 5.4: Time dependent evolution of the size distribution during March-May, 2004. Each plot represents the average during four hours intervals for the whole period (March-May).

6. European aerosol optical depth measurements from ground and space

by Thomas Holzer-Popp, Gerrit de Leeuw, Robin Schoemaker, Jan Schaug, Christoph Wehrli

The Integrated Global Observing Strategy (IGOS), which is a partnership of international organisations, recently presented an atmospheric chemistry theme report (WMO, 2004) with focus on the four grand challenges in atmospheric chemistry; the tropospheric air quality, the oxidation efficiency of the atmosphere, the stratospheric chemistry and ozone depletion, and the chemistry – climate interactions. Aerosols are important within all these four fields. At ground level the effects of anthropogenic PM smaller than 2.5 upon human health is well documented while the effect of aerosol/gas interactions on the tropospheric air quality and the oxidation capacity are not yet fully understood. Tropospheric aerosols cause a direct radiative forcing by scattering and absorbing solar radiation and indirectly by changing the radiative properties of clouds. Dependant on the aerosols' physical and chemical characteristics they may either reflect radiation, e.g. as white sulphates do, or they may absorb radiation, e.g. as black carbon particles will do. The magnitude of the total forcing remains unknown. In the stratosphere gas-particle interactions can affect the chemistry that controls the ozone layer.

A large number of sites at ground level record aerosol optical properties around the world. AERONET (<http://aeronet.gsfc.nasa.gov/>), short for Aerosol Robotic Network, aims at assessment of aerosol properties and validation of satellite retrieval of aerosol optical properties. This network compiles data from a large number of ground-measurement sites around the globe, and has about sixty European sites. More than twenty of the sites have currently reported cloud screened and quality assessed data (level 2) for more than one year. The sites span different site categories, from background sites such as Mace Head in Ireland, which also is a WMO GAW site, to city measurements, e.g. in Moscow.

The World Meteorological Organization, Global Atmosphere Watch (WMO GAW) programme runs a small trial network of 12 stations operating sunphotometers (precision-filter-radiometers) around the world (Wehrli, 2005). Six sites are, or will be operational in Europe. All sites are background sites. Data are available through the web (<http://rea.ei.jrc.it/netshare/wilson/WDCA/>).

AOD measurements have been included in EMEP since 2004 at the Level 3 monitoring. Level 3 is voluntary, but is considered important for the understanding of processes and for controlling the transboundary air pollution. Level 3 activities will typically be undertaken by research groups, may also include campaign data, and will hopefully include data that are not part of the networks above.

Satellites are, however, becoming increasingly important for measuring total vertical aerosol columns and vertical profiles. Ground-based networks will nevertheless continue to be important and necessary, both with respect to verification of satellite data and for filling in gaps in the space-based remote

monitoring of aerosols. Both NASA (<http://www.nasa.gov/home/>) and ESA have satellites returning information relevant to aerosol optical properties. PROMOTE (PROtocol MO尼Toring for the GMES Service Element) that is funded by ESA retrieves AOD data from satellites (<http://www.gse-promote.org/>), some examples have been given below. Below is also given some of the results from the three past years' measurements at the WMO GAW site at one single location, Ny-Ålesund, Spitsbergen, together with satellite derived fields for Europe.

6.1 Three years' measurements in Ny-Ålesund with the WMO-GAW precision-filter-radiometer

Figure 6.1 presents the aerosol optical density at 501 nm at Ny-Ålesund. As seen the AOD is higher during the Arctic spring compared to a measurement made during summer. This is due to the Arctic haze phenomenon in the boundary layer, and the suppression of removal mechanism during winter and early spring due to strong inversions. During summer precipitation removes the aerosols as well as water-soluble gases. The AOD measured in the Arctic is, as one would expect, quite low compared to corresponding measurements at the Continent, as seen from the satellite derived fields in Figure 6.3 and Figure 6.4.

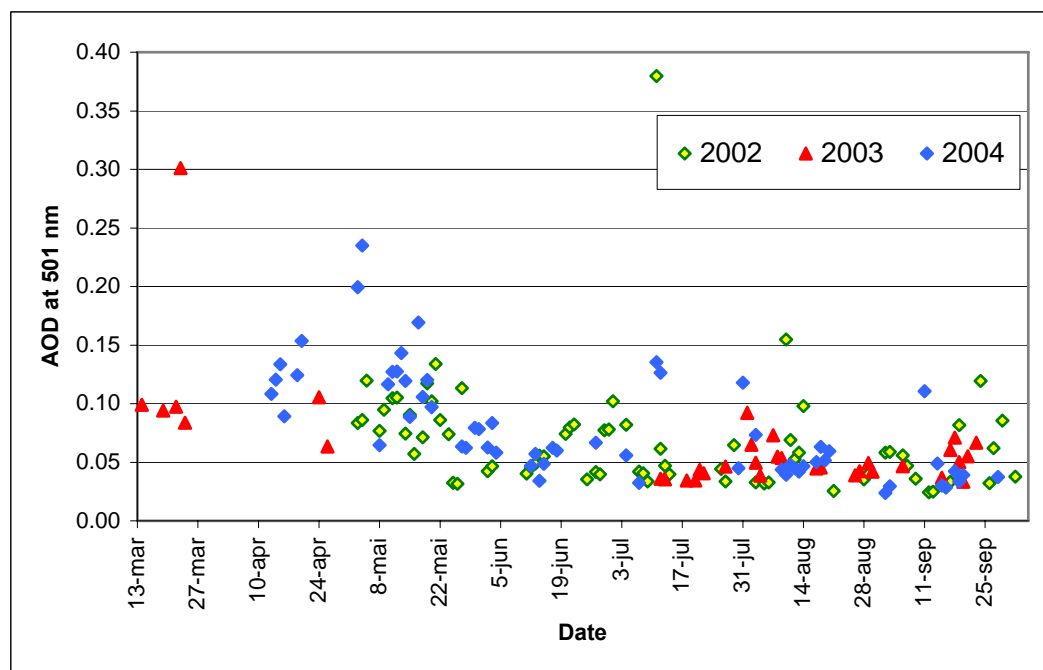


Figure 6.1: Aerosol optical depth at 501 nm measured in Ny-Ålesund during three years

There are a large number of days without results in Figure 6.1. The main problem is that clear sky conditions are needed for having a valid result and that clouds frequently occur at Spitsbergen. There are also more frequent cloudy or foggy conditions near the ground in Ny-Ålesund than at higher levels. After nearly four years with measurements there is therefore a strong desire to replace the measurement from the present location in Ny-Ålesund with measurements at the

nearby site at the Zeppelin mountain at 474 m asl. This will give more frequent valid results. A second problem at the current location is a drift in the pointing of the PFR instrument off the sun disc causing periods of rejected data.

Figure 6.2 presents Ångström's α parameter from its empirical formula for the wavelength dependence of the total haze scattering. $\sigma_A \sim \lambda^{-\alpha}$, where σ_A is the total fraction of light scattered by the particles within 1 cm^3 at the light wavelength λ . The exponent α varies mostly between 0.8 and 1.9 in Ny-Ålesund.

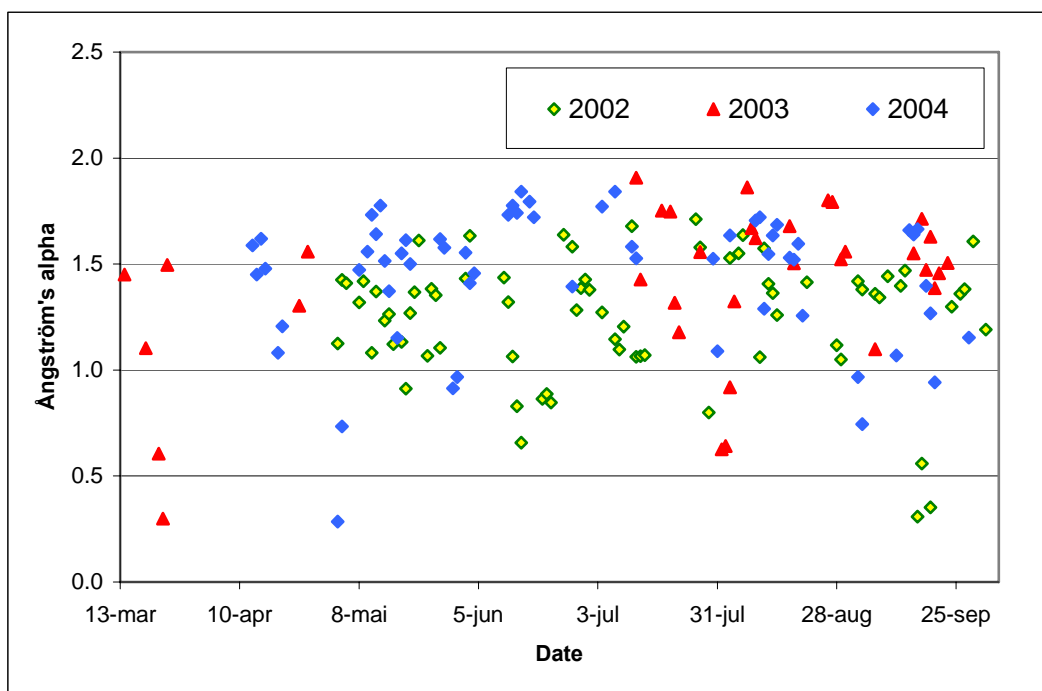


Figure 6.2: Ångström's alpha parameter measured in Ny-Ålesund.

6.2 ATSR-2 retrieved spatial distribution of aerosols over Europe

Algorithms for the retrieval of the aerosol optical depth (AOD) and derived parameters from ATSR-2 measurements have been developed and applied by TNO, The Hague, The Netherlands, for a variety of locations that are representative for the occurrence of characteristic aerosol types (Veefkind, 1999; Veefkind et al., 2000; Robles González et al., 2000; Robles González, 2003). The single view algorithm is applied over water surfaces and uses either the nadir or the forward view. The dual view algorithm is applied over land surfaces, which in general are brighter than water surfaces. The two views are combined to eliminate the effect of the land surface reflectance and the total reflectance received by ATSR at the top of the atmosphere (TOA). The actual retrieval is similar for both views. A radiative transfer model is applied to calculate the TOA reflectance (Doubling-Adding method at KNMI (DAK) (see Stammes, 2001). This is done for several aerosol models and the results are stored in look-up tables (LUT's). The calculated TOA reflectances are compared with the measured values and by selecting different LUT's the error function describing the difference between model and measurement, is minimized to find the most suitable aerosol model.

This procedure is applied for the ATSR-2 wavelengths of 0.55 μm , 0.67 μm , 0.87 μm (only over water) and 1.6 μm and hence the optimisation procedure determines the aerosol mixture that best fits the measurements over the applicable wavelength range. Thus in fact the parameters determined are the AOD at the suitable wavelengths, as well as the Ångström α parameter describing the wavelength dependence of the AOD, and the aerosol type and mixing ratio.

The aerosol types considered over Europe are marine aerosol ($r_{\text{eff}} = 1 \mu\text{m}$) (Shettle & Fenn, 1979) and anthropogenic aerosol (sulphate/nitrate water soluble, $r_{\text{eff}} = 0.05 \mu\text{m}$) (Volz, 1972), which are externally mixed. The vertical structure is described by the Navy Oceanic Vertical Aerosol Model (NOVAM) (de Leeuw et al., 1989). This model appears to work well over Europe, as evidenced from comparison with sun photometer derived AOD values. Other aerosol models have been implemented for areas such as South-East Asia and the Indian Ocean, and Africa (Robles González, 2003).

An important condition to retrieve aerosol properties from space-borne sensing is the absence of clouds. To accomplish this, three tests are applied as described in (Robles González, 2003), i.e. a 12 μm gross cloud test, a reflectance test for 0.67 μm , and a reflectance ratio test (0.67 μm / 0.87 μm). These procedures are based on the work of Koelemeijer et al. (2001). The scientific algorithms described above form the basis for the TNO quasi-operational ATSR-2/AATSR aerosol retrieval algorithm. The algorithm requires the AATSR level 1 GBTR (ATS-TOA-1P) product provided by ESA and delivers an output in ASCII and HDF format that can be used for further level-3 post-processing.

Figure 6.3 shows the AOD maps for August 2000 over Europe and part of North Africa, (20-80N; 20-40E) retrieved from ATSR-2 data. Retrieval is done over cloud-free scenes for the 1 x 1 km^2 sensor resolution and binned in pixels of 10x10 km^2 by means of an automated post-processing step. The final maps, however, cannot be considered as monthly averages; rather they are composites providing information on the spatial variation of aerosols, hot spots and other regions with high aerosol loading. The results are validated by comparison with collocated AERONET sun photometer AOD measurements, within 30 minutes of the satellite overpass. The sunphotometer AOD are determined with accuracy of 0.02. By comparison, the ATSR-2 AOD accuracy over land has been determined as 0.05.

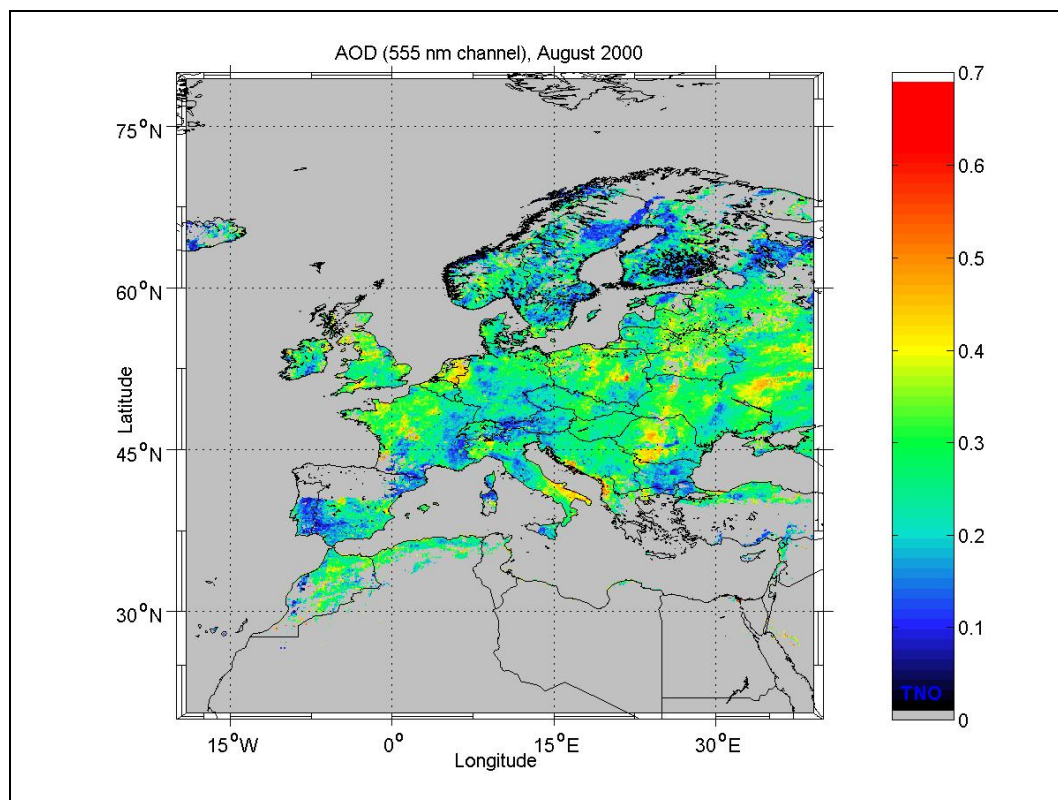


Figure 6.3: Composite that shows the mean AOD for the month of August 2000.

6.3 Synergetic ENVISAT aerosol optical depth and type

Aerosol parameters are retrieved at DLR-DFD with the new method SYNAER (SYNERgetic Aerosol Retrieval; Holzer-Popp et al., 2002a, 2002b) from a combination of simultaneous AATSR and SCIAMACHY measurements. The high spectral resolution of SCIAMACHY ideally supplements the high spatial resolution of AATSR. In this method cloud detection is first performed for all AATSR 1 km pixels with an improved version of the well-established APOLLO method (Kriebel et al., 2003). Secondly, dark fields (dark vegetation, water bodies) are selected automatically from these data by dynamical thresholds for the 1.6 μm and 3.7 μm channels and the Normalized Difference Vegetation Index (NDVI) calculated with the 670 and 870 nm channels. Then aerosol optical depth (AOD) values at 670 nm (over land) and 870 nm (over ocean) are derived for these dark AATSR nadir pixels for which the surface albedo can be estimated with good accuracy from a correlation to the 1.6 micron channel. AOD values over the irregularly distributed dark fields are interpolated to all cloud free AATSR pixels with a distance-weighting scheme. By atmospheric correction, the surface albedo values for the 3 wavelengths 560 nm, 670 nm and 870 nm are obtained for all cloud free pixels. All these AATSR derived parameters are then co-registered to SCIAMACHY pixels and interpolated spatially. AOD and surface albedo calculation is repeated for 40 different aerosol mixtures which are defined by external mixing of basic aerosol components from the OPAC database (Hess et al., 1998), where further differentiation of aerosol components for different absorption features has been added. Using the AATSR calculated values of optical depth and surface albedo, SCIAMACHY surface and consecutively top-of-the-

atmosphere spectra for the same set of different mixtures are simulated at 10 selected wavelengths. The measured SCIAMACHY spectra are corrected for cloud and ozone influence as well as radiometric errors (using simultaneous AATSR reflectances). Typically the simulated spectra do agree within a few percent noise level to the measured spectrum. Thus, a least square fit of the simulated to the measured SCIAMACHY spectrum can be used to select the most plausible type of aerosol and its corresponding AOD value at the reference wavelength of 550 nm inside a SCIAMACHY pixel of 60x30 km². Finally, a quality control and an ambiguity test are applied by comparing the fit error with deviations between different mixtures. A case study validation of the methodology applied to predecessor instruments GOME and ATSR-2 onboard ERS-2 against ground-based AERONET sunphotometer measurements showed proof of the SYNAER capabilities to derive accurate aerosol optical depth values better than 0.10 (0.07) at 670 (440) nm (Holzer-Popp et al., 2002b). Thus the spectral AOD gradient has been well captured indicating also a successful estimation of the type of aerosol between continental, maritime, polluted, desert outbreak and biomass burning / heavily polluted air masses as mixtures of 4 basic aerosol components (sulphate/nitrate, mineral dust, sea salt, soot). In the near future extended and systematic validation will be conducted based on the operational and reprocessed ENVISAT results.

Operational provision of the daily SYNAER ENVISAT aerosol results is currently in a concluding test loop and will be released by 1 September 2005 through the PROMOTE website and the ICSU world data centre for remote sensing of the atmosphere (<http://wdc.dlr.de/>). Results over Europe and Africa will be provided in near-real time. Reprocessing of ENVISAT data back to mid-2002 and the derivation of a 25-year aerosol climatology (1995-2020) with SYNAER applied to similar sensor pairs onboard ERS-2, ENVISAT and METOP is planned.

Figure 6.4 shows the preliminary SYNAER/ENVISAT 1-day overview maps of AOD₅₅₀ and type over Europe for 17 June 2005. Retrieved aerosol optical depth at 550 nm is shown in the upper part. Retrieved percentage contributions to AOD₅₅₀ of the basic aerosol components (depicted as percentage of the pixel area) are shown in the lower (IN/I2=insoluble with high/low absorption, WA=watersoluble, DI/BI= diesel/biomass burning soot, SA/SC=sea salt accumulation/Coarse mode, MT/ML=mineral transported with high/low hematite content; an "X" indicates that a high relative humidity component for hygroscopic aerosols was retrieved). Cloud covered SCIAMACHY pixels above 50% cloud fraction and erroneous pixels with fit error larger than 0.01 are excluded. The image shows the typical daily coverage with SCIAMACHY nadir observations with the large gaps along the orbit due to intermediate limb scan sequences.

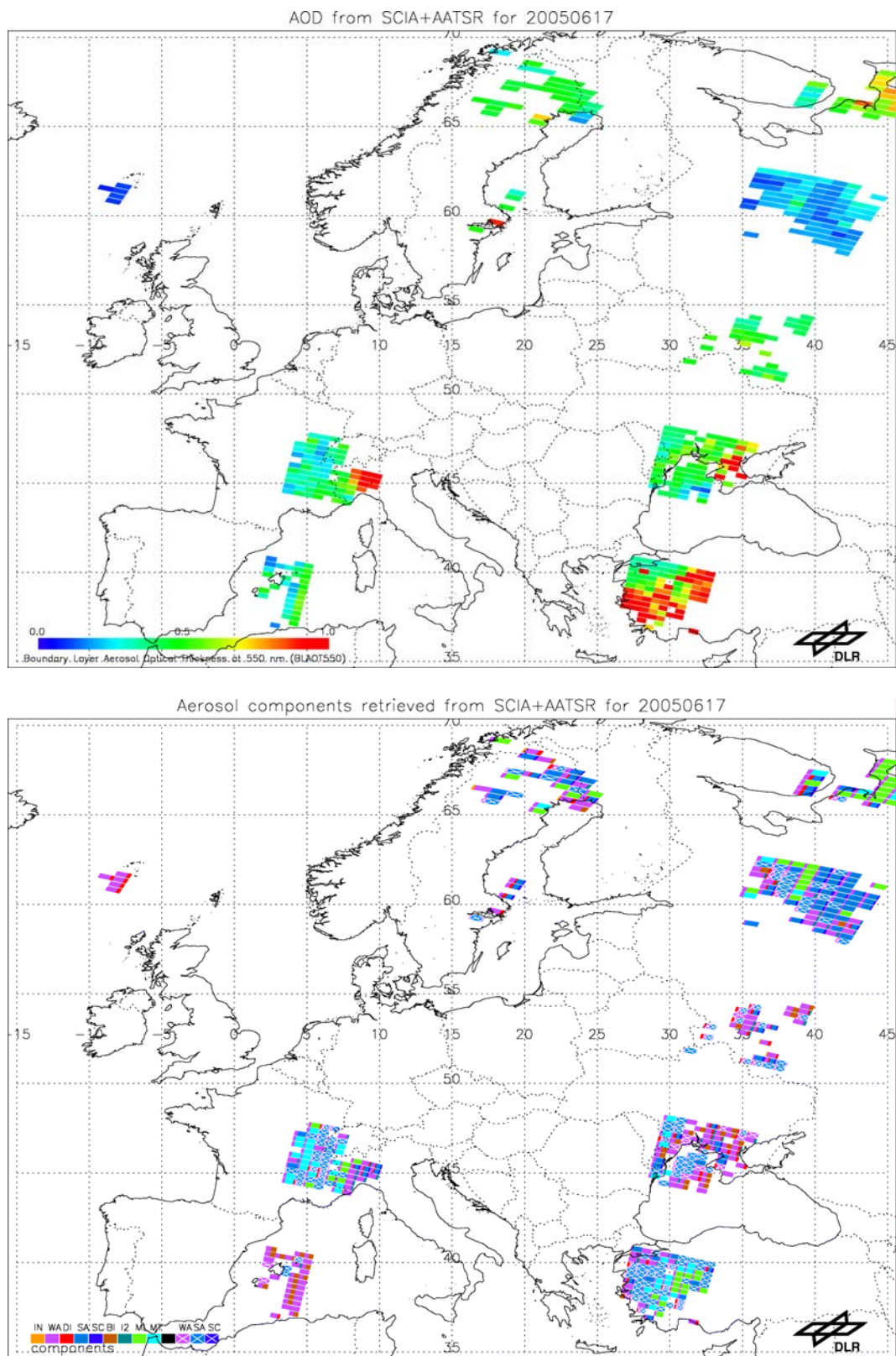


Figure 6.4: SYNAER daily aerosol for 17 June 2005 (upper: AOD550 at 550nm; bottom: contribution of the basic components to AOD550).

7. Construction, use and delivery of an European aerosol database

by S.G. Jennings

7.1 Introduction

CREATE is a Thematic Project initiated under the 5th Framework Programme “Energy, Environment and Sustainable Development” in support of GMES (Global Monitoring for Environment and Security). GMES represents the main European contribution to the Group on Earth Observation (GEO). The project was established to address issues relating to measuring, modelling and monitoring of atmospheric aerosols within the priority theme: Global Atmosphere Monitoring. It has had close synergy with its sister Thematic Project DAEDALUS in the same key action topic: Global Atmosphere Monitoring, sharing a common Description of Work, and participating in joint Workshop Meetings.

The consortium consisted of 11 partners from 9 countries and coordinated by NUI, Galway, Ireland. A web site <http://macehead.nuigalway.ie/create/> facilitated the management and coordination of the project CREATE.

The primary objective of CREATE is: to construct, use and deliver an European aerosol database.

7.2 European Aerosol Database

- a) A European aerosol database has been established at:
www.nilu.no/projects/ccc/create/database.htm
- b) Through CREATE a formal agreement has been sanctioned between NILU which is hosting the EMEP-CCC/NILU database and JRC which hosts the WMO-GAW World Data Centre for Aerosols (WDCA) on establishing a coordinated data flow in order to facilitate data submission. Details of the Agreement can be found on the CREATE web site and on the EMEP web site.

Field Research Stations closely linked to CREATE Partners, which have contributed to the CREATE European Aerosol Database are as follows:

Mace Head Atmospheric Research Station
The High Altitude Research Station Jungfrauoch
Finokalia Station - University of Crete (Greece) – ECPL
Pallas-Sodankylä Research Station
Melpitz Atmospheric Research Station
SMEAR II (Station for Measuring Forest Ecosystem – Atmosphere Relations)
Zeppelin Mountain Atmospheric Research Station

7.3 Descriptions of aerosol data sets, housed at NILU

Data linked to the following aerosol parameters have been submitted to the database:

- Total aerosol number concentration
- Aerosol (PM₁₀, PM_{2.5}) mass concentration
- Aerosol particle size distribution
- Aerosol inorganic composition (nitrate, ammonium, and sulphate)
- Mass concentration of organic (OC), black carbon (BC) and total carbon (TC)
- Aerosol radiative data (aerosol absorption, scattering coefficient, aerosol optical depth at specified wavelengths).

Table 7.1 shows the data submitted to the database by end of March 2005. All data can be downloaded from the Internet at <http://www.nilu.no/projects/ccc/create/database.htm> which has been specially created both for the submission of aerosol data and for access to data. This database is run by EMEP and is housed at NILU, Norway. It caters for all the aerosol parameters cited above except for aerosol optical depth which is submitted to the World Data Centre for Aerosols (WDCA) through its web site: <http://ies.irc.cec.eu.int/wdca/>

Table 7.1: Aerosol data submitted to the database.

Station	Component	Instrument	Time period
CH01 Jungfraujoch	Aerosol absorption coefficient	Aethalometer	1995-2003
	Aerosol light scattering/backscattering coefficient	Nephelometer	1995-2003
	Aerosol number concentration	CPC	1995-2003
	Aerosol number distribution	SMPS	1997-1998
	Aerosol composition	Filterpack	1999-2001
DE43 Hohenpeissenberg	Particle number distribution Total particle number	DMPS	1998-2000
DE44 Melpitz	Particle number distribution Total particle number Chemical composition of PM ₁₀	DMPS High volume PM10 sampler	1996-1997 2003 2000
FI50 Hyytiälä	Particle number distribution Total particle number Particle mass	DMPS 3-stage impactor	1996-2003 1999,2000
FI96 Pallas	Particle number distribution Aerosol number concentration Aerosol light scattering coefficient	DMPS CPC Nephelometer	2000-2003 2000-2003 2002
GR02 Finokalia	Aerosol number concentration Absorption coefficient Aerosol light scattering coefficient Suspended particulate matter Aerosol inorganics	CPC PASP Nephelometer Filterpack Filterpack	1997 2000 2002 1998-1999 1996-1999
IE31 Mace Head	Average attenuation coefficient Particle number distribution Aerosol number concentration Aerosol light scattering coefficient	Aethalometer SMPS CPC Nephelometer	1989-2002 2002-2004 2000-2004 2000-2004
NL11 Cabauw	Nitrate mass distribution	SJAC-MOI	2002
NO01 Birkenes	Particle number distribution EC/OC Aerosol inorganics	DMPS KFG filterpack	2002-2003 2001-2003 1972-2003
NO42 Zeppelin	Particle number distribution Aerosol inorganics	DMPS filterpack	2000-2004 1993-2003

7.4 Technical information on instrumentation, techniques used, meta-data, references, data sources and comments for selected aerosol parameters

Technical information on instrumentation, techniques used, meta-data, references, data sources and comments for selected aerosol parameters shown in Table 7.2 has been compiled and is contained in Appendix B of the CREATE Final Report – accessible from the CREATE web site.

Table 7.2: Selected aerosol parameters

1. Total particle concentration (CPC)
2. Particulate Matter (PM) mass concentration
3. Aerosol particle size distribution
4. Chemical composition of aerosol constituents and size resolved aerosol composition measurements
5. Aerosol scattering coefficient

Table 7.2: The following table is a compilation of the total particle number concentration data sets provided in the CREATE database. The data sets are listed alphabetically after their station code.

No.	Station code	Measurement site	Years	Method/Instrument	Contact person
1	CH01	Jungfraujoch	1995-2003	CPC	Urs Baltensperger, Ernest Weingartner
2	DE43	Hohenpeissenberg	1998-2000	Calculated from DMPS	Wolfram Birmili
3	DE44	Melpitz	1996-1997, 2003	Calculated from DMPS	Wolfram Birmili
4	FI50	Hyytiälä	2000-2003	Calculated from DMPS	Michael Boy, Pasi Aalto
5	FI96	Pallas	2000-2003	CPC 3010	Heikki Lihavainen, Mika Komppula
6	GR02	Finokalia	1997	CPC	Nikos Mihalopoulos
7	IE31	Mace Head	2000-2003	CPC	Gerry Jennings

Technical information on these data sets is provided on the following issues relating to total particle number concentration and is accessible in the CREATE Final Report, Appendix B.

- a) **Instrument** type (i.e., CPC type)
- b) Lower **size cut-off** (either calibrated or presumed)
- c) Type and height of the **inlet** used to sample ambient aerosol
- d) Information on whether a **dryer** was used for sample aerosol or not
- e) Maintenance; quality control
- f) Comments

Table 7.3: The following list compiles the ambient particle size distribution data sets provided in the CREATE database. The data sets are listed alphabetically after their station code.

No.	Station code	Measurement site	Years	Method/Instrument	Contact person
1	CH01	Jungfraujoch	1997-1998	SMPS	Urs Baltensperger, Ernest Weingartner
2	DE43	Hohenpeissenberg	1998-2000	TDMPs	Wolfram Birmili
3	DE44	Melpitz	1996-1997, 2003	TDMPs	Wolfram Birmili
4	FI50	Hyytiälä	1996-2003	TDMPs	Pasi Aalto
5	FI96	Pallas	2000-2003	DMPS	Veli-Matti Kerminen, Mika Komppula
6	IE31	Mace Head	2002-2004	SMPS	Gerry Jennings
7	NO01	Birkenes	2002-2003	DMPS	Kjetil Tørseth
8	NO42	Zeppelin	2000-2004	DMPS	Johan Ström

In the following, technical information on each of these data sets is provided (in the CREATE Final Report, Appendix B) on issues regarding:

- g) **Instrumental components** (DMAs, CPCs, neutralisers, sheath air preparation)
- h) Brief information on **corrections** applied to raw data and type of **inversion**
- i) Type and height of the **inlet** used to sample ambient aerosol
- j) Information on whether a **dryer** was used for sample aerosol or not
- k) **Maintenance; quality control**
- l) **Comments**

Table 7.4: The following Table summarizes aerosol chemical composition data sets provided in the CREATE database. The data sets are listed alphabetically after their station code.

No.	Station code	Measurement site	Years	Method/Instrument Chemical Species	Contact person
1	CH01	Jungfrauoch	1999-2001	Filterpack - Inorganics	Urs Baltensperger, Ernest Weingartner
3	DE44	Melpitz	2000	High Volume PM10	Wolfram Birmili
6	GR02	Finokalia	1996-1999 1998-1999	Filterpack- Inorganics Filterpack-SPM	Nikos Mihalopoulos
8	NL11	Cabauw	2002	SJAC-MOI - Nitrate	Harry ten Brink
9	NO01	Birkenes	2001-2003	KFG - EC/OC	Kjetil Torseth
10	NO42	Zeppelin	1993-2003	Filterpack - inorganics	Kjetil Torseth

7.5 Summary

Guidelines on aerosol chemical measurements at WMO GAW stations are documented by Baltensperger et al. (2003). That report gives a detailed account of sampling details of aerosol chemical measurements and includes detailed descriptions of:

- (a) Recommended chemical sampling techniques and analysis
- (b) Sampling media and methods
- (c) Sampling set-up for aerosol chemical analysis
- (d) Flow measurements
- (e) Sampling frequency
- (f) Recommended analyses
- (g) Sample handling protocol
- (h) Continuous instrumentation
- (i) Quality assurance and quality control

Further detail on two of the dominant nitrogen-containing compounds in airborne aerosols – that of nitrate and ammonium is given in Section 6 of the Final Report of CREATE. This includes a description of filter types (inert filters, impregnated filters etc), artefacts, sampling methods using denuder filter packs, and impactors with filters. A more detailed discussion is included together with a useful reference list.

Carbon is a dominant component of the European aerosol. However, the actual concentrations are as yet uncertain, because of severe problems in collection and analysis of the compounds containing the carbon. Therefore it is considered premature to give a definitive description of measurement details as more research is needed towards an artefact-free and generally agreed procedure for the determination of TC, OC, EC, and BC.

7.5.1 Size resolved aerosol composition measurements

Data on size resolved aerosol composition measurements, and source of the data are based on a comprehensive literature search and are described in Appendix B of the CREATE Final Report.

Since reviews on measurement involving two size fractions are available (Van Dingenen et al., 2004; Putaud et al., 2004), only data covering a minimum of three size fractions were included in this report. In principle, only data covering more than a two-week measurement period were accepted. Shorter time periods were included in case the measured particle size-resolution was exceptionally good. Data published in the literature were preferred over unpublished data. No data measured prior to 1980 were accepted.

The available data was first divided into three categories based on the measured quantity: 1) gravimetric mass, 2) elements and 3) inorganic (and organic) ions. Very few size-segregated measurements on various components associated with carbonaceous were available, so these data were not included here.

Basic information associated with the available data was listed when available. These are the name of the measurement site, its location, measurement period, number of collected samples, number of size ranges measured, and relevant literature references.

Table 7.5: The following Table is a compilation of aerosol scattering coefficient data sets provided in the CREATE database. The data sets are listed alphabetically after their station code.

No.	Station code	Measurement site	Years	Method/Instrument	Contact person
1	CH01	Jungfrauoch	1995-2003	Nephelometer	Urs Baltensperger, Ernest Weingartner
2	DE43	Hohenpeissenberg	Submitted to WDCA	Nephelometer	Wolfram Birmili
5	FI96	Pallas	2002	Nephelometer	Veli-Matti Kerminen, Mika Komppula
6	GR02	Finokalia	2002	Nephelometer	Nikos Mihalopoulos
7	IE31	Mace Head	2000-2004	Nephelometer	Gerry Jennings

The aerosol light scattering coefficient, σ_{sp} , is measured with an integrating nephelometer (see e.g., Heintzenberg and Charlson, 1996). At present, there are about a dozen sites monitoring σ_{sp} routinely around the globe, and many of them are part of the WMO GAW global network. A few of these are operating single-

wavelength units, but most are measuring σ_{sp} at three wavelengths. At present, there is only one multi-wavelength integrating nephelometer that is commercially available: the TSI model 3563 (TSI, Inc., St. Paul, USA). This instrument operates at wavelengths of 450, 550, and 700 nm, and has the added feature of being able to measure σ_{sp} over two angular ranges: total scattering (7-170° degrees) and hemispheric backscattering (90-170°, denoted as σ_{bsp}).

A detailed account of measurement guidelines (standard operating procedures) and calibration procedures for measurement of aerosol scattering coefficient is given in Appendix H of the CREATE Final Report.

8. References

- Baltensperger, U. et al. (2003) Aerosol measurement procedures, guidelines and recommendations. Geneva, WMO (WMO/GAW Report No. 153).
- Bergametti, G., Dutot, A.-L., Buat-Ménard, P., Losno, R. and Remoudaki, E. (1989) Seasonal variability of the elemental composition of atmospheric aerosol particles over the Northwestern Mediterranean. *Tellus*, 41B, 353-361.
- Danalatos D. and Glavas S. (1999) Gas phase nitric acid, ammonia and related particulate matter at a Mediterranean coastal site, Patras, Greece. *Atmos. Environ.*, 33, 3417-3425.
- de Leeuw, G., Davidson, K.L., Gathman, S.G. and Noonkester, R.V. (1989) Modeling of aerosols in the marine mixed-layer. In: *Propagation Engineering*. Ed. by N.S. Kopeika and W.B. Miller. Bellingham (SPIE Proceedings, 1115). pp. 287-294.
- Draxler, R.R. (1994) Hybrid single-particles Lagrangian integrated trajectories. Version 3.2 NOAA-ARL.
- Dulac, F., Buat-Ménard, P., Arnold, M., Ezat, U. and Martin, D. (1987) Atmospheric input of trace metals to the Western Mediterranean Sea: 1. Factors controlling the variability of atmospheric concentrations. *J. Geophys. Res.*, 92, 8437-8453.
- Dye, C. and Yttri, K.E. (2005) Determination of monosaccharide anhydrides in atmospheric aerosols by use of high-resolution mass spectrometry combined with high performance liquid chromatography. *Anal. Chem.*, 77, 1853-1858.
- EMEP (2003) Transboundary particulate matter in Europe. Ed. by M. Kahnert and L. Tarrasón. Kjeller, Norwegian Institute for Air Research (EMEP Report 4/2003).
- EMEP/CCC (2003) Measurements of particulate matter: Status report 2003. Ed. by M. Kahnert. Kjeller, Norwegian Institute for Air Research (EMEP/CCC-Report 5/2003).
- EMEP/CCC (2004) Measurements of particulate matter: Status report 2004. Ed. by J. Schaug. Kjeller, Norwegian Institute for Air Research (EMEP/CCC-Report 3/2004).
- European Commission (2001) A global strategy for atmospheric interdisciplinary research in the European research area, AIREs in ERA. Luxembourg, Office for Official Publications of the European Communities (Air Pollution Research Report 76) (EUR 19436).
- Fine, P.M., Cass, G. and Simoneit, B.R.T. (2001) Chemical characterization of fine particle emissions from fireplace combustion of woods grown in the Northeastern United States. *Environ. Sci. Technol.*, 35, 2665-2675.

- Fine, P.M., Cass, C.R. and Simoneit, B.R.T. (2002a) Organic compounds in biomass smoke from residential wood combustion: Emissions characterization at a continental scale. *J. Geophys. Res.*, *107D*, 8349, doi: 10.1029/2001JD000661.
- Fine, P.M., Cass, G. and Simoneit, B.R.T. (2002b) Chemical Characterization of Fine Particle Emissions from the Fireplace Combustion of Woods Grown in the Southern United States. *Environ. Sci. Technol.*, *36*, 1442-1451.
- Fine, P.M., Cass, G.R. and Simoneit, B.R.T. (2004) Chemical characterization of fine particle emissions from the fireplace combustion of wood types grown in the Southern Midwestern and Western United States. *Environ. Eng. Sci.*, *21*, 387-409.
- Graham, B., Guyon, P., Taylor, P.E., Artaxo, P., Maenhaut, W., Glovsky, M.M., Flagan, R.C. and Andreae, M.O. (2003) Organic compounds present in the natural Amazonian aerosol: Characterization by gas chromatography-mass spectrometry. *J. Geophys. Res.*, *108D*, 4766, doi: 10.1029/2003JD003990.
- Gray, H.A., Cass, G.R., Huntzicker, J.J., Heyerdahl, E.K. and Rau, J.A. (1986) Characterization of atmospheric organic and elemental carbon particles concentrations in Los-Angeles. *Environ. Sci. Technol.*, *20*, 580-589.
- Guerzoni, S., Correggiari, I. and Miserochi, S. (1990) Wind-blown particles from ships and land-based stations in the Mediterranean Sea: A review of trace metal sources. *Water Poll. Res. Rep.*, *20*, 377-386.
- Hawthorne, S.B., Miller, D.J., Langenfeld, J.J. and Krieger, M.S. (1992) PM-10 High-volume collection and quantification of semi- and nonvolatile phenols, methoxylated phenols, alkanes, and polycyclic aromatic hydrocarbons from winter urban air and their relationship to wood smoke emissions. *Environ. Sci. Technol.*, *26*, 2251-2262.
- Heintzenberg, J. and Charlson, R.J. (1996) Design and applications of the integrating nephelometer: a review. *J. Atmos. Oceanic Technol.*, *13*, 987-1000.
- Hess, M., Köpke, P. and Schult, I. (1998) Optical Properties of Aerosols and Clouds: The Software package OPAC. *Am. Meteorol. Soc. Bull.*, *79*, 831-844.
- Holzer-Popp, T., Schroedter, M. and Gesell, G. (2002a) Retrieving aerosol optical depth and type in the boundary layer over land and ocean from simultaneous GOME spectrometer and ATSR-2 radiometer measurements, 1, Method description. *J. Geophys. Res.*, *107D*, 4578, doi: 10.1029/2001JD002013.
- Holzer-Popp, T., Schroedter, M. and Gesell, G. (2002b) Retrieving aerosol optical depth and type in the boundary layer over land and ocean from simultaneous GOME spectrometer and ATSR-2 radiometer measurements, 2, Case study application and validation. *J. Geophys. Res.*, *107D*, 4770, doi: 10.1029/2002JD002777.

- Kahnert, M. and Kylling, A. (2004) Radiance and flux simulations for mineral dust aerosols: Assessing the error due to using spherical or spherical model particles. *J. Geophys. Res.*, 109, D20203, doi: 10.1029/2003JD004318.
- Kerminen, V.M., Pirjola, L. and Kulmala, M. (2001) How significantly does coagulation limit atmospheric particle production? *J. Geophys. Res.*, 106D, 24119-24125.
- Kerr, R.A. (2003) Climate Change: Warming Indian Ocean wringing moisture from the Sahel. *Science*, 302, 210-211.
- Kiss, G., Varga, B., Galambos, I. and Ganszky, I. (2002) Characterization of water-soluble organic matter isolated from atmospheric fine aerosol. *J. Geophys. Res.*, 107D, 8339, doi: 10.1029/2001JD000603.
- Kleefeld, S., Hoffer, A., Krivácsy and Jennings, S.G. (2002) Importance of organic and black carbon in atmospheric aerosols at Mace Head, on the west coast of Ireland. *Atmos. Environ.*, 36, 4479-4490.
- Kleeman, M.J., Schauer, J.J. and Cass, G. (1999) Size and composition distribution of pine particulate matter emitted from wood burning, meat charbroiling, and cigarettes. *Environ. Sci. Technol.*, 33, 3516-3523.
- Koelemeijer, R.B.A., Stammes, P., Hovenier, J.W. and de Haan, J.D. (2001) A fast method for retrieval of cloud parameters using oxygen-A band measurements from the Global Ozone Measurement Instrument. *J. Geophys. Res.*, 106D, 3475-3490.
- Kriebel, K.T., Gesell, G., Kästner, M. and Mannstein, H. (2003) The cloud analysis tool APOLLO: Improvements and Validation. *Int. J. Remote Sens.*, 24, 2389-2408.
- Krivácsy, Z., Hoffer, A., Sarvari, Z., Temesi, D., Baltensperger, U., Nyeki, S., Weingartner, E., Kleefeld, S. and Jennings, S.G. (2001) Role of organic and black carbon in the chemical composition of atmospheric aerosol at European background sites. *Atmos. Environ.*, 35, 6231-6244.
- Lelieveld, J. et al. (2002) Global air pollution crossroads over the Mediterranean. *Science*, 298, 794-799.
- Luria, M., Peleg, M., Sharf, G., Tov-Alper, D.S., Spitz, N., Ben Ami, Y., Gawii, Z., Lifschitz, B., Yitzchaki, A. and Seter, I. (1996) Atmospheric sulfur over the East Mediterranean region. *J. Geophys. Res.*, 101D, 25917-25930.
- Mader, B.T., Yu, J.Z., Xu, J.H., Li, Q.F., Wu, W.S., Flagan, R.C. and Seinfeld, J.H. (2004) Molecular composition of the water-soluble fraction of atmospheric carbonaceous aerosols collected during ACE-Asia. *J. Geophys. Res.*, 109D, D06206, doi: 10.1029/2003JD004105.
- Maenhaut, W., Ptasiński, J. and Cafmeyer, J. (1999) Detailed mass size distributions of atmospheric aerosol species in the Negev desert, Israel, during ARACHNE-96. *Nucl. Instrum. Meth. B*, 150, 422-427.

- Mayol-Bracero, O.L., Guyon, P., Graham, B., Roberts, G., Andreae, M.O., Decesari, S., Facchini, M.C., Fuzzi, S. and Artaxo, P. (2002) Water-soluble organic compounds in biomass burning aerosols over Amazonia - 2. Apportionment of the chemical composition and importance of the polyacidic fraction. *J. Geophys. Res.*, *107D*, 8091, doi: 10.1029/2001JD003249.
- Meehl, G.A. and Tebalki, C. (2004) More intense, more frequent, and longer lasting heat waves in the 21st century. *Science*, *305*, 994-997.
- Millán, M.M., Salvador, R., Mantilla, E. and Kallos, G. (1997) Photooxidant dynamics in the Mediterranean basin in summer: Results from European research projects. *J. Geophys. Res.*, *102D*, 8811-8823.
- Myhre, G. and Stordal, F. (2001) Global sensitivity experiments of the radiative forcing due to mineral aerosols. *J. Geophys. Res.*, *106D*, 18193-18204.
- NOAA Air Resources Laboratory (2002) 'Archived backward trajectories' at <https://www.arl.noaa.gov/ready/sec/hysplit4.html>.
- Novakov, T. and Corrigan, C.E. (1996) Cloud condensation nucleus activity of the organic component of biomass smoke particles. *Geophys. Res. Lett.*, *23*, 2141-2144.
- Pal, J.S., Giorgi, F. and Bi, W. (2004) Consistency of recent European summer precipitation trends and extremes with future regional climate projections. *Geophys. Res. Lett.*, *31*, L13202, doi:10.129/2004GL019836.
- Putaud, J.P., Raes, F., Van Dingenen, R., Brüggemann, E., Facchini, M.C., Decesari, S., Fuzzi, S., Gehrig, R., Hüglin, C., Laj, P., Lorbeer, G., Maenhaut, W., Mihalopoulos, N., Müller, K., Querol, X., Rodriguez, S., Schneider, J., Spindler, G., ten Brink, H., Tørseth, K., Wiedensohler, A. (2004) A European aerosol phenomenology-2: chemical characteristics of particulate matter at kerbside, urban, rural and background sites in Europe. *Atmos. Environ.*, *38*, 2579-2595.
- Ramdahl, T., Schjoldager, J., Currie, L.A., Hanssen, J.E., Møller, M., Klouda, G.A. and Alfheim, I. (1984) Ambient impact of residential wood combustion in Elverum, Norway. *Sci. Total Environ.*, *36*, 81-90.
- Robles González, C. (2003) Retrieval of aerosol properties using ATSR-2 observations and their interpretation. Ph. D Thesis. Utrecht, Utrecht University.
- Robles González, C., Veefkind, J.P. and de Leeuw, G. (2000) Aerosol optical depth over Europe in August 1997 derived from ATSR-2 data. *Geophys. Res. Lett.*, *27*, 955-958.
- Rodriguez, S., Querol, X., Alastuey, A. and Mantilla, E. (2002) Origin of high summer PM₁₀ and TSP concentrations at rural sites in Eastern Spain. *Atmos. Environ.*, *36*, 3101-3112.

- Rodriguez, S., Querol, X., Alastuey, A., Viana M. M. and Alarcon, M. (2004) Comparative PM₁₀-PM_{2.5} source contribution study at rural, urban and industrial sites during PM episodes in Eastern Spain. *Sci. Tot. Environ.*, 328, 95-113.
- Ruellan, S. and Cachier, H. (2001) Characterisation of fresh particulate vehicular exhaust near a Paris high flow road. *Atmos. Environ.*, 35, 453-468.
- Seinfeld, J.H. and Pandis, S.N. (1998) Atmospheric chemistry and physics. New York, Wiley.
- Shettle, E.P. and Fenn, R.W. (1979) Models for the aerosols of the lower atmosphere and the effects of humidity variations on their optical properties. Hanscom, Air Force Geophysics Laboratory (Environmental Research Papers, 676; AFGL-TR-79-0214).
- Stammes, P. (2001) Manual for the DAK program. De Bilt, Royal Netherlands Meteorological Institute.
- Tunved, P., Hansson, H.-C., Kulmala, M., Aalto, P., Viisanen, Y., Karlsson, H., Kristensson, A., Swietlicki, E., Dal Maso, M., Ström, J. and Komppula, M. (2003a) A one-year study of the Nordic aerosol. *Atmos. Chem. Phys. Discuss.*, 3, 2783-2833.
- Tunved, P., Hansson, H.-C., Kulmala, M., Aalto, P., Viisanen, Y., Karlsson, H., Kristensson, A., Swietlicki, E., Dal Maso, M., Ström, J. and Komppula, M. (2003b) One year boundary layer aerosol size distribution data from five Nordic background stations. *Atmos. Chem. Phys.*, 3, 2183-2205.
- Turpin, B.J. and Lim, H.-J. (2001) Species contributions to PM_{2.5} mass concentrations: Revisiting common assumptions for estimating organic mass. *Aerosol Sci. Technol.*, 35, 602-610.
- Van Dingenen, R., Raes, F., Putaud, J.P., Baltensperger, U., Charron, A., Facchini, M.C., Decesari, S., Fuzzi, S., Gehrig, R., Hansson, H.C., Harrison, R.M., Hüglin, C., Jones, A.M., Laj, P., Lorbeer, G., Maenhaut, W., Palmgren, F., Querol, X., Rodriguez, S., Schneider, J., ten Brink, H., Tunved, P., Tørseth, K., Wehner, B., Weingartner, E., Wiedensohler, A. and Wåhlin, P. (2004) A European aerosol phenomenology-1: physical characteristics of particulate matter at kerbside, urban, rural and background sites in Europe. *Atmos. Environ.*, 38, 2561-2577.
- Veefkind, J.P. (1999) Aerosol Satellite Remote Sensing. Ph.D Thesis. Utrecht, Utrecht University.
- Veefkind, J.P., de Leeuw, G., Stammes, P. and Koelemeijer, R.B.A. (2000) Regional distribution of aerosol over land, derived from ATSR-2 and GOME. *Remote Sens. Environ.*, 74, 377-386.
- Volz, F.E. (1972) Infrared refractive index of atmospheric aerosol substances. *Appl. Optics*, 11, 755-759.

- Wehrli, C. (2005) *GAWPFR: A network of Aerosol Optical Depth observations with Precision Filter Radiometers*. In: *WMO/GAW Experts workshop on a global surface based network for longterm observations of column aerosol optical properties*. Report GAW No. 162 (WMO TD No. 1287). pp. 36-39.
URL: <http://www.wmo.ch/web/arep/gaw/gawreports.html>.
- World Meteorological Organisation (2004) *The changing atmosphere. An integrated global atmospheric chemistry observation theme for the IGOS partnership*. Report GAW No. 159 (WMO TD No. 1235).
URL: <http://www.wmo.ch/web/arep/gaw/gawreports.html>.
- Yttri, K.E., Dye, C., Braathen, O.-A. and Steinnes, E. (2005a) *Ambient aerosol concentrations of elemental carbon, organic carbon, water-insoluble organic carbon and water-soluble organic carbon at three different sites in Norway*. Submitted to *Atmos. Environ.*
- Yttri, K.E., Dye, C., Slørdal, L.H. and Braathen, O.-A. (2005b) *Quantification of monosaccharide anhydrides by negative electrospray HPLC/HRMS-TOF – Application to aerosol samples from an urban and a suburban site influenced by small scale wood burning*. *J. Air & Waste Managem. Assoc.* In press.
- Yttri, K.E. and Kahnert, M. (2004) *Preliminary results from the EMEP EC/OC-campaign*. In: *Measurements of particulate matter: Status report 2004*. Ed. by J. Schaug, Kjeller, Norwegian Institute for Air Research (EMEP/CCC-Report 3/2004). pp. 17-29.
- Zdráhal, Z., Oliveira, J., Vermeylen, R., Claeys, M. and Maenhaut, W. (2002) *Improved method for quantifying levoglucosan and related monosaccharide anhydrides in atmospheric aerosols and application to samples from urban and tropical locations*. *Environ. Sci. Technol.*, 36, 747-757.

Annex 1

Overview of sampling methods for particulate matter 2003

Country: Austria			Year: 2003	
	Station	Sampling	Sampling frequency	Analysis method
PM ₁₀	All	High Volume Sampler, glass fibre filters with organic binder, 720 m ³ /day, EN 12341	Daily	Micro balance
PM _{2.5}	AT02	High Volume Sampler, glass fibre filters with organic binder, 720 m ³ /day, EN 12341	Daily	Micro balance
PM ₁	AT02	High Volume Sampler, glass fibre filters with organic binder, 720 m ³ /day, EN 12341	Daily	Micro balance

Country: Denmark			Year: 2003	
	Station	Sampling	Sampling frequency	Analysis method
PM ₁₀	DK 05	Millipore RAWP in a SM200-monitor, 22 m ³ /day	Daily	Gravimeetric

Country: Germany			Year: 2003	
	Station	Sampling	Sampling frequency	Analysis method
PM ₁₀	All	Digitel High Volume Sampler DHA 80, round aerosol filters ø15 cm, Machery Nagel MN 85/90	Daily	Gravimetric by weight
PM _{2.5}	DE02, DE04, DE05	Digitel High Volume Sampler DHA 80, round aerosol filters ø15 cm, Machery Nagel MN 85/90	Daily	Gravimetric by weight

Country: Italy: IT01 (lab.: CNR)			Year: 2003	
	Station	Sampling	Sampling frequency	Analysis method
PM ₁₀	IT01	Beta gauge monitor 24 m ³ /day	Daily	Beta gauge monitor

Country: Italy, IT04 (lab.: JRC)			Year: 2003	
	Station	Sampling	Sampling frequency	Analysis method
PM ₁₀		Whatman quartz fibre filter QFF, 55 m ³ /day	Daily	Weighing at 50% RH
PM _{2.5}		Whatman quartz fibre filter QFF, 55 m ³ /day	Daily	Weighing at 50% RH

Country: Norway			Year: 2003	
	Station	Sampling	Sampling frequency	Analysis method
PM ₁₀	NO01	Dichotomous sampler, Pall Zefluor, 24 m ³ /day	Daily	Weighing at 50% RH
	NO01	Dichotomous sampler, Pall Zefluor, 24 m ³ /day	Daily	Weighing at 50% RH

Country: Slovakia			Year: 2003	
Main components and ozone - EMEP				
	Station	Sampling	Sampling frequency	Analysis method
PM ₁₀	SK04, SK05, SK06	Partisol R&P, Sartorius nitrocellulose filter, 24 m ³ /day	Weekly	Gravimetric method
Suspended particulate matter	SK02, SK07	Sartorius nitrocellulose filter, 8-10 m ³ /day	Weekly	Gravimetric method

Country: Slovenia			Year: 2003	
Main components and ozone - EMEP				
	Station	Sampling	Sampling frequency	Analysis method
PM ₁₀	SI08	Low volume sampler, 2.3 m ³ /h, Quartz filter, Schleicher and Schuell 47 mm	Daily	Gravimetric method

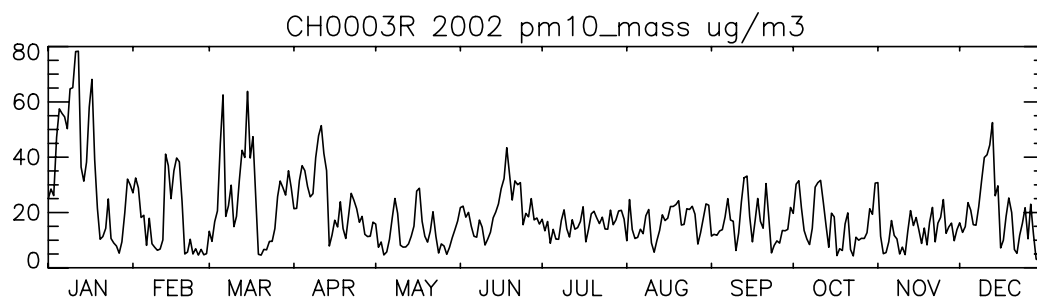
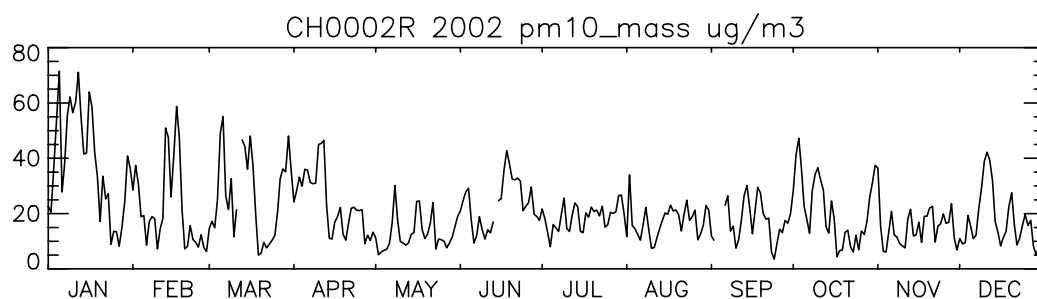
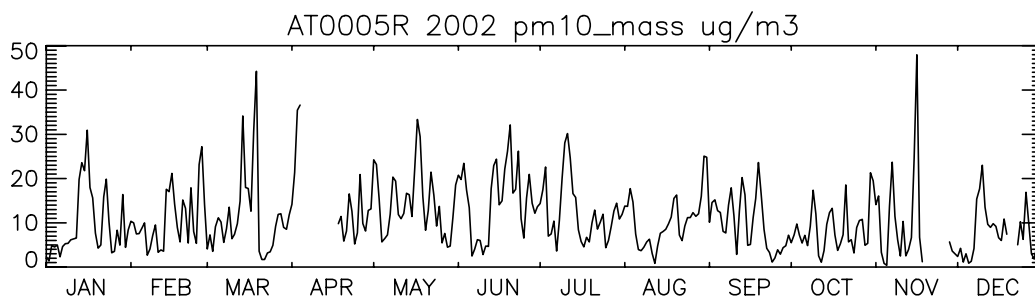
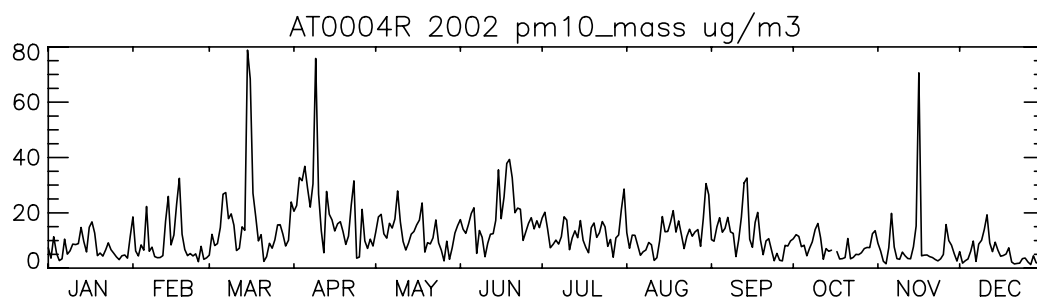
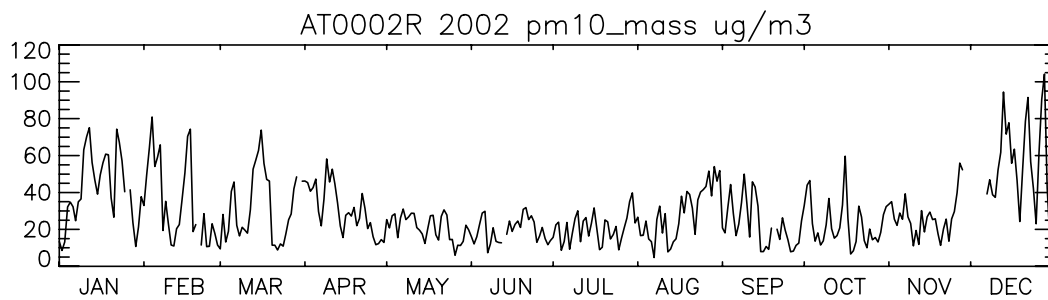
Country: Spain		Main components and ozone - EMEP	Year: 2003	
	Station	Sampling	Sampling frequency	Analysis method
PM ₁₀	All		Daily	Gravimetric method
PM _{2.5}	All		Daily	Gravimetric method

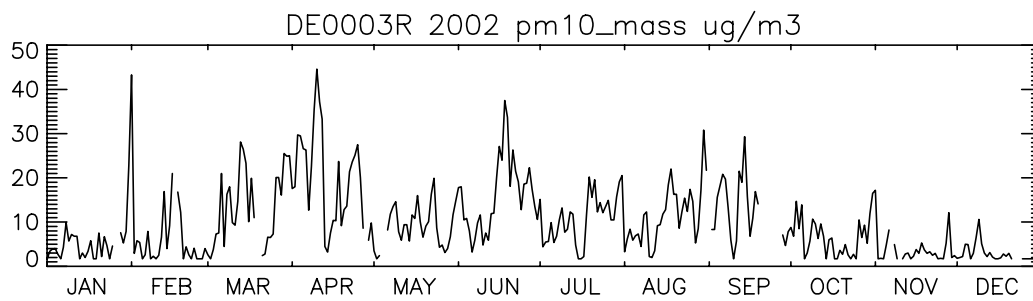
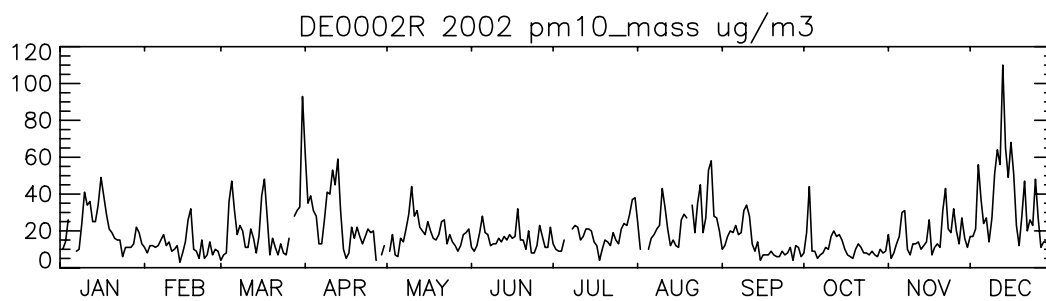
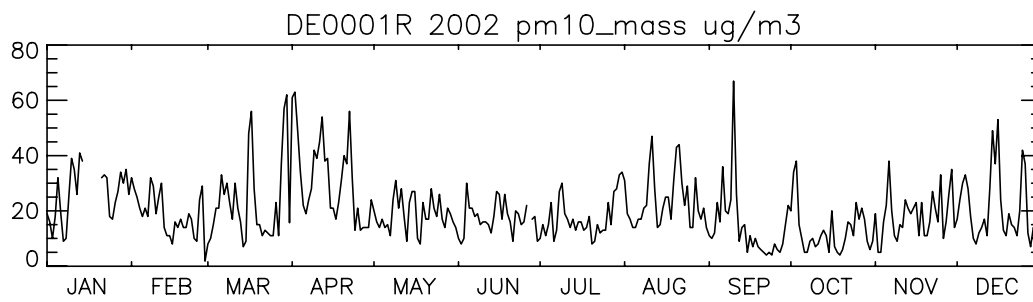
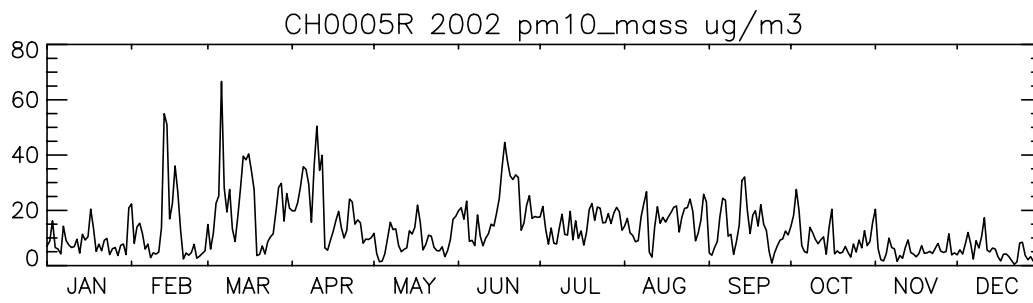
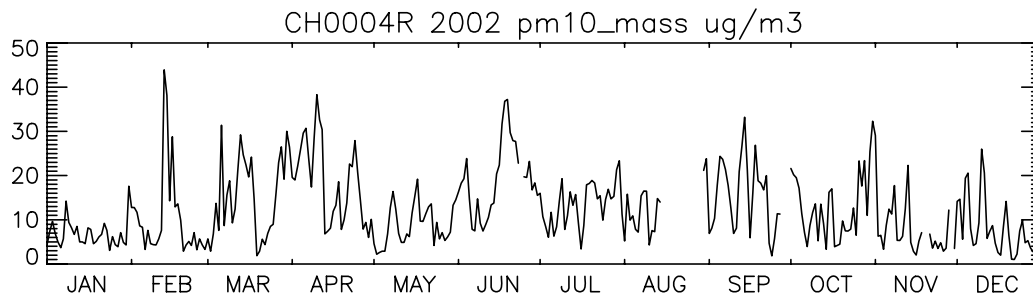
Country: Sweden		Main components and ozone - EMEP	Year: 2003	
	Station	Sampling	Sampling frequency	Analysis method
PM ₁₀		TEOM (Tapered Element Oscillating Microbalance)	Hourly	TEOM
PM _{2.5}		TEOM (Tapered Element Oscillating Microbalance)	Hourly	TEOM
Suspended particulate matter	All	Black smoke on Whatman-filter	Daily	Reflectance

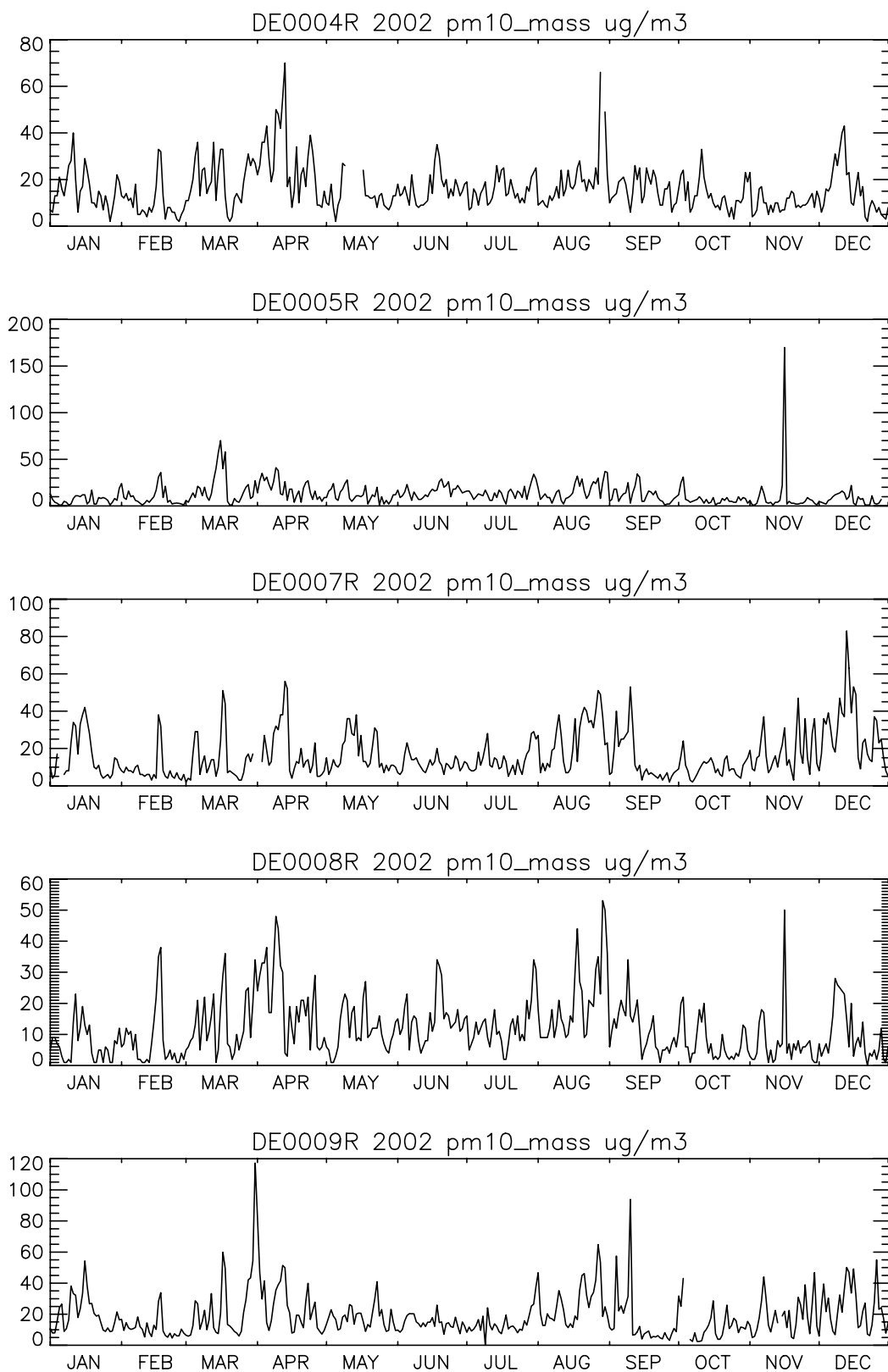
Country: Switzerland		Main components and ozone - EMEP	Year: 2003	
	Station	Sampling	Sampling frequency	Analysis method
PM ₁₀	All	High Volume Samplers, Ederol 227/1/60, 720 m ³ /day	Daily (CH01 2-day-samples)	Gravimetry
PM _{2.5}	CH02, CH04	High Volume Samplers, Ederol 227/1/60, 720 m ³ /day	Daily	Gravimetry
PM ₁	CH04	High Volume Samplers, Ederol 227/1/60, 720 m ³ /day	Daily	Gravimetry

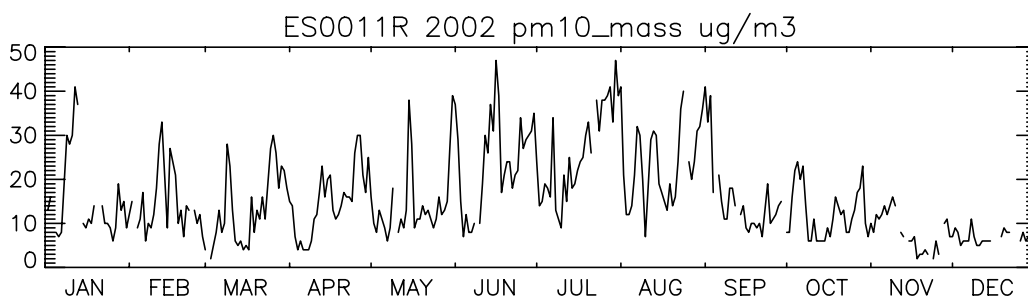
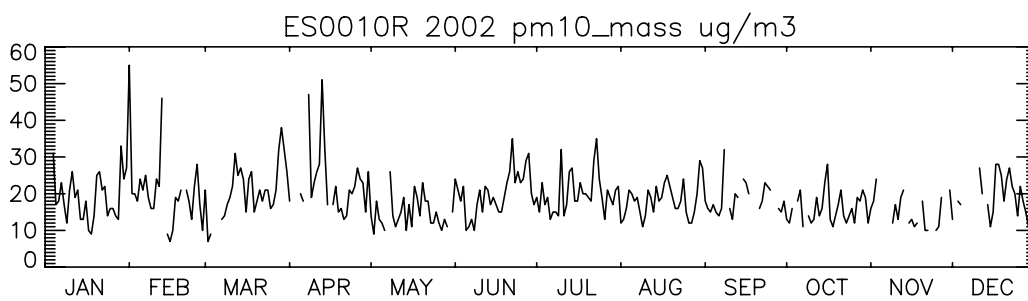
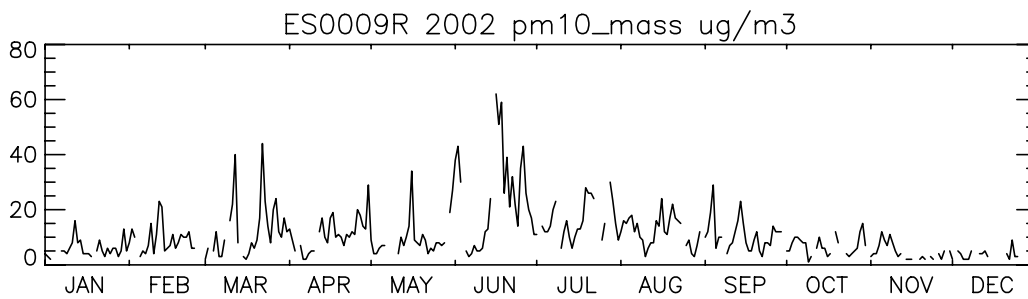
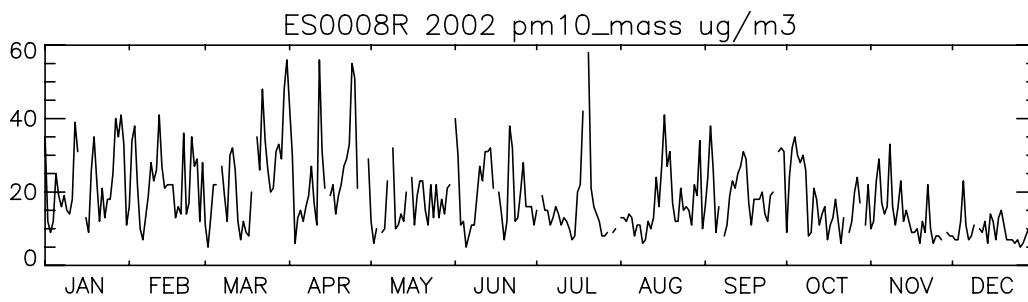
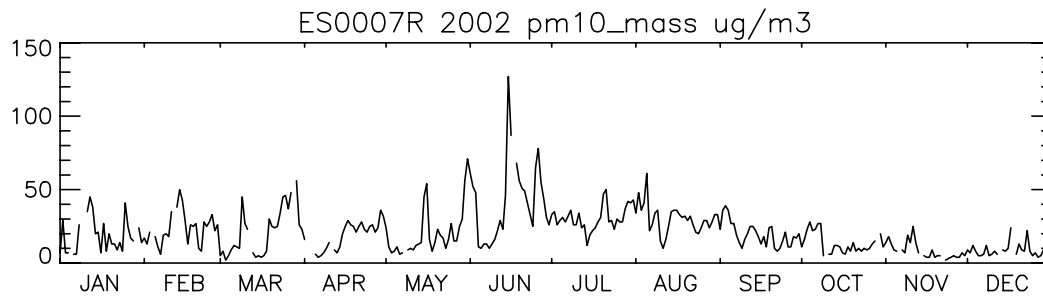
Annex 2

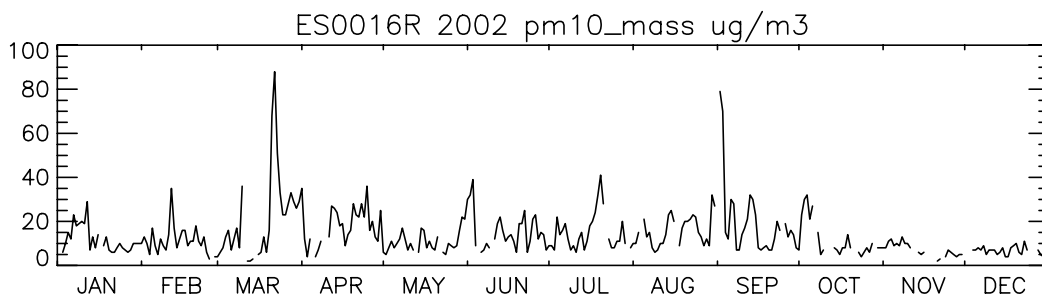
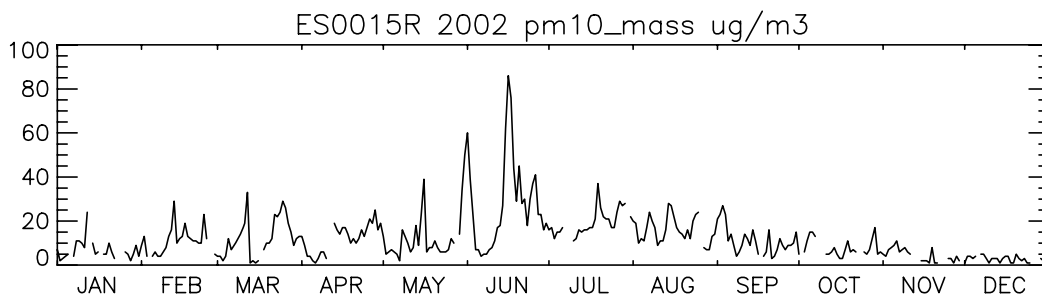
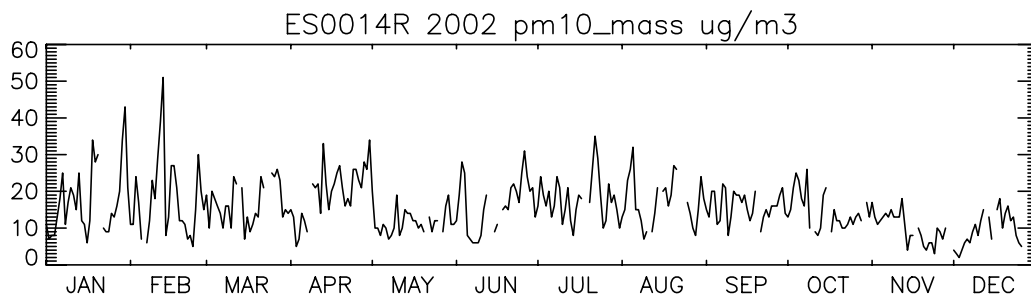
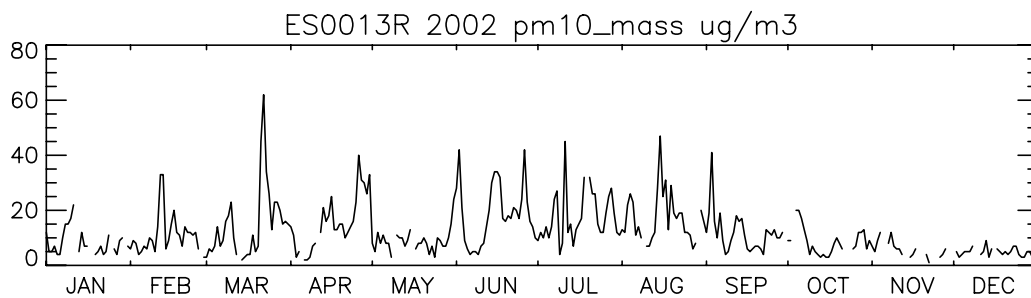
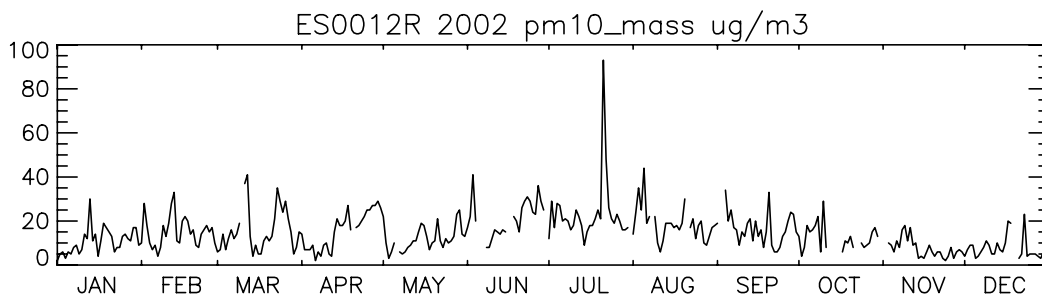
Time series of particulate matter mass concentrations at EMEP stations in 2002 and 2003

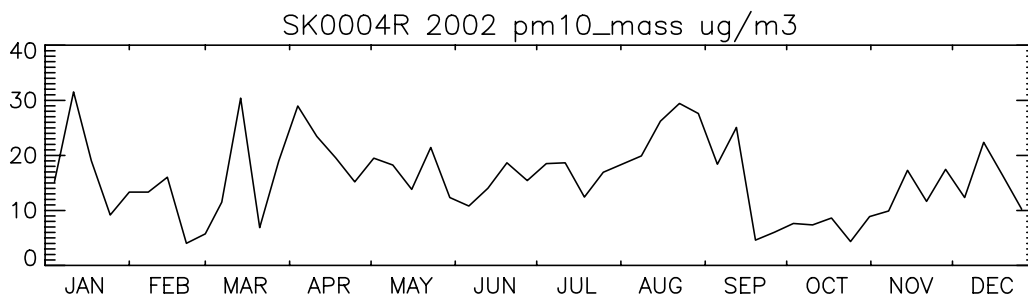
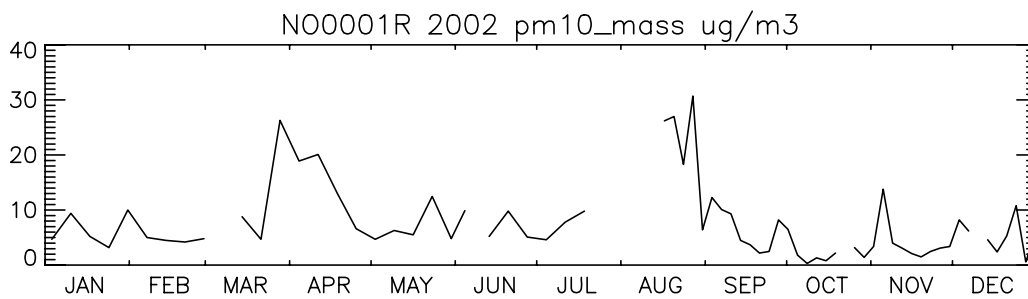
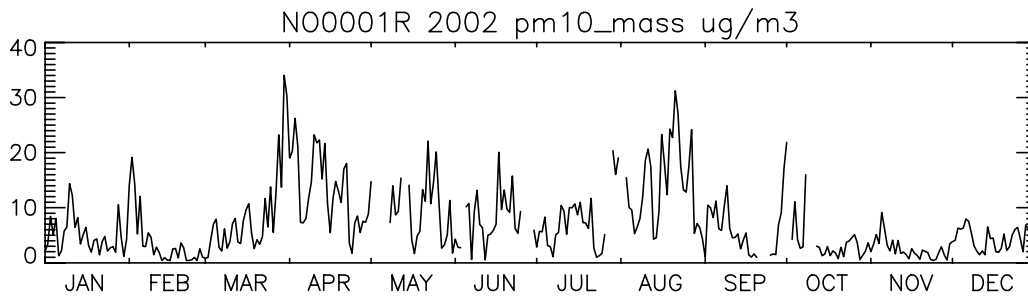
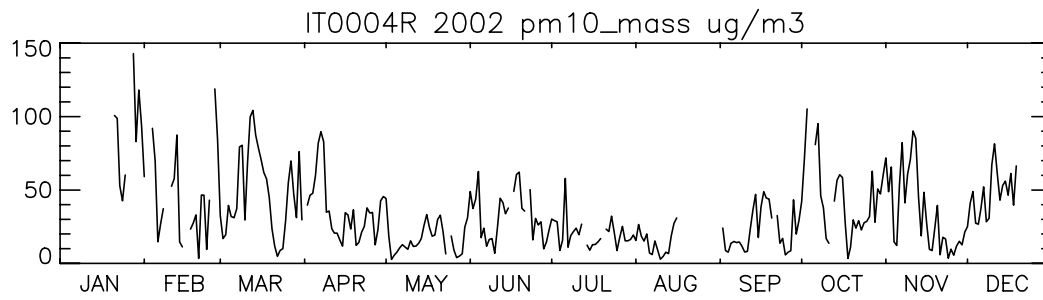
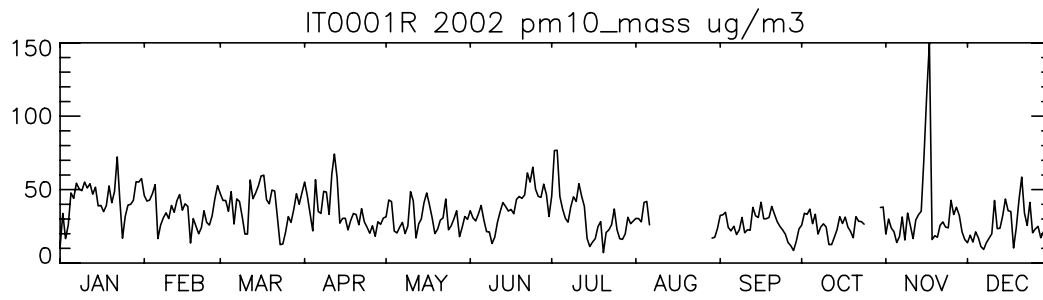


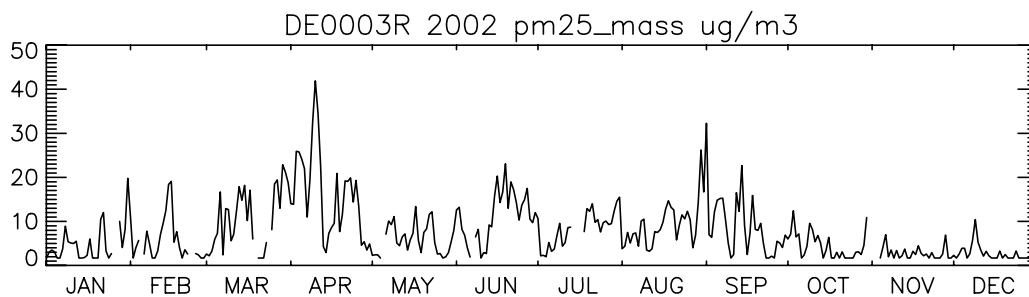
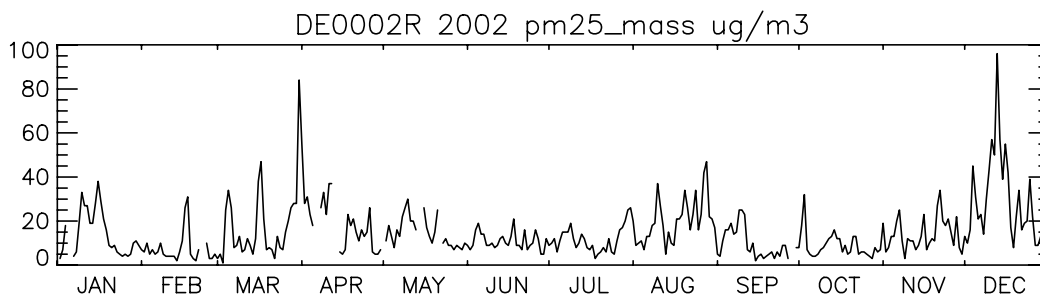
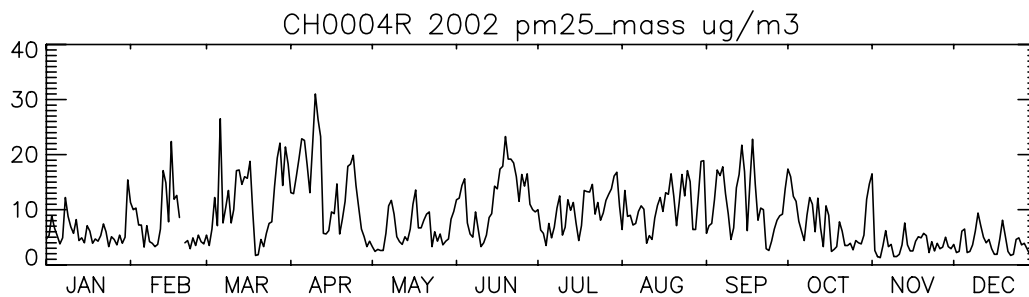
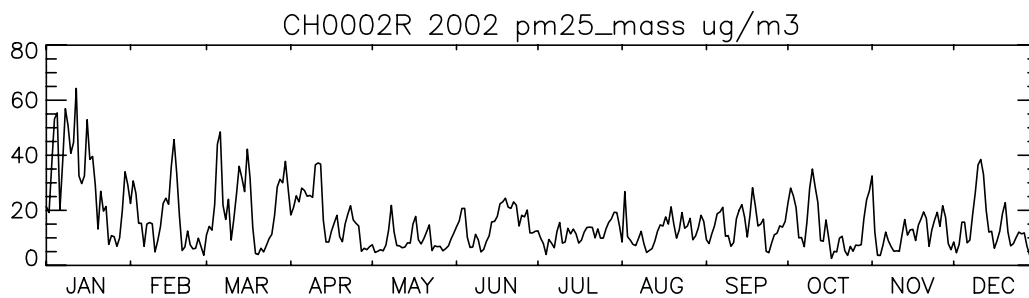
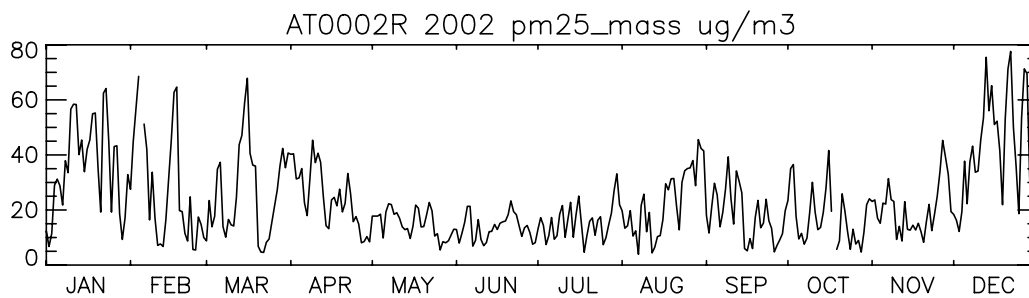


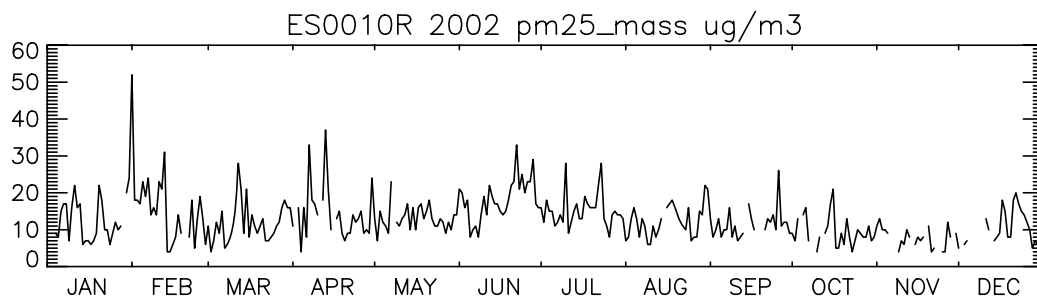
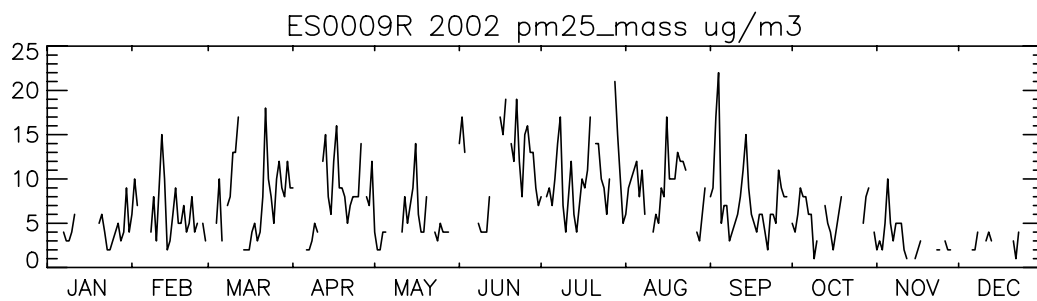
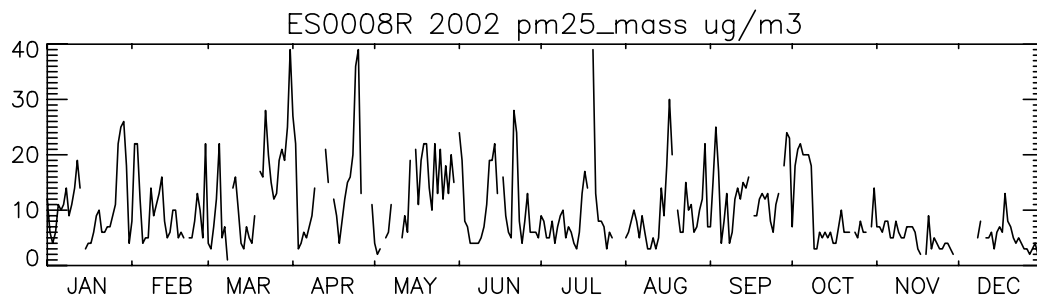
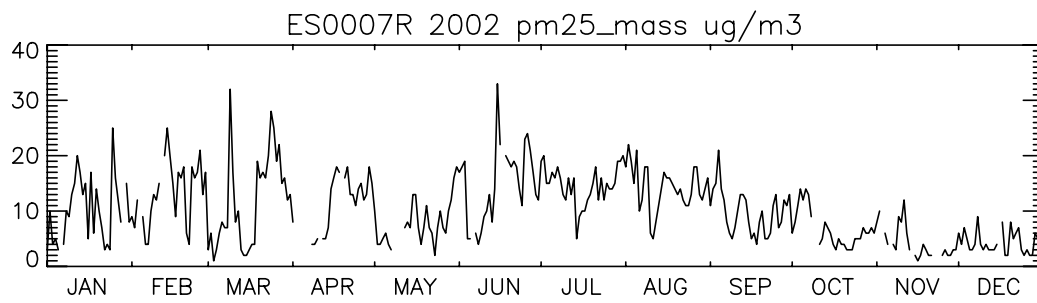
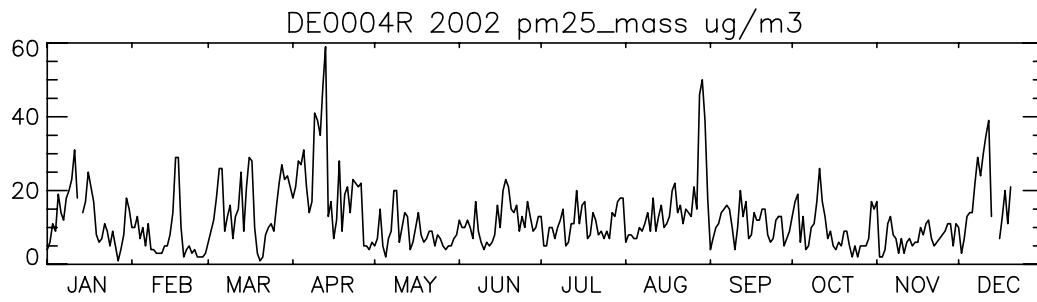


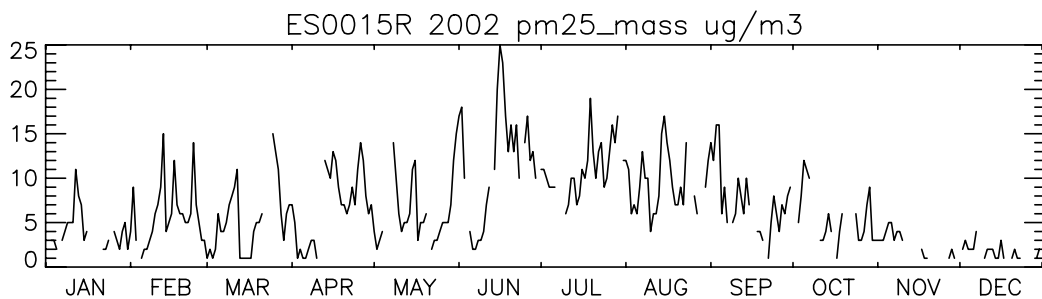
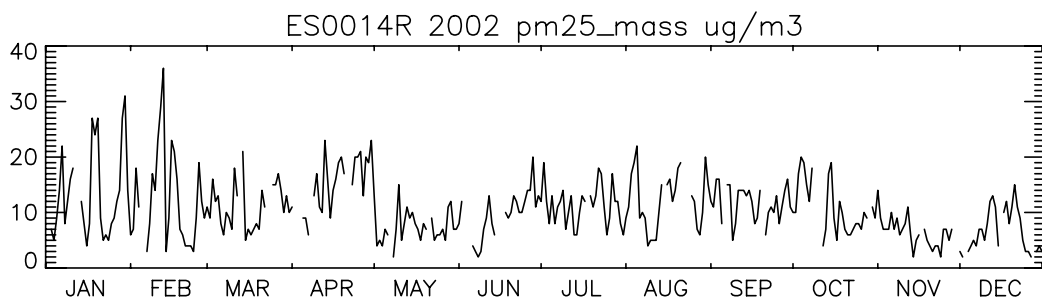
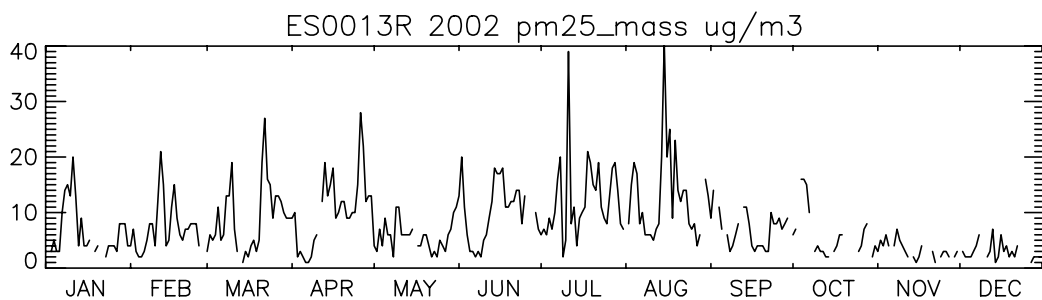
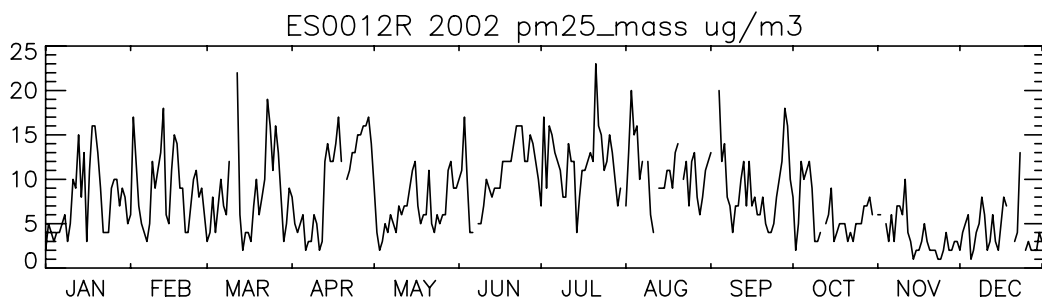
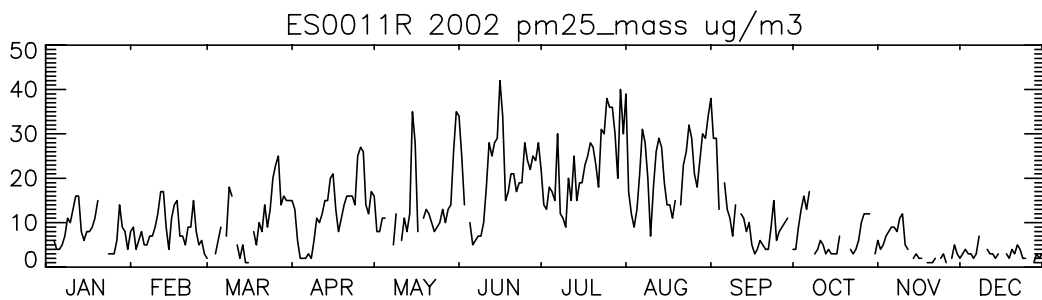


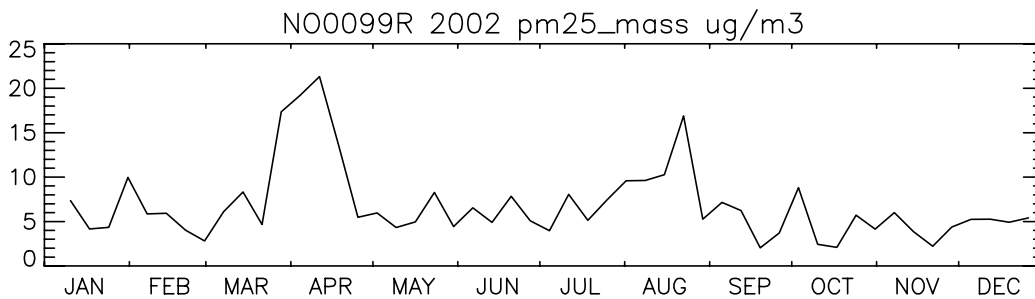
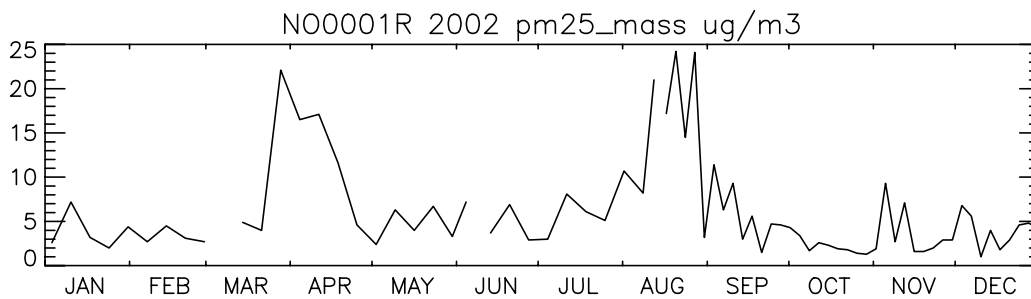
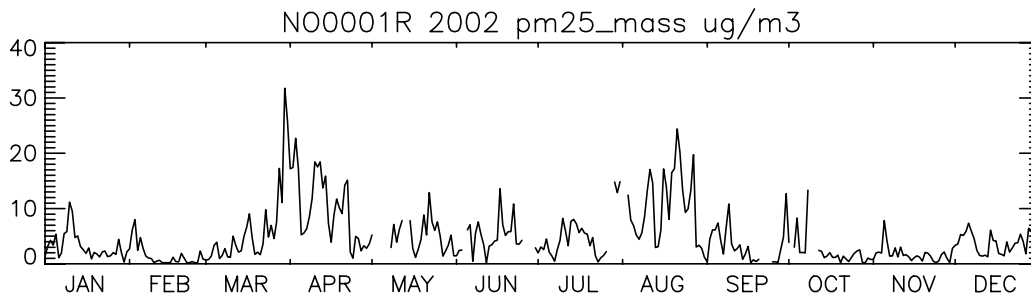
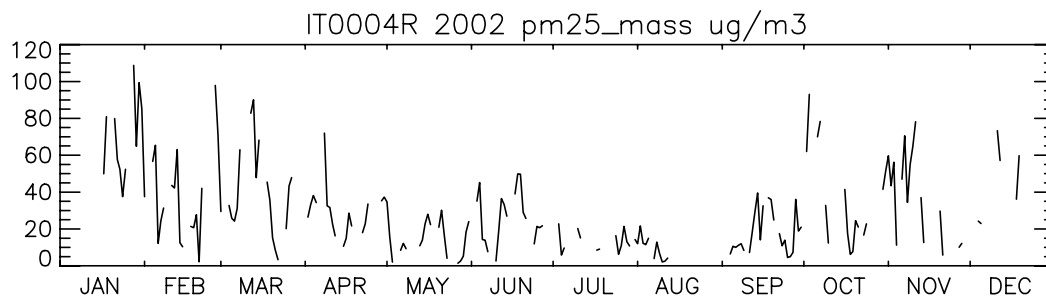
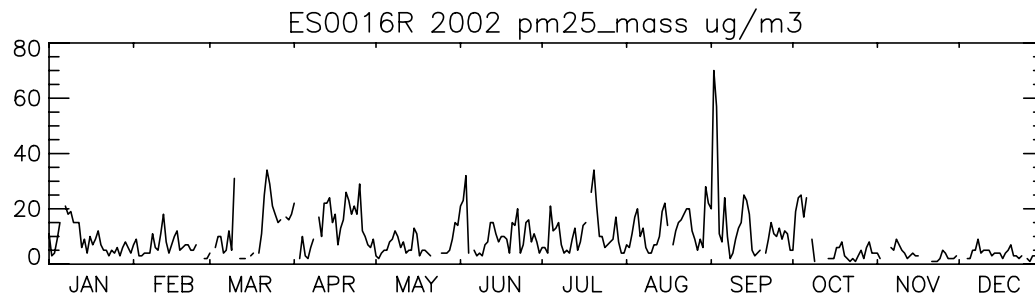


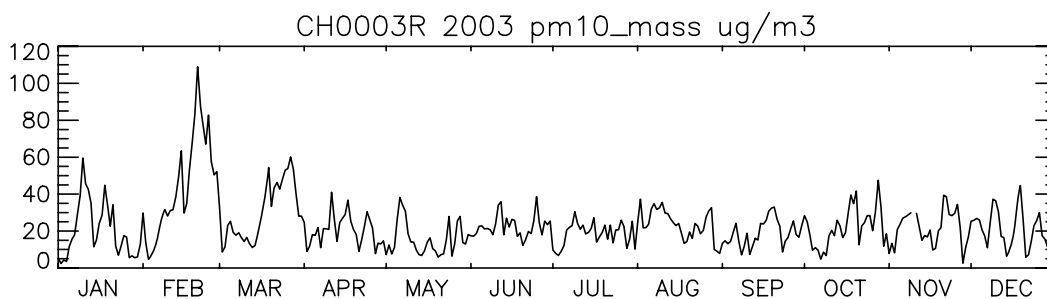
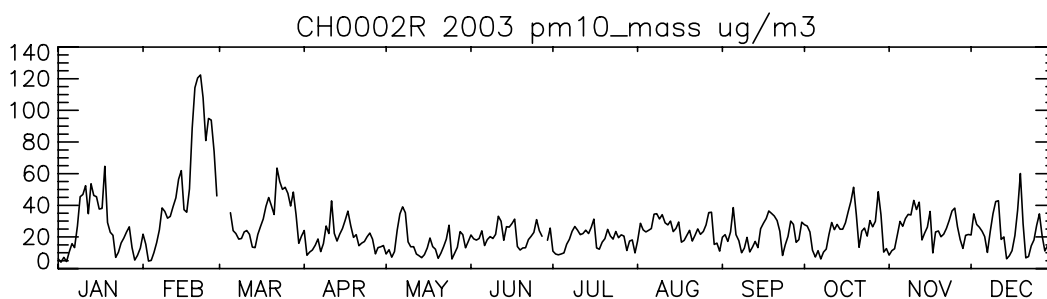
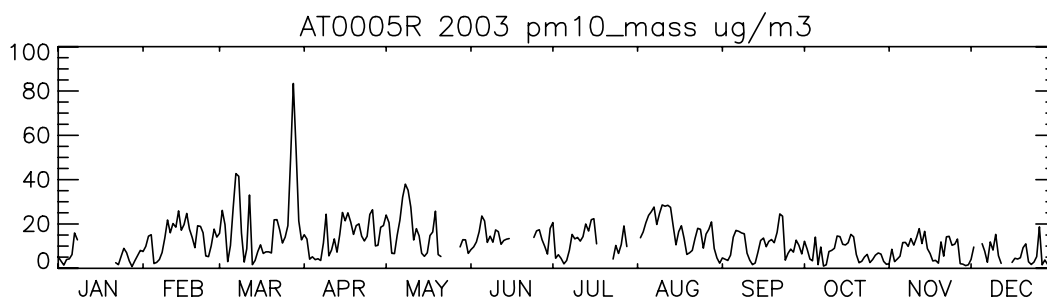
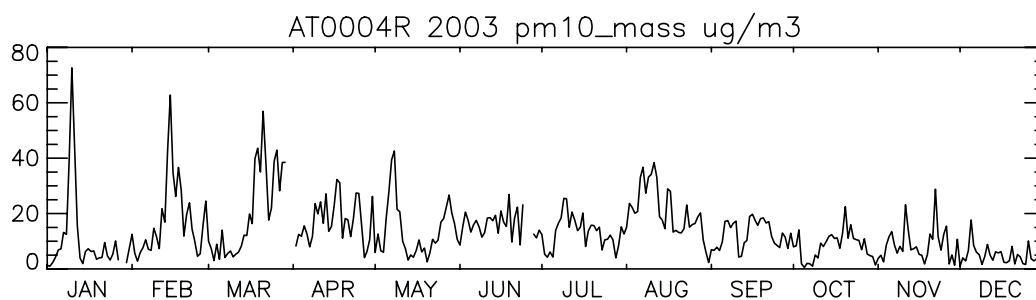
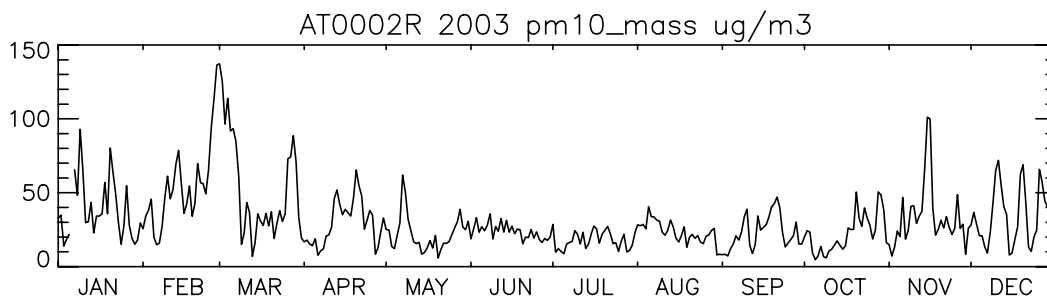


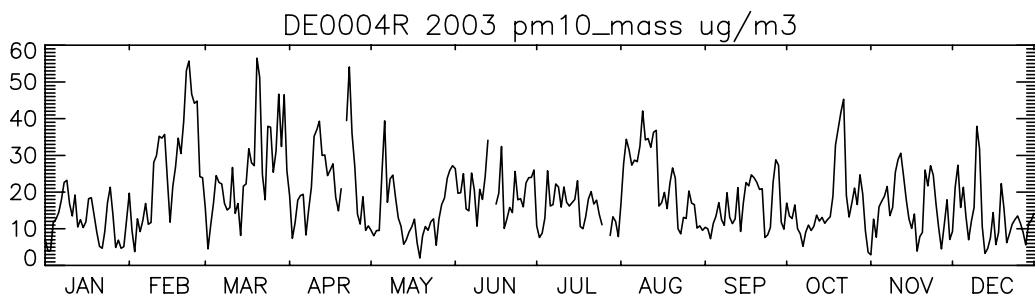
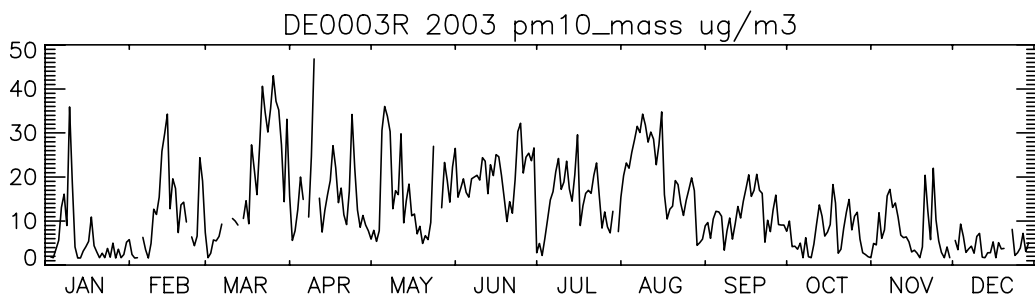
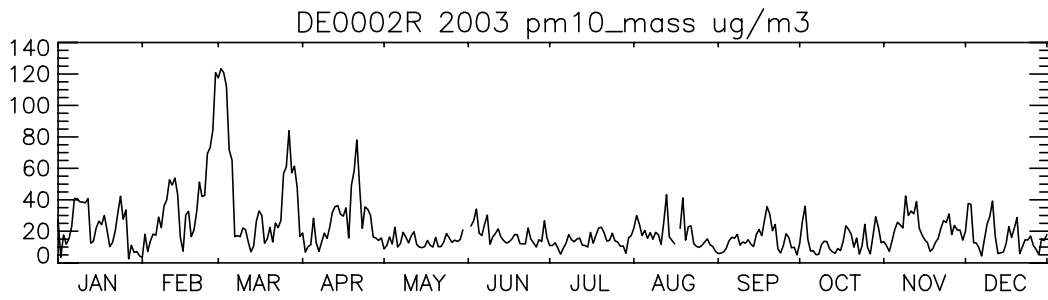
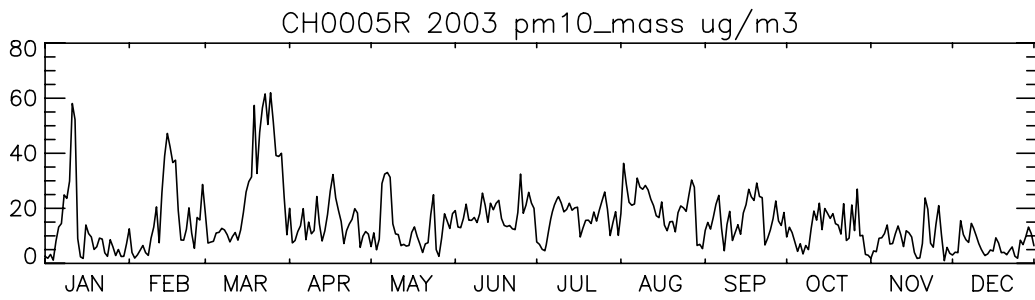
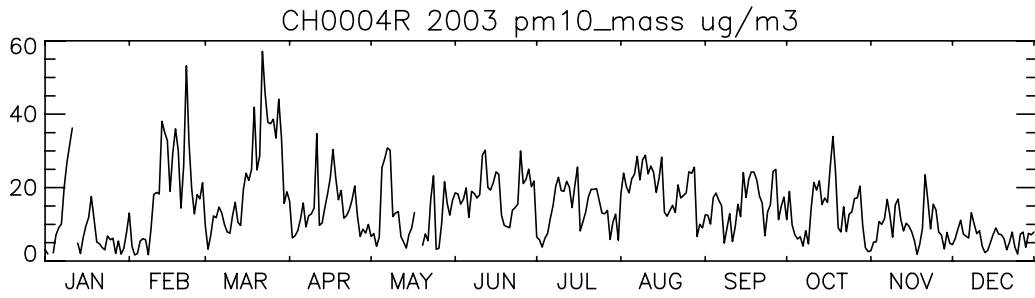


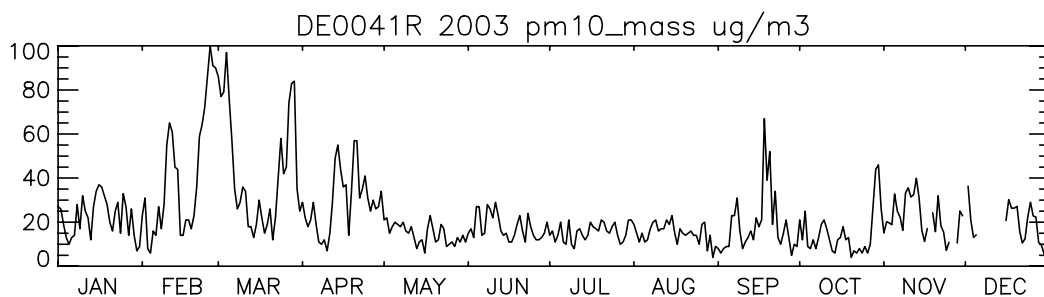
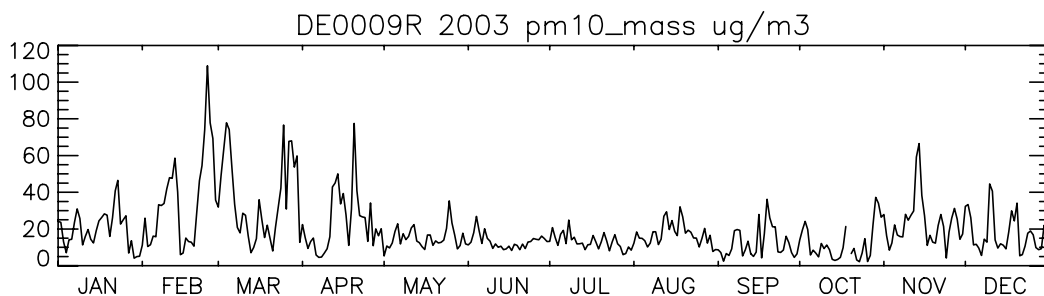
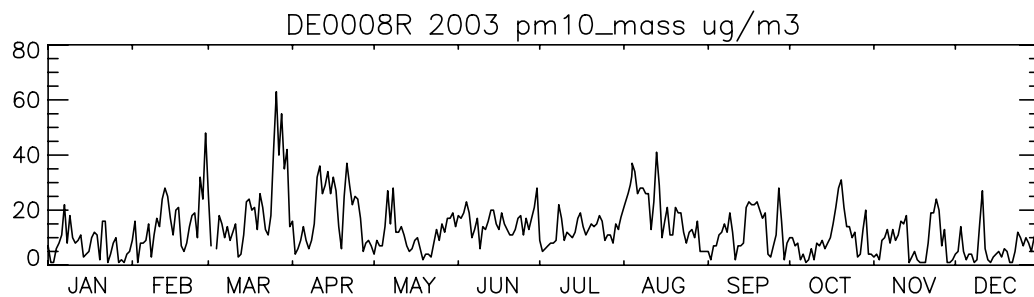
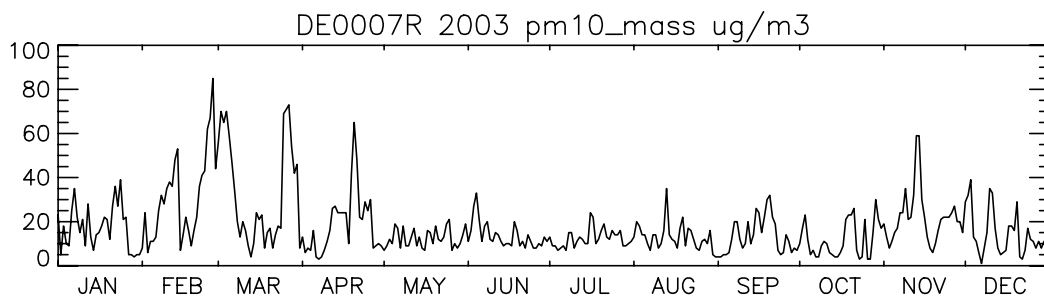
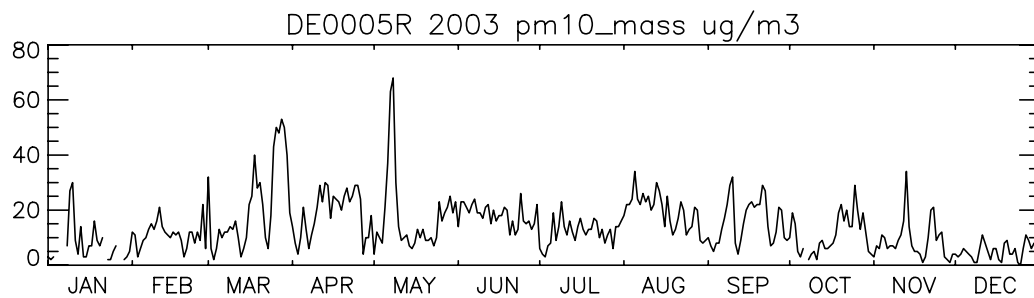


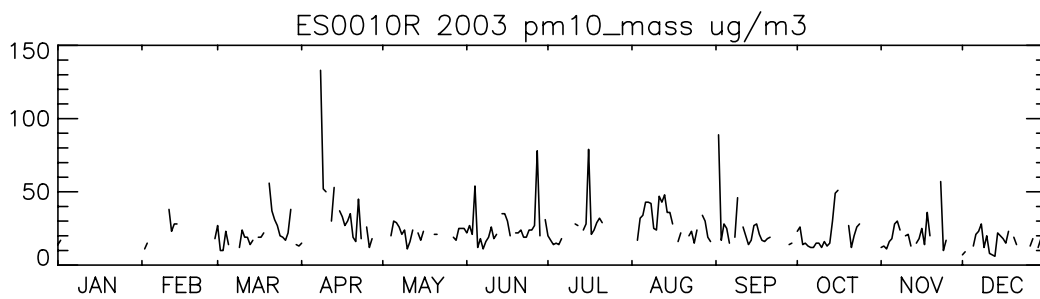
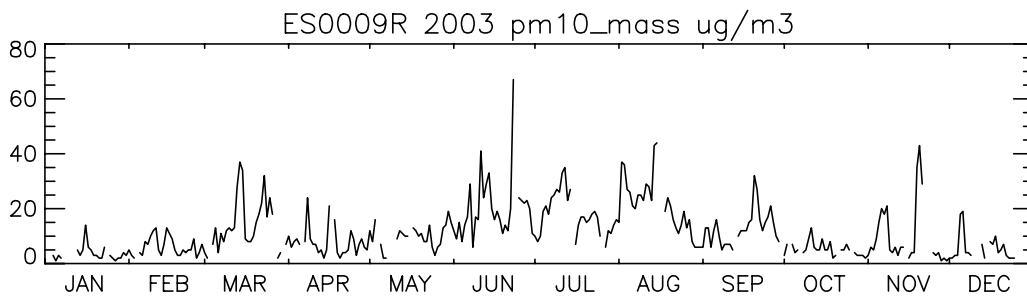
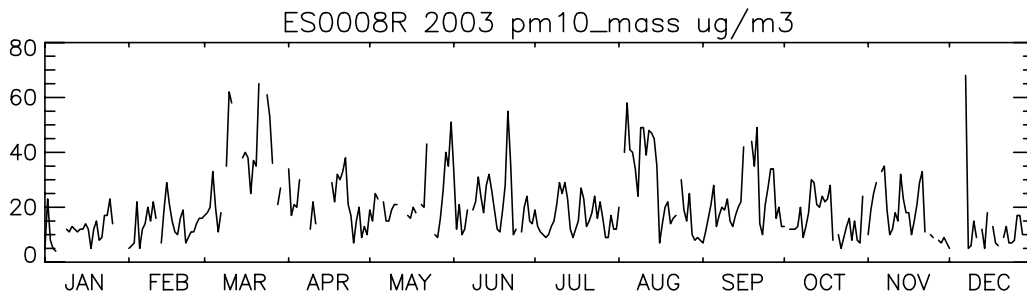
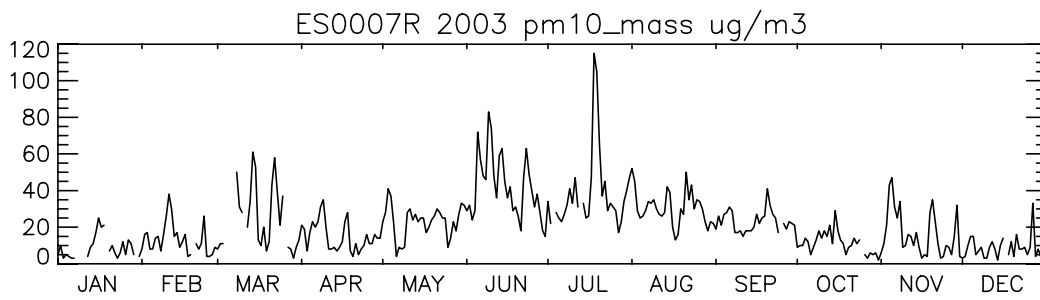
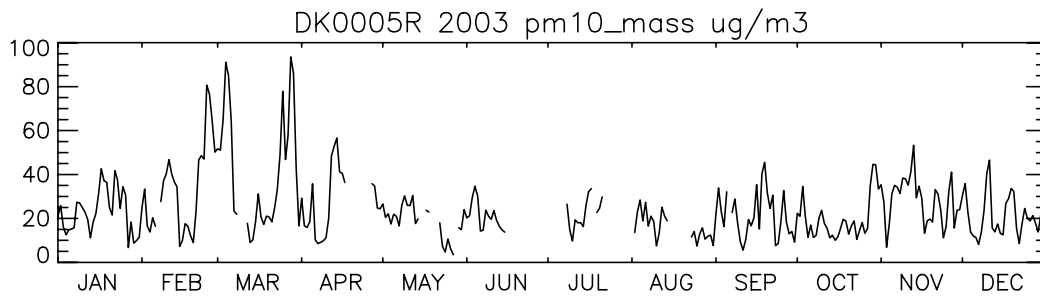


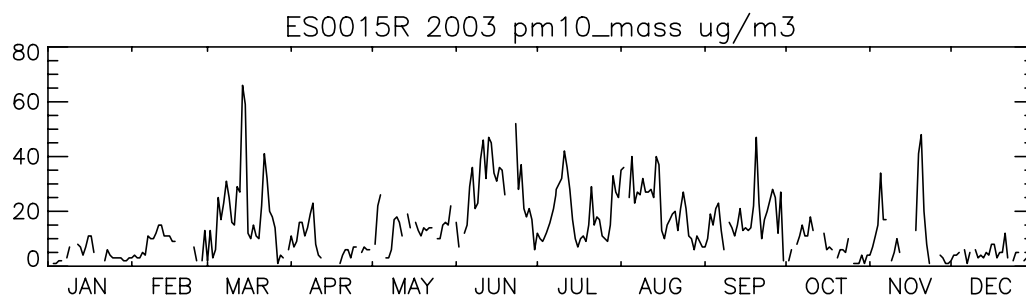
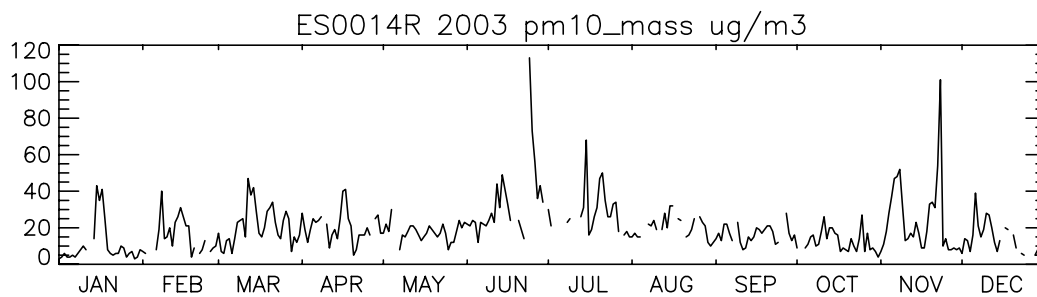
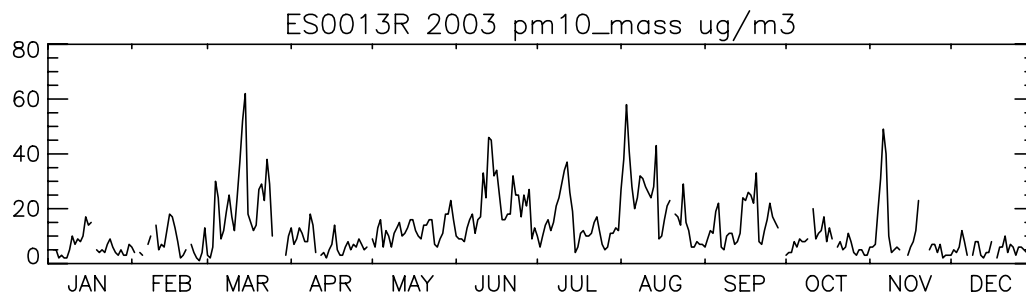
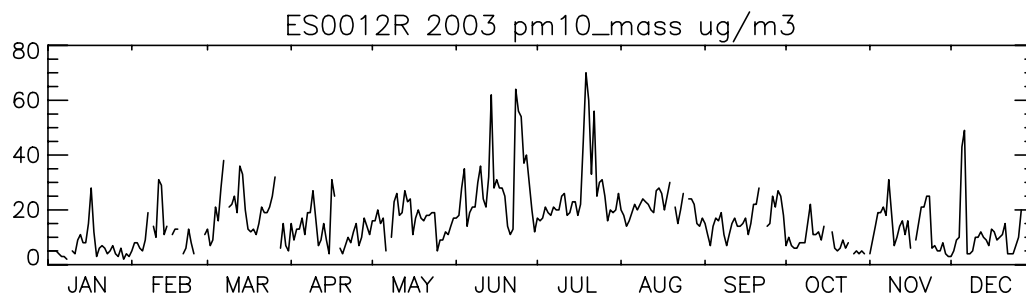
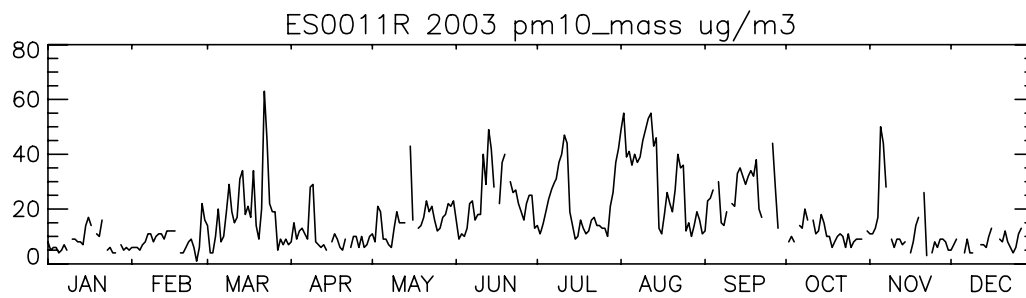


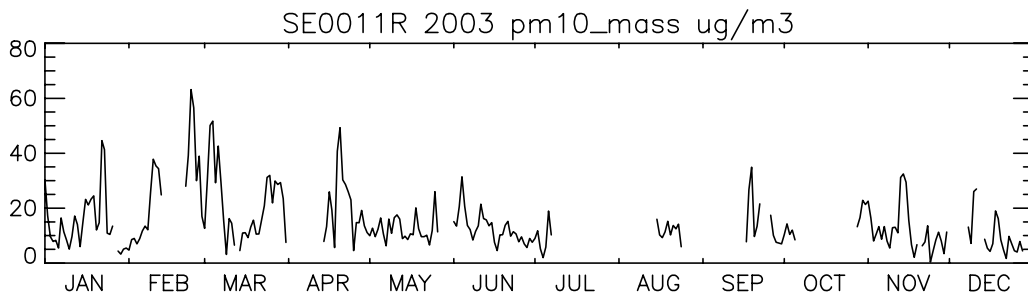
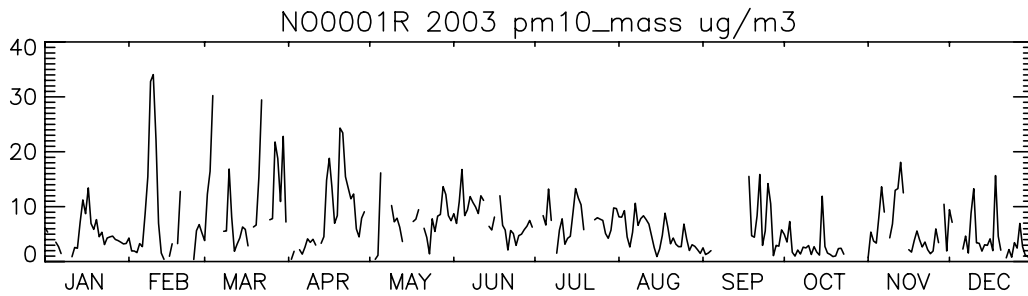
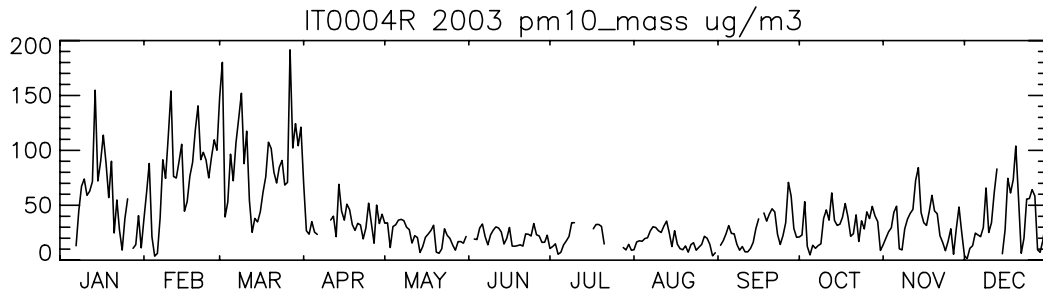
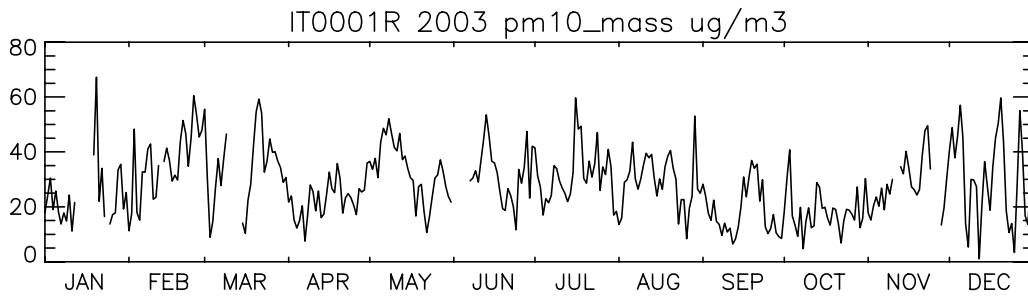
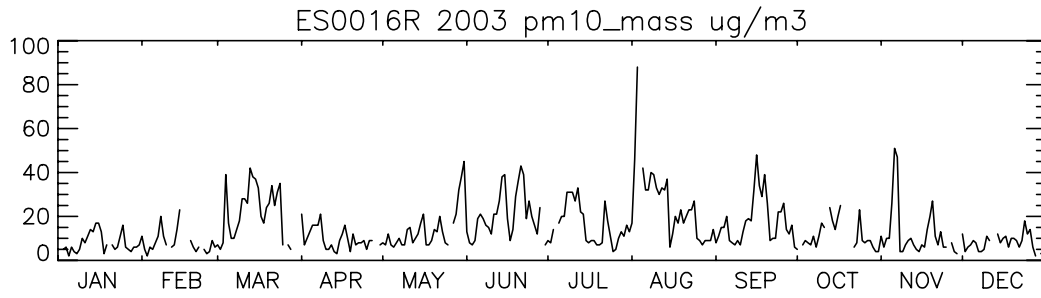


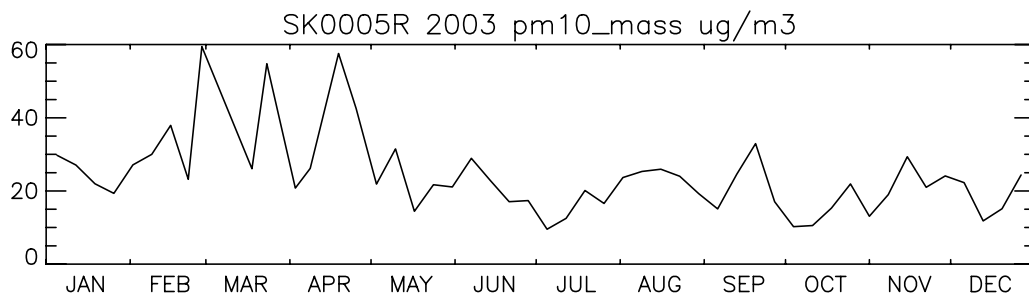
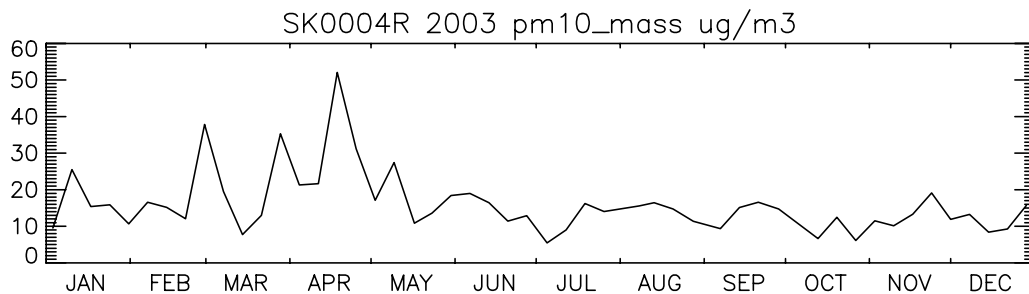
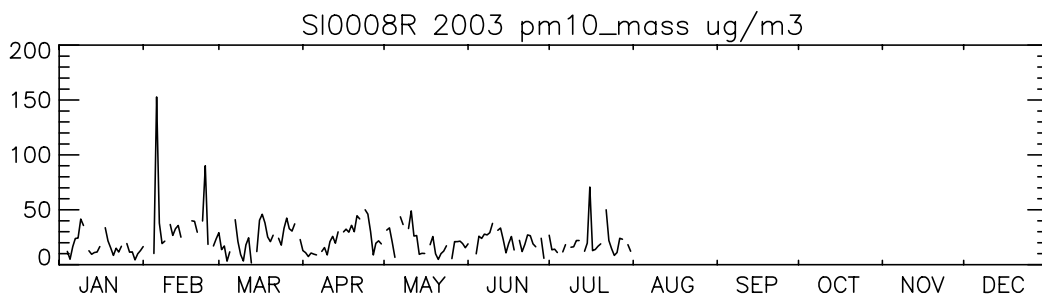
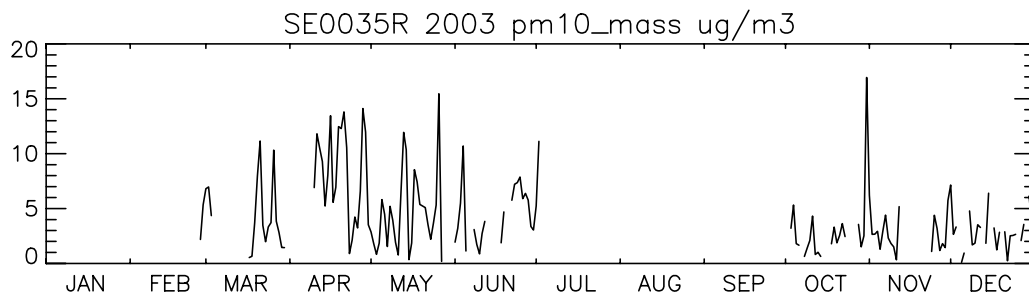
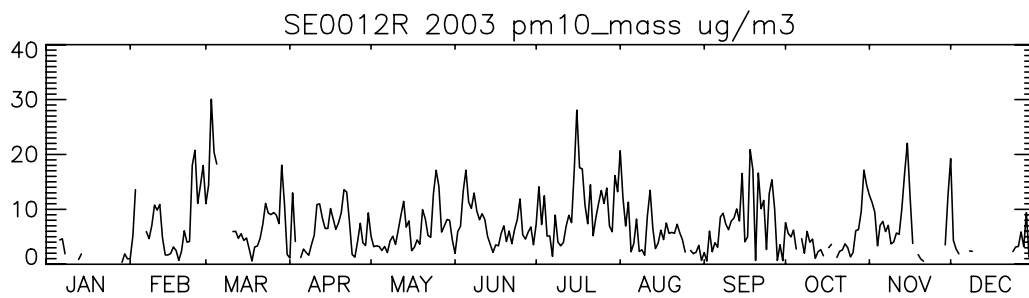


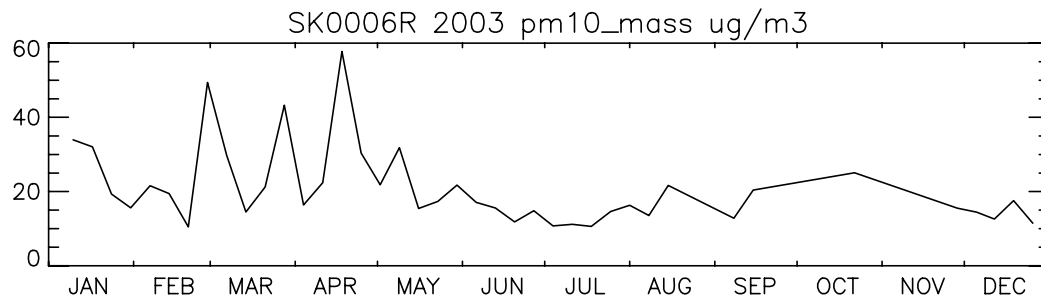


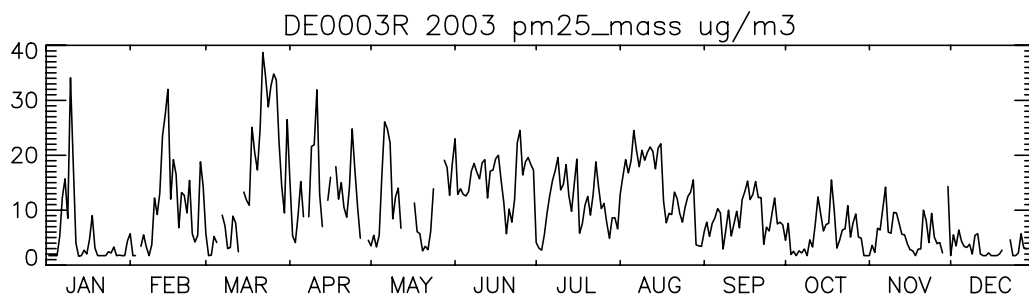
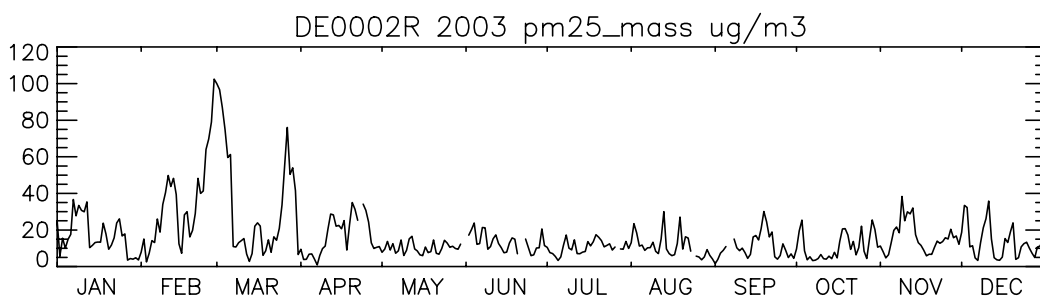
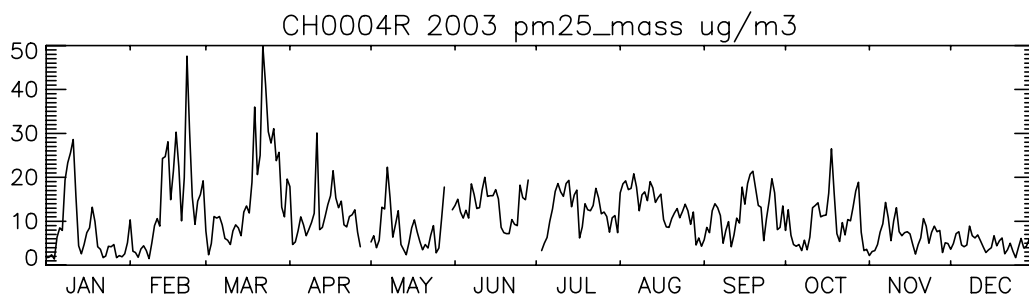
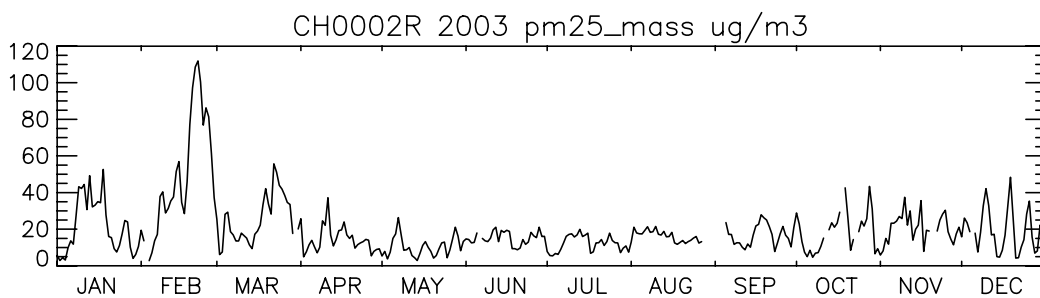
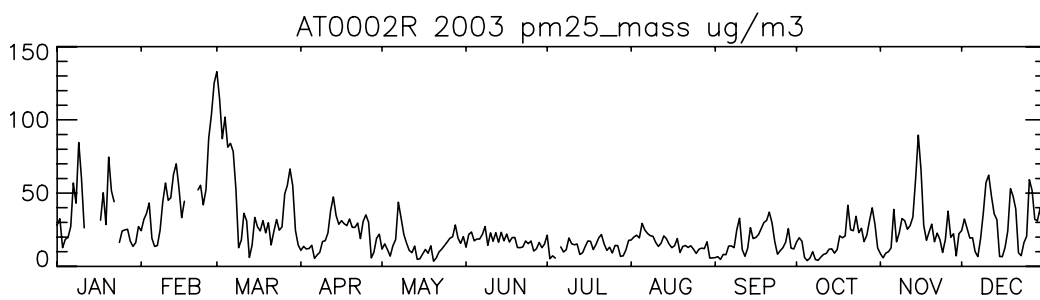


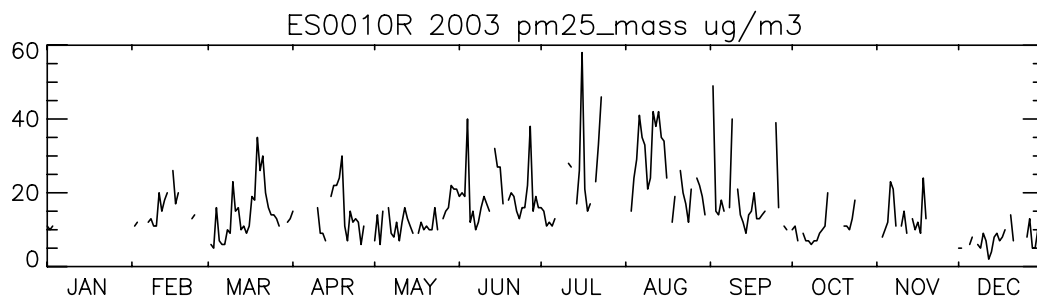
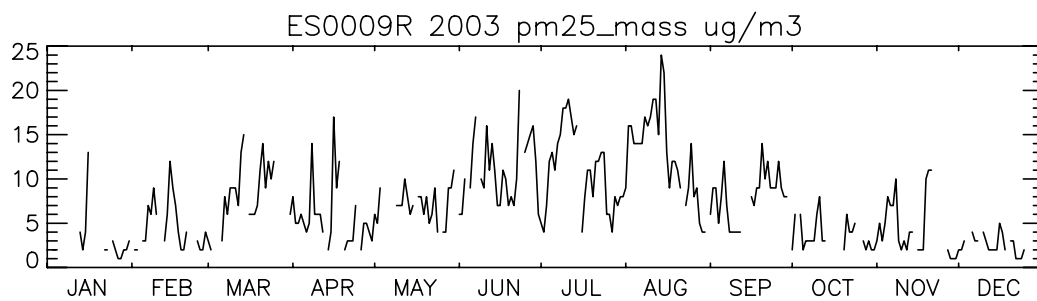
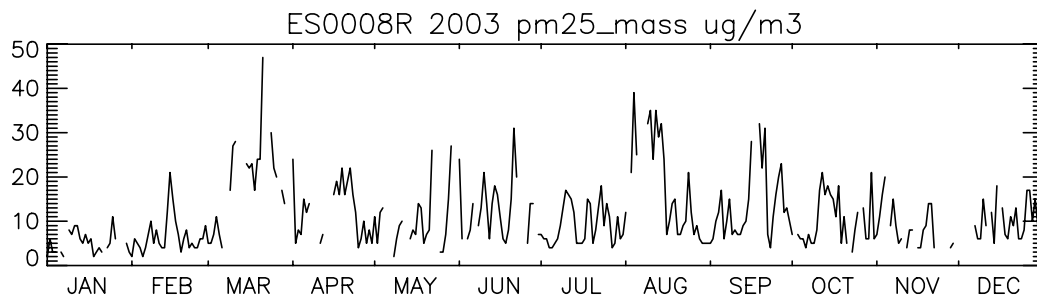
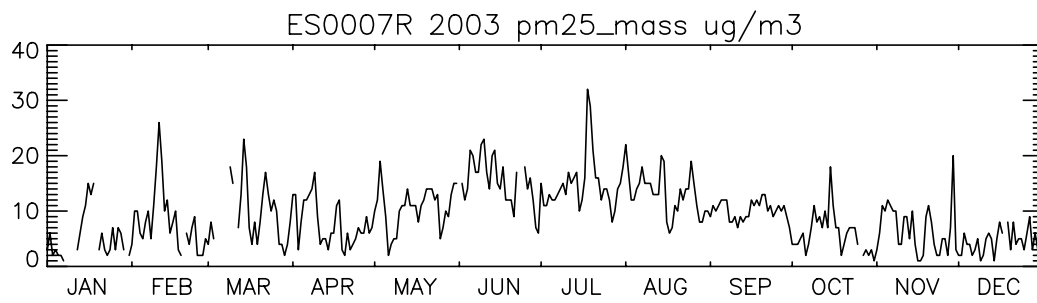
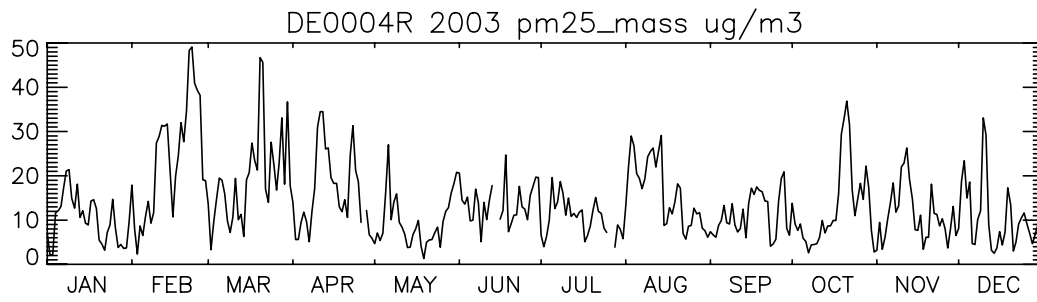


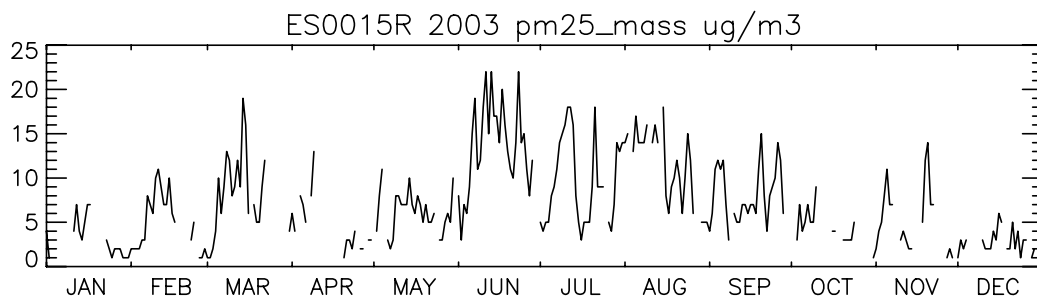
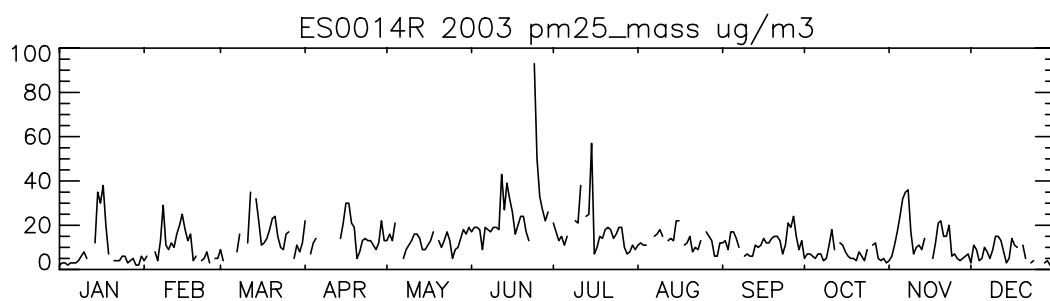
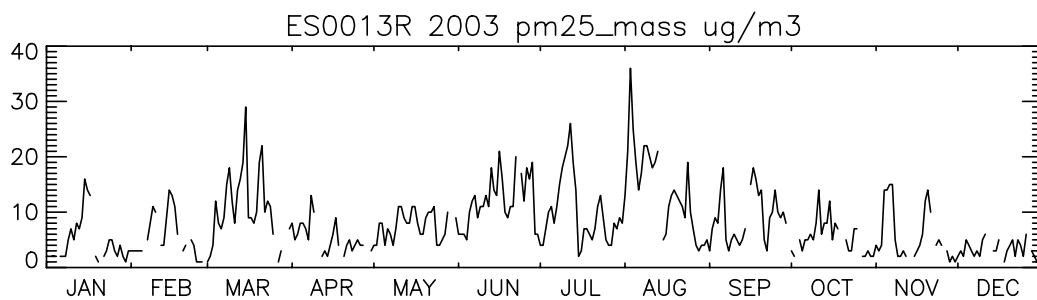
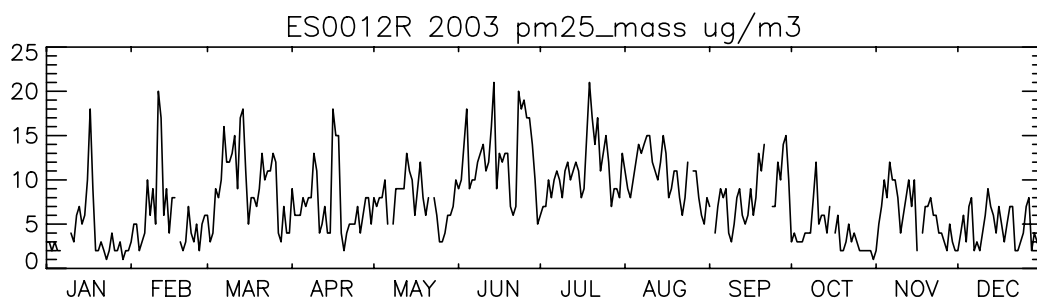
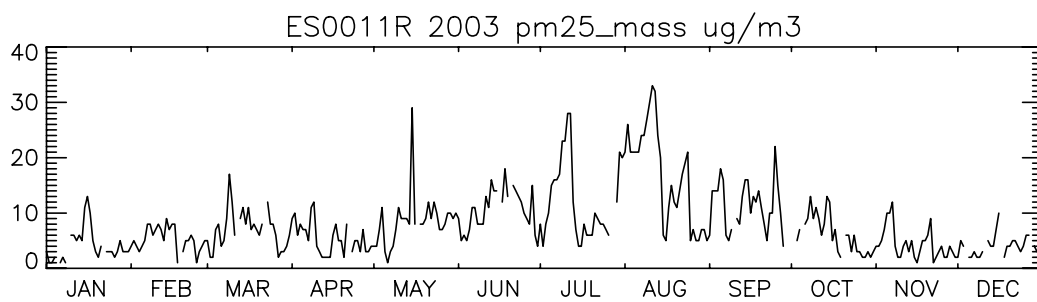


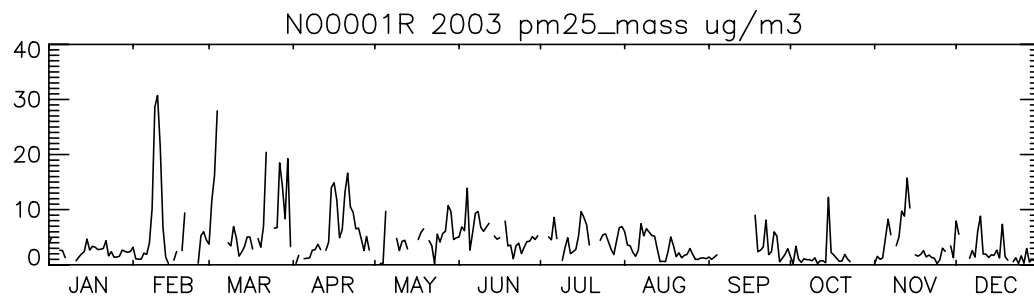
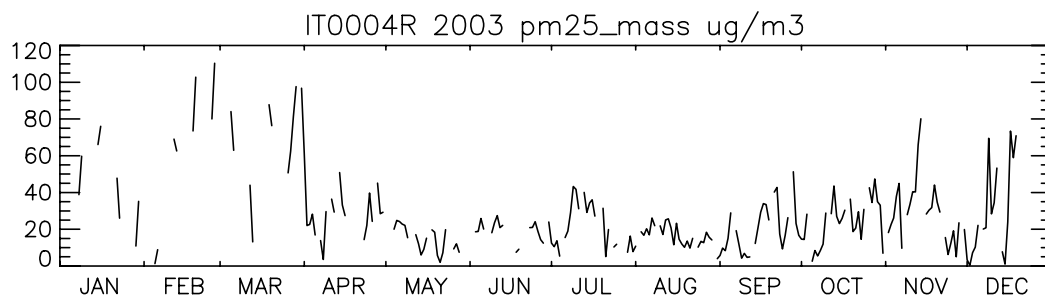
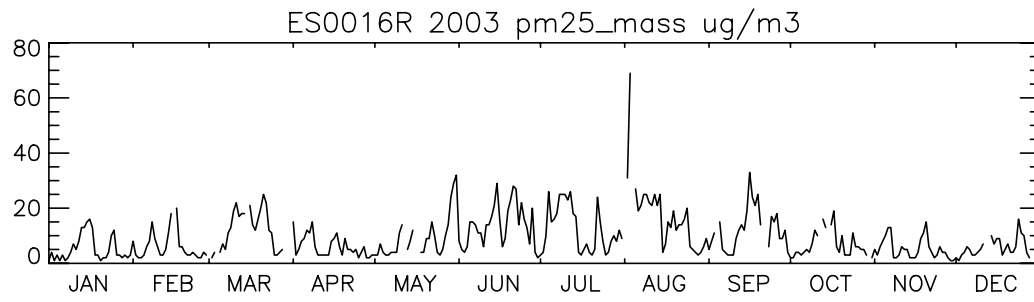


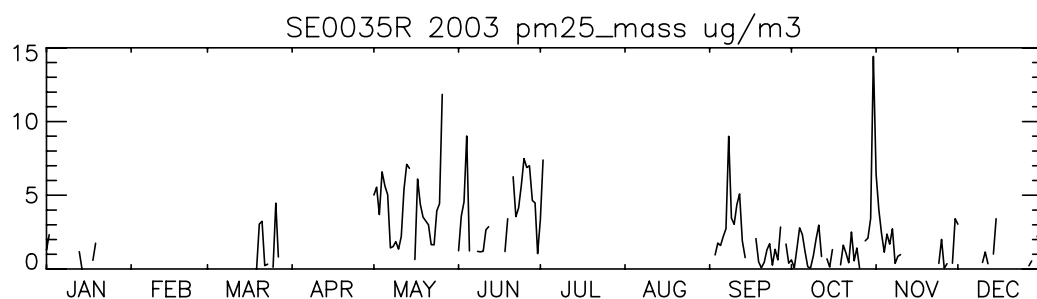
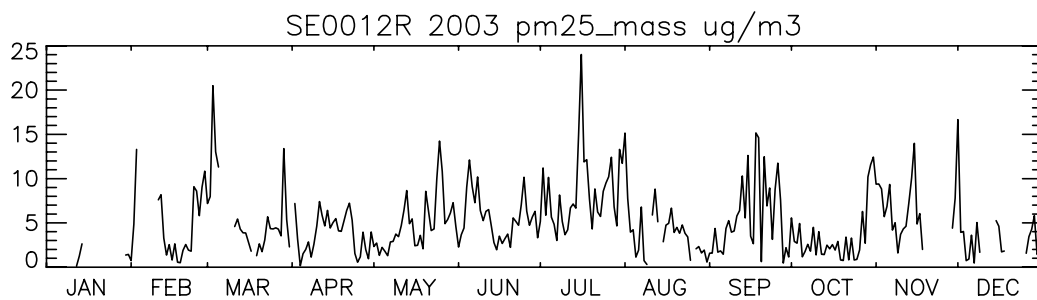
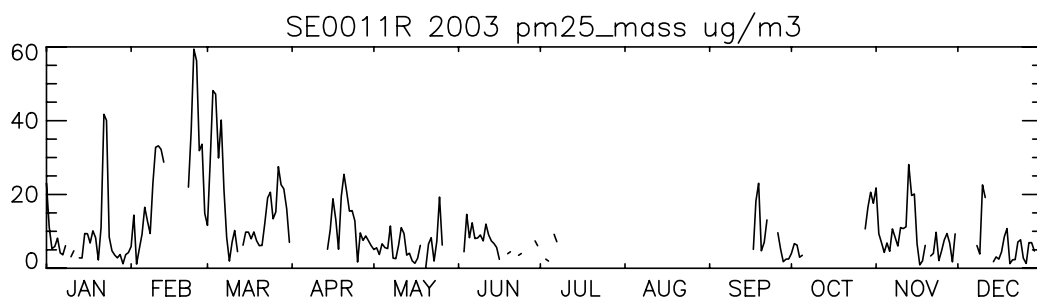
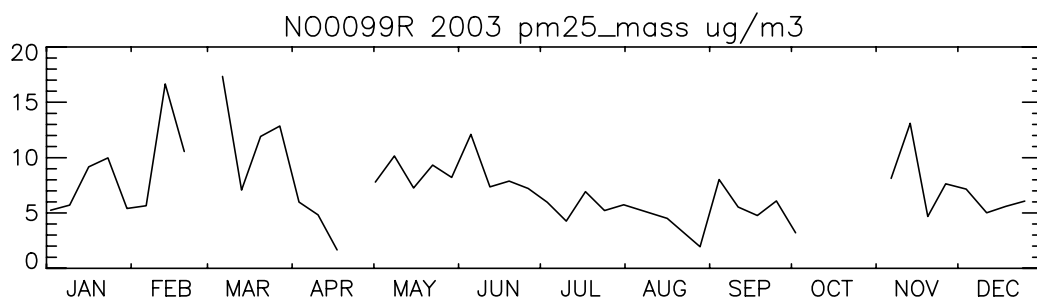


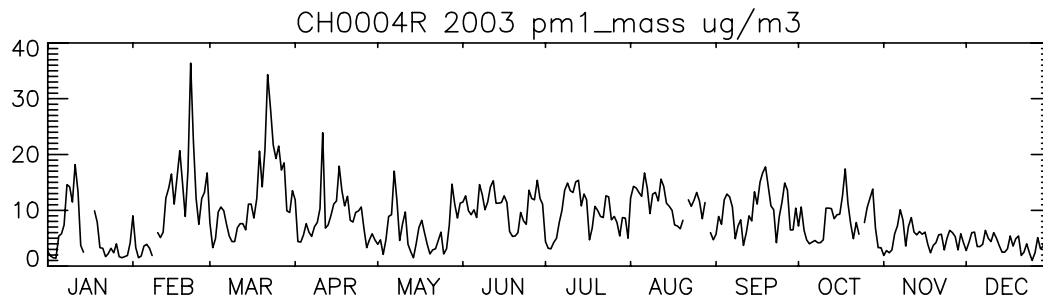
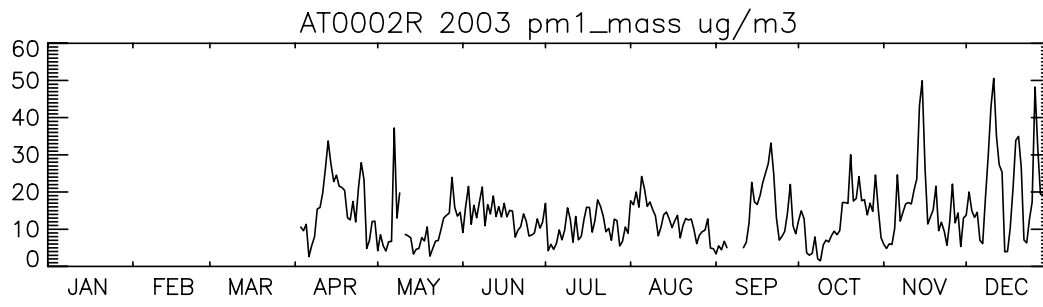












Annex 3

Trends in yearly mean particulate mass concentrations at selected EMEP stations

